SQT

NASA CR-159506

(NASA-CR-159506) DEVELOPMENT OF FLEXIBLE ROTOR BALANCING CRITERIA Final Report (Rochester Inst. of Tech., N. Y.) 115 p HC A06/MF A01 CSCL 13I

N80-32720

G3/37 Unclas 33742

DEVELOPMENT OF FLEXIBLE ROTOR BALANCING CRITERIA

by

Wayne W. Walter and Neville F. Rieger

Rochester Institute of Technology
Rochester, New York

Prepared for

NATIONAL AERONAUTICS AND SPACE ADMINISTRATION
Lewis Research Center
Cleveland, Ohio 44135

March 1979

Grant NSG-3072

TABLE OF CONTENTS

1. DESCRIPTION OF STUDIES UNDERTAKEN

1.1 Scope

The objective of the studies in this report was to develop rotordynamic analysis procedures for obtaining numerical criteria for the balancing of flexible rotors. Present numerical criteria for flexible rotor balancing are based on related practical experience. This study attempts to develop flexible rotor balancing criteria, through the use of rotor analysis techniques. Such a formulation should validate existing criteria, and would provide a general procedure for establishing criteria values for specific rotor types.

The procedure used in this study was to use a rotor response computer program to calculate the response of a range of flexible rotors in a systematic manner. This provided rotor response charts by which criteria for many similar rotor types could be obtained directly, as follows. First, a comprehensive analysis was made of the unbalance response of a uniform flexible rotor in several types of fluid-film bearings. Charts of rotor whirl amplitude vs. speed were plotted for ranges of bearing-rotor stiffness parameter, C/δ. Second, a procedure for representing a non-uniform rotor as an equivalent uniform rotor with similar dynamic properties was developed. This was based on using the lowest rigid-bearing flexural critical speed value and the mass of the rotor to define an equivalent rotor stiffness, which was then matched to that of the uniform diameter rotor. A further procedure was developed for making equivalent bearing representations. This is important in cases where a rotor is supported in two end bearings which do not have identical stiffness and damping properties.

The third step was to test the equivalent rotor procedure for its ability to represent bearing whirl amplitudes. This was done by computing the response of the equivalent rotor system and that of the actual non-uniform rotor system, and comparing results. This comparison was made for twelve different non-uniform rotor cases, to compare the effectiveness of the equivalent rotor method amplitudes for the first whirl mode.

The fourth step in the procedure was to compare results from the equivalent rotor method with results available from other calculations done on six practical rotors. In several cases test data on rotor whirl amplitudes was available for these practical rotors. This data allowed information on rotor unbalance/rotor journal whirl amplitude and on other response details to be developed. Equivalent rotors were developed in each instance, and whirl amplitudes were calculated for specified rotor residual unbalance. These results were checked against results based on actual $(\frac{r}{a})$ values. The results provided an assessment of the validity of the proposed method, and gave new information on the suitability of existing rotor balance criteria.

The above four steps are demonstrated herein, and typical results are shown. The remainder of this report discusses progress made toward improved flexible rotor criteria, with suggestions for additional studies to supplement the above.

1.2 Need

The need to develop improved balancing criteria arises from both the lack of an established data base for flexible rotor balancing, and from the lack of a procedure by which specific criteria for a given rotor can be obtained. Such data have been developed for rigid rotors in two end bearings. The method for selection of an appropriate numerical criterion for a rigid industrial rotor requires that the rotor be classified into a specific quality grade suited to its function. A corresponding residual unbalance value is then selected for its speed of operation. Charts for both the above steps are given in I.S.O. Standard Document 1940 (1973): Balancing of Rigid Rotors, reference [1]. The charts in this document are based on comprehensive data for rigid rotors from a range of industrial applications: see Muster and Flores [2].

Similar data for flexible rotors are in the process of practical development. This development is presently based on two sources: (a) from established machinery vibration standards and, (b) from prior

experience with typical flexible rotor machines. Data obtained from both procedures is empirical. Without questioning its validity, the data base for such information must be somewhat restricted. Also, it is difficult to quantify in a consistent manner. These reasons suggest that additional data developed by analysis should represent a useful addition to existing criteria. Once developed, an analytical criterion would apply to a rotor of any shape, size, or speed.

1.3 Previous Work

Early computer studies of unbalance response of a rotor in fluid-film bearings were made by Lund and Sternlicht [3] in 1961. A single-disk rotor was studied to determine the influence of the oil film in attenuating rotor vibrations, especially during operation near the flexural critical speed of the system. Data on the dynamic properties of several types of fluid-film bearings is included in this report, with comparisons of their relative influence on rotor unbalance amplitudes. The response of a symmetrical two-disk rotor in partial bearings was studied by Warner and Thoman [4], who gave design charts for evaluation of amplitude response and transmitted force. The computer analysis of rotor-bearing systems has been discussed by several authors including Lund and Orcutt [5] who compared theoretical whirl amplitudes with test results for a given high-speed flexible rotor. These results were later verified by Thomas [6] who wrote the initial version of the computer program described herein. A parametric study of the unbalance response of a uniform flexible rotor in fluid-film bearings was made by Rieger [7].

Criteria for rotor balancing were initially proposed by Feldman [8] based on work by Federn [9], Rathbone [10], and others. Muster and Flores [2] collected data on rigid rotors from a variety of industries, and from this data made a statistical determination of acceptable rotor vibration levels for various rotor types, sizes, weights and speeds. These results

were used as the basis for the rigid rotor criteria charts in I.S.O. Document 1940 (1973) [1]. This document also contains much valuable guidance on rigid rotor balancing technology. Other standards for rigid rotor balancirg (AGMA, NEMA, API) are also available, but I.S.O. 1940 is more comprehensive.

Flexible rotor balancing procedures and concepts are described in I.S.O. Draft International Standard I.S.O. DIS 5343 (1976), ref. [11]. This document describes suitable procedures for balancing the five basic rotor classes mentioned previously. Numercial criteria for flexible rotor balancing were proposed by Giers [12] based on values given in a German Vibration Standard Document VDI 2953. In revised form these criteria plus a guide to their application is given in I.S.O. draft International Standard 2905 (1978), ref. [13]. These criteria values make allowance for rotor size, quality, operating speed, and location of measurement. Further detail form I.S.O. 5343 and I.S.O. 2916 are given in the present report.

2. UNBALANCE RESPONSE COMPUTER PROGRAM

2.1 Program Details

The computer program used in this study was a general rotor system unbalance response program, based on the system model shown in figure 1. Practical rotors are modeled using a sequence of cylindrical sections which are rigidly joined together at their ends. Disk sections of the rotor with mass and gyroscopic properties are also incorporated at these end junctions, as shown. Rotor unbalance is included at the rotor junctions, and a spatial distribution of unbalance along the rotor may be introduced through the use of sine and cosine unbalance components at the rotor unbalance stations.

Bearings are represented in this program by the model shown in figure 2, using the conventional linearized eight stiffness and damping coefficient procedure. Bearings are introduced into the system model at suitable rotor section ends, as shown in figure 1. This procedure allows the influence of any desired bearing geometry or bearing operating conditions to be investigated for which the coefficient data is available. The influence of given plain cylindrical bearings, tilting-pad bearings, axial groove bearings, and partial arc bearings on the response of several rotor configurations was investigated during this investigation.

The rotor-bearing formulation used allows the shaft to whirl in a elliptical orbit, where required by the bearing conditions. The magnitude of the rotor whirl ellipse maximum radius is plotted for selected rotor locations on the rotor response charts. These response charts are used in developing the balance criteria with which this report is concerned.

The computer program was developed and verified by Thomas [6]. A matrix formulation is used, based on the dynamic stiffness procedure of McCallion and Rieger [14]. Excellent correlation with previous rotor-bearing system studies was demonstrated during program verification. A program listing with input and output details is given in the Appendix of this report.

3. UNIFORM ROTOR RESPONSE CALCULATIONS

3.1 System Parameters

It has been shown by Rieger [7] that the unbalance response of a uniform rotor in fluid-film bearings may be described in terms of:

a) bearing geometry and operating conditions

b) axial location of unbalance

c) type of unbalance (force, couple)

The dimensionless parameters used to describe rotor unbalance response are:

1. Amplitude ratio

$$\frac{r}{a} = \frac{\text{maximum radius of whirl orbit, ins.}}{\text{eccentricity of rotor mass, ins.}} \qquad U = Wa$$

2. Speed ratio

$$\frac{\omega}{\omega_c} = \frac{\text{shaft speed of rotation, rad/sec}}{\text{lowest rigid bearing critical speed, rad/sec}}$$

3. Stiffness ratio

$$\frac{c}{\delta} = \frac{\text{radial machined clearance of bearing}}{\text{Mid-span deflection of uniform rotor in rigid bearings}}$$

4. Eccentricity ratio

$$\frac{e}{c} = \frac{\text{eccentricity of journal center from bearing center}}{\text{radial machined clearance of bearing}}$$

3.2 Uniform Rotor Response Charts

Figures 4 through 29 show charts of unbalance response for a uniform rotor in:

a) Plain cylindrical journal bearings

b) Four-shoe tilting pad bearings

c) Partial arc bearings

d) Four axial groove bearings

Details of the conditions for which the above results apply are specified in table 1. These results apply for a uniform cross-section end-bearing rotor as shown in figure 3. In each instance, the unbalance force is a single force vector located at the axial position specified in table 1.

The unbalance response computer program described in section 2 was used to calculate the rotor response results. In most instances, the rotor was represented in two sections as shown in figure 3. These sections join at the unbalance vector location. This representation includes the distributed mass and distributed stiffness properties of the rotor, which are incorporated directly through the rotor dynamic stiffness mentioned previously. The other ends of the rotor sections are each supported in fluid-film bearings of the type specified. The validity of results obtained using this rotor model was verified against data from ref [7] before proceeding.

Data given in the charts of unbalance response applied for conditions of constant bearing eccentricity ratio, ε. This representation simplified the calculation procedure. To use these charts it is necessary to know in advance the bearing operating eccentricity for the conditions under which the rotor unbalance response data is required. Bearing eccentricity can be obtained from standard steady-state performance charts, for the appropriate bearing type, slenderness ratio (L/D), and Sommerfeld number

TABLE 1. Details of Uniform Rotor Cases Calculated

Case Number	Bearing Type	$\frac{L}{D}$ ratio	Operating Eccentricity ε	$\frac{c}{\delta}$ ratio	Unbalance Position Z/L	Response Location	Figure Number
B1	Plain	1.0	0.2	0.3, 3, 10, 30	0.5	Midspan	4
B3			0.5				5
B5			0.7				6
B7			0.2			Journal	7
B9			0.5				8
B11			0.7				9
B13	Axial Groove	1.0	0.2	0.3, 3, 10, 30	0.5	Midspan	10
B15			0.5				11
B17			0.7				12
B19			0.2			Journal	13
B21			0.7				14
B23			0.5				15

TABLE 1. Details of Uniform Rotor Cases Calculated (Con't)

Case Number	Bearing Type	$\frac{L}{D}$ ratio	Operating Eccentricity ε	$\frac{c}{\delta}$ ratio	Unbalance Position Z/L	Response Location	Figure Number
B25	Partial Arc	1.0	0.2	0.3, 3, 10, 30	0.5	Midspan	16
B27	↓	↓	0.5	↓	↓	↓	17
B29	↓	↓	0.7	↓	↓	↓	18
B31	↓	↓	0.2	↓	↓	Journal	19
B33	↓	↓	0.5	↓	↓	↓	20
B35	↓	↓	0.7	↓	↓	↓	21
B37	Tilting Pad	1.0	0.2	0.3, 3, 10, 30	0.5	Midspan	22
B39	↓	↓	0.5	↓	↓	↓	23
B41	↓	↓	0.7	↓	↓	↓	24
B43	↓	↓	0.2	↓	↓	Journal	25
B45	↓	↓	0.5	↓	↓	↓	26
B47	↓	↓	0.7	↓	↓	↓	27
B49	Plain	0.5	0.3	3, 10, 30, 100	0.5	Midspan	28
B50	Plain	1.0	0.5	0.3, 3, 10, 30	0.25	Midspan	29

for the given bearing operating conditions. Bearing eccentricity may also be obtained by a measurement from an actual bearing. Additional details of pad length, groove geometry, etc., for which the bearing coefficients apply must also be considered. When applying the results of this report it should be borne in mind that variations from the calculated bearing geometry details and operating conditions may cause response results to differ somewhat from the computed results, especially in the region of the critical speed peak amplitudes.

3.3 Uniform Rotor Response Results

Figures 4 through 29 are charts of rotor whirl amplitude results obtained using the computer program described in Section 2. These results indicate the variation of:

a) bearing type (plain, axial groove, partial arc, tilting pad)

b) stiffness ratio (c/δ = 0.3, 1.0, 3.0, 10.0, 30.0)

c) speed ratio (ω/ω_n = 0.1 through 25.0, relative to rigid bearing critical speed, ω_n)

d) response location (midspan response, journal response)

The curves shown apply for the case of midspan unbalance. The charts are discussed in detail below.

a) Plain cylindrical bearings

Figure 4 shows the variation of mid-span rotor response with mid-span unbalance over the speed range at eccentricity ratio ε = 0.2, for various stiffness ratio (c/δ) values. Low stiffness ratios, e.g., c/δ = 0.3 correspond to the rigid bearing case (high δ, low C), which is seen to peak at ω/ω_n = 1.0, and 9.0, as expected. The peak at ω/ω_n = 4.0 is absent because the mid-span unbalance does not excite non-symmetric modes. Higher stiffness ratio values tend toward rigid-rotor flexible-bearing conditions. For c/δ = 0.3 the minor peak at ω/ω_n = 0.5 is a

damped rigid-rotor critical speed, and the peaks at 2.25 and 12.0 represent free-free rotor modes. At ω/ω_n = 2.25 the bearing damping is still significant, whereas at 12.0 the bearing damping is less effective and large whirl amplitudes occur. Similar trends are evident in figure 5 for ε = 0.5. More rigid bearing conditions exist with ε = 0.7 as shown in figure 6.

For this case, the rigid bearing curve c/δ = 30 shows two low-speed peaks at ω/ω_n = 0.2 and 0.5, corresponding to the damped rigid rotor critical speeds. This stiff bearing case also brings out the free-free criticals at ω/ω_n = 2.25 and 12.0 (strongly).

Results for journal whirl amplitudes with mid-span unbalance are shown in figures 7, 8 and 9, corresponding to eccentricity ratios of ε = 0.2, 0.5 and 0.7. Amplitudes are generally less than at mid-span, though similar trends may be observed in the results. For ε = 0.2 the rigid bearing case c/δ 0.3 shows resonant peaks at ω/ω_n = 1.0 and at 9.0, as previously. The rigid rotor case shows resonant peaks at ω/ω_n = 2.25 and 12.0 as previously, but the low-speed rigid rotor modes below ω/ω_n = 1.0 are evidently suppressed probably by over-critical damping in the bearings. Similar results are apparent for ε = 0.5. The stiff bearing case ε = 0.7 shows the rigid body critical speeds below ω_n = 1.0, possibly because the bearing damping is effectively smaller for this case.

b) Four axial groove bearings

Similar trends are evident in the axial groove bearing results to those observed for the cylindrical bearing rotor results. For ε = 0.2 in figure 10 the rigid bearing curve c/δ = 0.3 again shows a sharp resonant peak at ω/ω_n = 9.0~10.0, though this appears to have been suppressed by damping, as was the peak around ω/ω_n = 16.0. Thus even at mid-span the rigid bearing rotor tends to be adequately damped in its higher modes. The rigid rotor trends differ from these results. A rigid body mode is observed at ω/ω_n = 0.46, and the rotor free-free mode occurs at 2.25. The peak amplitude in this mode is larger than the rigid-body mode, and

the next resonant mode at ω/ω_n = 12.0 is even stronger, showing the decreasing influence of damping for higher rotor frequency ratios. As the rotor stiffness ratio c/δ increases the above trends become more pronounced.

For ε = 0.5 figure 11 all resonant peaks are very distinct, i.e., the system is losing its effective damping. The rigid bearing case c/δ = 0.3 is evident at ω/ω_n = 1.0, 9.0 and 16.0. The rigid rotor case is also sharp and distinct at ω/ω_n = 0.45, 2.25, and 12.0 as discussed previously. All resonant peaks apart from c/δ = 0.3 blend into a single response above ω/ω_n = 9.0 with a strong common response peak at 12.0

For ε = 0.7, figure 12, the rigid bearing rotor resonances occur at ω/ω_n = 1.0 (strong), 4.5 (damped, weak), 7.0, and 12.0 (very strong). The rigid rotor criticals for c/δ = 30 occur at ω/ω_n = 1.5, 0.4 (damped), 2.25 (strong) and 12.0 (very strong). c/δ curves except 0.3 appear to blend around ω/ω_n = 2.0 and so form common resonant peaks at 2.25 and 12.0.

The journal response at the above conditions is shown in figures 13 through 15. Figure 13 shows the journal response for ε = 0.2 which is similar to that observed for the plain cylindrical bearings. The rigid bearing case has the lowest journal whirl amplitudes with resonant conditions at ω/ω_n = 1.0, 7.5 and 16.0. Amplitudes generally increase as rotor stiffness increases for c/δ = 30. A rigid critical is observed at 3.0 (stronger) and 12.0. Again the stiffer rotor responses appear to form a common peak around ω/ω_n = 12.0, though this trend is apparent in the lower resonance at ω/ω_n = 2.25 to 4.0. The peaks become sharper as the rotor stiffness increases.

For an eccentricity of ε = 0.5 the resonant peaks become sharper, due to the overall decrease in bearing damping, i.e., ($B\omega/k$) (effective) decreases. This effect is evident in figure 12. The tendency toward blending for stiffness ratios above c/δ = 0.3 is again observed at ω/ω_n = 8.0 and beyond. It is also evident that all response peaks have maximum values of about the same value, in each resonant range.

An eccentricity of $\varepsilon = 0.7$ the first mode peaks are relatively small and of similar maximum value, X/a = 5.0, as shown in figure 15. The second resonance at $\omega/\omega_n = 2.25$ shows all stiffness characteristics blended, and again at $\omega/\omega_n = 12.0$, with the exception of $c/\delta = 0.3$. Generally speaking, the axial groove peaks are greater than the plain cylindrical maxima by between 2:1 and 3:1.

c) Partial Arc Bearings

Trends observed for the two previous bearing types are again evident for partial arc bearings. For a flexible shaft in rigid bearings and an eccentricity ratio of $\varepsilon = 0.2$, figure 16, mid-span amplitude peaks are evident at $\omega/\omega_n = 1.0$, 9.0 (minor) and $\omega/\omega_n = 12.0$. Rigid rotor conditions give rise to larger amplitudes below $\omega/\omega_n = 1.0$ with damped rigid-body criticals in this region. Free-free modes occur at $\omega/\omega_n = 2.25$ and 13.0. Again the rigid shaft characteristics begin to blend above $\omega/\omega_n = 2.0$, with a common peak at $\omega/\omega_n = 12.0$. In general mid-span whirl amplitudes are somewhat higher than with plain cylindrical bearings.

At an eccentricity ratio of $\varepsilon = 0.5$, figure 17, rigid-body critical speeds are evident for each shaft stiffness ratio above $c/\delta = 0.3$, at speeds below $\omega/\omega_n = 1.0$. Above $\omega/\omega_n = 1.0$ the $c/\delta = 0.3$ curve response again has critical speeds at $\omega/\omega_n = 3.5$, 9.0, and 13.0, whereas the rigid shaft criticals are at $\omega/\omega_n = 2.25$ and 13.0. Similar trends are evident in the curves for $\varepsilon = 0.7$, figure 18, except that the rigid body criticals are more evident at the higher eccentricity ratio than for $\varepsilon = 0.2$. At $\varepsilon = 0.7$, the curves are again similar to the responses at lower eccentricity ratios. The response amplitudes are somewhat higher than at $\varepsilon = 0.2$ and 0.5.

The journal whirl characteristics shown in figures 19, 20 and 21 are similar to those for the plain cylindrical bearing. A minor peak occurs for the flexible shaft case at $\omega/\omega_n = 1.0$, for stiffness of $c/\delta = 0.3$ all other stiffness ratios show common resonant peaks at ω/ω_n and 2.25 and 12.0. Magnitude of the peaks is similar to the plain cylindrical

journal amplitude ratios. At $\varepsilon = 0.5$ the curves are all blended above $\omega/\omega_n = 1.0$, with peaks at 2.25 and 12.0. Below $\omega/\omega_n = 1.0$, minor rigid rotor critical speed peaks are evident. These peaks are again evident for $\varepsilon = 0.7$, and the rigid rotor peaks at 2.25 and 12.0 are again present. The flexible rotor characteristic shows a small rigid bearing critical at $\omega/\omega_n = 0.8$ and at 3.5. The lower critical speeds suggest that the partial bearing acts somewhat more flexible than the plain cylindrical bearing for given stiffness ratio.

d) Tilting pad bearings

Response characteristics with tilting pad bearings shown in figures 22 through 27 again resemble the characteristics seen with plain cylindrical bearings. The rigid bearing flexible shaft curve shows critical speeds at $\omega/\omega_n = 1.0$ and 12.0. The higher critical is more heavily damped, and both peaks are lower than for corresponding plain cylindrical bearing case, in the ratio 0.4:1.0 approximately. The indication is that tilting pad bearings dampen flexible shaft modes more than plain bearings. Rigid rotor criticals of low magnitude appear below $\omega/\omega_n = 1.0$, and at $\omega/\omega_n = 2.25$ and 12.0. The magnitude of these peaks is of the same order as with the plain cylindrical bearing.

At $\varepsilon = 0.5$, figure 23, the above pattern is repeated. The flexible shaft $c/\delta = 0.3$ is lower at $\omega/\omega_n = 1.0$ and higher at $\omega/\omega_n = 12.0$. The rigid rotor peaks are higher at low speed, but otherwise similar. At $\varepsilon = 0.7$, figure 24, conditions are similar to $\varepsilon = 0.5$ and the peaks are of the same general magnitude.

The journal response curve for $\varepsilon = 0.2$, figure 25, also resembles the response seen in plain cylindrical bearings. Flexible shafts in rigid bearings have lower response amplitudes below $\omega/\omega_n = 1.0$, and then grow to a peak at $\omega/\omega_n = 12.0$. Rigid rotor response is larger, but no critical peak appears below $\omega/\omega_n = 1.0$ for $\varepsilon = 0.2$. The free-free peak appears at $\omega/\omega_n = 2.25$, and all curves blend closely into the peak at $\omega/\omega_n = 12.0$. Similar trends are evident at $\varepsilon = 0.5$, figure 26, and again at $\varepsilon = 0.7$, figure 27. Amplitudes appear to be larger at higher operating eccentricities by between 25 to 35 percent over amplitudes at $\varepsilon = 0.2$.

4. THE EQUIVALENT ROTOR BEARING SYSTEM

4.1 Equivalent Rotor Calculation Procedure

In the present context, an equivalent rotor-bearing system is a uniform rotor in fluid-film bearings which has similar dynamical properties to those of the complex rotor-bearing system on which it is based. The equivalent system is a convenient means of representing the actual rotor system by which balance criteria suited to an actual rotor system may be obtained from the uniform rotor response charts discussed in Section 3. Both an equivalent rotor and equivalent bearings may be required to model a given system. The concept of an equivalent rotor system is shown in figure 30. The procedure for defining the equivalent rotor is as follows:

Step 1: Calculate the first bending critical speed N^r_{cl} of the actual rotor, mounted in rigid radial supports which are located at the axial midpoint of the rotor journals.

Step 2: Calculate the diameter of the equivalent uniform shaft in rigid bearings which has the same bending critical speed N^r_{cl} as the actual rotor in rigid bearings, given the same material properties E and w, and the same bearing span L. To do this let:

$$N^r_{cl}\ \text{Actual} = N^r_{cl}\ \text{Equivalent} = 9.55\,\frac{\pi^2}{L^2}\,\sqrt{\frac{EIg}{wA}}$$

$$= 9.55\,\frac{\pi^2}{L^2}\cdot\frac{D_e}{4}\cdot\sqrt{\frac{Eg}{w}}\quad \text{rpm}$$

or

$$D_e = \frac{N^r_{cl}}{2.39}\cdot\frac{L^2}{\pi^2}\cdot\sqrt{\frac{w}{Eg}}\quad \text{ins}$$

D_e is the diameter of the equivalent rotor in rigid bearings which has the same first bending N_1^r critical speed as the equivalent rotor in rigid bearings.

Step 3: Determine the operating eccentricity ε_e of the bearings of diameter D_e for the equivalent uniform rotor system. The theory for this step is given in the following section.

The above steps define an equivalent rotor-bearing system for which the unbalance amplitude response properties may be determined from the charts given in Section 2.

4.2 Theory of Equivalent Bearing Procedure

The theory for determining the equivalent bearing eccentricity from the actual bearings is based on several assumptions:

(a) The ratio of bearing radius to radial clearance (R/C) remains the same for the uniform rotor as for the actual rotor.

(b) The actual bearings are sufficiently close in size and loading that the operating eccentricity for both bearings is approximately the same.

This allows the equivalent bearings to be based on the average operation eccentricity, or

$$\varepsilon_a = \frac{\varepsilon_L + \varepsilon_R}{2} \qquad \begin{matrix} L = \text{left} \\ R = \text{right} \end{matrix} \qquad (1)$$

For dynamically similar bearings, the assumption is made that

$$\frac{R^U}{C^U} = \frac{R_a^S}{C_a^S} \qquad \begin{matrix} U = \text{uniform} \\ S = \text{stepped} \end{matrix} \qquad (2)$$

where R is the bearing radius, C is the bearing clearance, U refers to the uniform rotor, and 'a' is the average value for the stepped rotor. Then

$$C^U = \left(\frac{D_e}{2}\right) \frac{C_a^S}{R_a^S} \quad , \qquad \text{as} \quad R^U = \frac{D_e}{2} \tag{3}$$

The maximum static deflection due to gravity of a uniform-section beam in rigid supports is:

$$\delta^U = \frac{5}{384} \frac{wAL^4}{EI} = \frac{5}{384} \frac{w}{E} \frac{16L^4}{D_e^2}$$

Thus $(C/\delta)^U$ may now be easily calculated.

Now, let ε_a be the average bearing eccentricity of the stepped rotor, i.e.

$$\varepsilon_a = \frac{\varepsilon_L + \varepsilon_R}{2}$$

then since the average Sommerfeld number of the stepped rotor $S_A = f(1/\varepsilon_A)$, it follows that

$$\frac{\varepsilon_A}{\varepsilon_U} = \frac{S_U}{S_a} = \frac{\left\{\frac{\mu NDL}{W}\left(\frac{R}{C}\right)^2\right\}_U}{\left\{\frac{\mu NDL}{W}\left(\frac{R}{C}\right)^2\right\}_A}$$

If we again preserve R/C, and also L/D, μ, and N (where μ is the viscosity, and N the speed in rev/sec) then

$$\frac{\varepsilon_a}{\varepsilon_U} = \frac{D_e^2}{D_a^2} \frac{W_a}{W_U} \qquad \varepsilon_U = \left(\frac{W_U}{W_A}\right)\left(\frac{D_a}{D_e}\right)^2 \varepsilon_a$$

where W_U is the weight of the equivalent uniform rotor, W_a, is the weight of the stepped rotor, D_a is the average diameter of the stepped rotor, and D_e is the diameter of the equivalent uniform rotor.

Knowing $(C/\delta)_U$ and ε_U, the unbalance response of the stepped rotor can be determined by referring to the appropriate uniform rotor curve in this report, or it can be calculated using ROTOR2, or another unbalance response program.

4.3 Sample Calculation of Equivalent Rotor-Bearing System

Consider a non-uniform steel rotor of the type shown in table 2, case 1, which has a bearing span of L = 100 in. and weight W = 6224.2 lb. The lowest rigid-support critical speed for this system is N_1^r = 6400 rpm. Calculate the diameter of the equivalent uniform shaft having similar dynamic properties and the eccentricity of the equivalent plain cylindrical bearing with L/D ratio = 1.0.

Step 1: Equivalent diameter D_e

Given N_1^r = 6400 rpm

and $$D_e = \frac{N_1^r}{2.39}\left(\frac{L}{\pi}\right)^2\sqrt{\frac{W}{Eg}}$$

$$= \frac{6400}{2.39}\left(\frac{100}{\pi}\right)^2\sqrt{\frac{0.283}{(30.10^6)(386.4)}}$$

$$D_e = 13.13 \text{ ins.}$$

Step 2: Equivalent bearing eccentricity

$$I_e = \frac{\pi}{64} D_e^4 = \frac{\pi}{64}(13.13)^4 = 1569.9 \text{ in}^4$$

TABLE 2. System Details for Equivalent Rotor Studies

Case		Midspan whirl amplitude ratio
1.	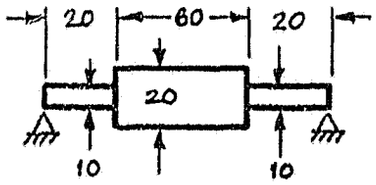	$\frac{A_e}{A_U} = 2.3$
2.	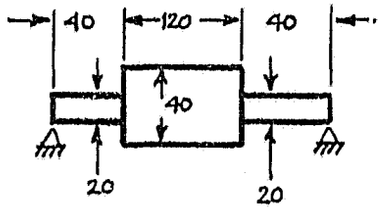	$\frac{A_e}{A_U} = 2.5$
3.		$\frac{A_e}{A_U} = 1.7$
4.	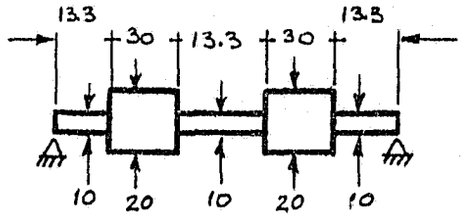	$\frac{A_e}{A_U} = 1.7$

TABLE 2. System Details for Equivalent Rotor Studies (Con't)

Case		Midspan whirl amplitude ratio
5.	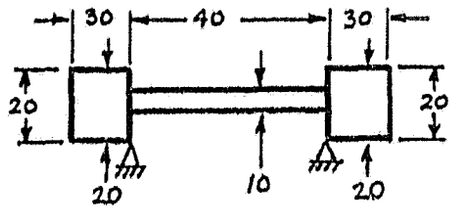	$\frac{A_e}{A_U} = 11.5$
6.	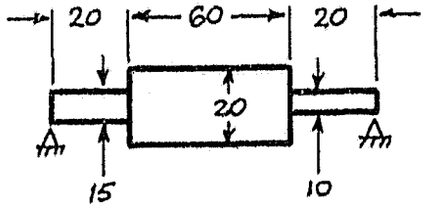	$\frac{A_e}{A_U} = 1.67$
7.	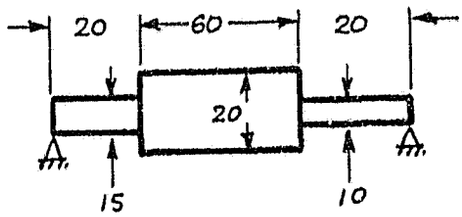	$\frac{A_e}{A_U} = 1.63$
8.	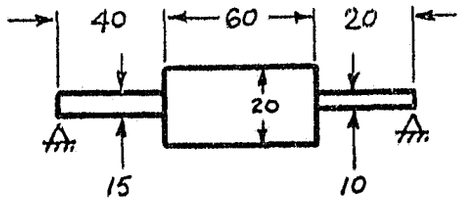	$\frac{A_e}{A_U} = 1.71$
9.	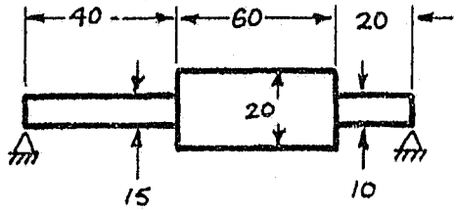	$\frac{A_e}{A_U} = 2.01$

$$A_e = \frac{\pi}{4} D_e^2 = \frac{\pi}{4} (13.13)^2 \quad 141.66 \text{ in}^2$$

Rotor mid-span deflection $\delta_e = \frac{5}{384} \cdot \frac{wAL^4}{EI}$

$$= \frac{5}{384} \cdot \frac{(0.283)(141.66)(10^8)}{(30.10^6)(1569.9)}$$

$$= 1.0896 \times 10^{-3} \text{ ins.}$$

Effective bearing machined clearance:

$$C_e = \frac{R_e}{R_a} \cdot C_a = (\frac{6.57}{7.5})10 \times 10^{-3} = 8.953 \times 10^{-3} \text{ ins.}$$

Stiffness ratio:

$$\frac{C_e}{\delta_e} = \frac{8.953 \times 10^{-3}}{1.0896 \times 10^{-3}} = 8.217$$

If the rotor in case 1 operates with eccentricity $\varepsilon_a = 0.2$, and the uniform rotor weight W_e is

$$W_e = wAL = 0.283(141.6t)(100) = 4008.98 \text{ lb.}$$

the equivalent bearing operating eccentricity is:

$$\varepsilon_e = \left(\frac{W_e}{W_a}\right)\left(\frac{D_a}{D_e}\right)^2 \varepsilon_a = \left(\frac{4008.98}{6224.2}\right)\left(\frac{15.0}{13.13}\right)^2(0.2) = 0.16$$

The parameters required for determining the unbalance response of the equivalent rotor-bearing system are therefore:

Stiffness ratio: $\left(\frac{C}{\delta}\right)_e = 8.217$

Eccentricity ratio: $\varepsilon_e = 0.16$

for plain cylindrical bearings or L/D = 1.0 mounted in rigid supports. These values may now be used to determine the response of the given rotor system using the equivalent uniform rotor system response charts.

The following section describes a range of tests which were applied to the above theory, to determine whether the equivalent rotor procedure could be used to predict the unbalance response of non-uniform rotors, using the uniform rotor response charts given in Section 3. The general result of the following study is that for the range of two-end-bearing rotors shown in table 2, the equivalent rotor theory predict resonant response amplitudes which are approximately 1.6 to 2.5 times as great as the true rotor response. Accepting this excess amplitude as a safety factor will therefore allow the equivalent rotor theory to be used as a basis for selecting rotor balancing criteria. This concept is further tested in Section 6 on several specific rotors.

5. STEPPED ROTOR CALCULATIONS

5.1 Rotor System Details

The non-uniform rotor configurations shown in table 2 were selected to study the effectiveness of the proposed equivalent rotor method for unbalance response calculation. Dimensions of each rotor are given in table 2. Fluid-film bearings with L/D = 1.0 were used in each case. An unbalance response calculation was made with each rotor in each of the four bearing types mentioned: Plain cylindrical bearings, partial bearings, tilting-pad bearings, and axial-groove bearings. The results obtained are shown in figures 31 through 45.

In each case, the rotor was assumed to be a continuous flexible steel structure, without any deformable joints or hinges. Each rotor was supported in two bearings located near its ends, as shown in table 2. Effects arising from shaft overhangs were examined in several cases. Each rotor model was composed of two or three basic shaft sections, each of which had differing diameters and lengths. Where the bearings have different sizes, they have different eccentricity ratios, denoted by ε_L and ε_R, respectively.

Three calculations were made for each rotor as follows:

(a) Response of stepped rotor to unbalance when operating in rigid bearings,
(b) Response of stepped rotor in damped, flexible bearings,
(c) Response of equivalent rotor in equivalent damped, flexible bearings.

Table 2 gives results for the ratio of the mid-span amplitude of the equivalent rotor to the mid-span amplitude of the stepped rotor, A_e/A_s, both in flexible bearings. It is shown that the equivalent rotor whirl amplitude exceeds the stepped rotor amplitude for all end-bearing rotors by a

factor of between 1.63 and 2.5. The overhung rotors in cases 5 and 7 appear to be strongly influenced by whether a mid-span mass exists, and by the overhangs themselves. Further discussion of these results is given in section 5.4.

5.2 Comparison of Whirl Amplitude Ratios

Case 1 is a typical non-uniform rotor system with identical plain cylindrical end bearings, L/D = 1.0, operating with eccentricity ratios $\varepsilon_R = \varepsilon_L = 0.2$. The response of this rotor in plain cylindrical bearings is shown in figure 32. To obtain the natural frequency of such rotors in rigid bearings, the following bearing coefficients were used:

$$K_{xx} = K_{yy} = 100 \times 10^6 \text{ lb/in}$$

$$K_{xy} = K_{yx} = 0.0 \text{ lb/in}$$

$$B_{xx} = B_{yy} = 0.0 \text{ lb sec/in}$$

$$B_{xy} = B_{yx} = 0.0 \text{ lb sec/in}$$

The response of the equivalent rotor for this system is shown in figure 33. It may be observed that the maximum first-mode stepped shaft response amplitude at mid-span is 2.2×10^{-3} in and that the mid-span whirl amplitude of the equivalent shaft is 5.0×10^{-3} in. The ratio of these numbers is:

$$\frac{A_e}{A_s} = \frac{5.0 \times 10^{-3}}{2.2 \times 10^{-3}} = 2.3, \text{ as indicated previously}$$

Case 2 is the same as case 1, but with all dimensions multiplied by 2.0: See table 2. The operating eccentricity of both bearings is $\varepsilon = 0.2$. The rigid bearing response is shown in figure 34, the flexible stepped rotor response is shown in figure 35, and the equivalent rotor response in equivalent bearings is shown in figure 36. The ratio of the maximum first

mode mid-span whirl amplitude of the equivalent rotor to that of the stepped shaft is $A_e/A_s = 20.10^{-3}/8.10^{-3} = 2.5$ in this case.

Case 3 is the same as case 1, but with all dimensions multiplied by 3.0. Operating eccentricity ratio is again $\varepsilon = 0.2$. Results are shown in figures 37, 38 and 39. The amplitude ratio for this case is $A_e/A_s = 1.7$.

Case 4 shows the influence of two steps on the shaft, with two moderately-long cylindrical shaft sections supported in end bearings. The bearing eccentricity ratio is again $\varepsilon = 0.2$. Results for the rigid bearing case, stepped rotor case, and equivalent rotor case, are shown in figures 40, 41 and 42, respectively. The amplitude ratio is $A_e/A_s = 1.7$.

Case 5 is a double overhung rotor with a flexible shaft between bearings. The bearing operating eccentricity is $\varepsilon = 0.2$. Results are shown in figures 43, 44 and 45. The amplitude ratio for this case is $A_e/A_s = 11.5$. This result is high because modeling as an end-bearing rotor is unsuited to this case.

Case 6 considers the influence of unsymmetrical shaft sections, and also the influence on rotor response of bearings which operate at different eccentricity ratios. Results are not shown for this and remaining cases in the interest of brevity. The amplitude ratio, in this case, was $A_e/A_s = 1.7$.

Case 7 has the same rotor as case 6 and the operating eccentricity of the left bearing is increased to $\varepsilon = 0.4$. The amplitude ratio was $A_e/A_s = 1.63$.

Case 8 is a modification of the case 6 rotor, with a longer left section in the same bearings as case 6. The amplitude ratio is $A_e/A_s = 1.7$.

Case 9 is the case 8 rotor for which the operating eccentricity of the left bearing has been changed to $\varepsilon = 0.4$, with the longer left section of the case 8 rotor. The amplitude ratio is $A_e/A_s = 2.0$.

Case 10 is a three mass rotor with an overhang at each end. The connecting shaft section is slender. The rotor operates at eccentricity $\varepsilon = 0.2$

for both bearings. The lowest rotor whirl mode is a free-free mode. As with case 5, response results for the actual rotor and for the equivalent rotor are not similar in form. The amplitude ratio A_e/A_s = 0.27, primarily due to the lack of damping in the bearings. This result is not regarded as relevant because the end bearing equivalent rotor is too strongly affected by bearing stiffness to assume a free-free bending mode.

5.3 Results

The main result from these studies was that the equivalent rotor procedure appeared to give results for maximum mid-span amplitude ratio A_e/A_s which lay between 1.63 and 2.50. Thus the equivalent rotor predicted mid-span amplitudes which always exceeded those of the stepped rotor by between 63 percent and 150 percent. The equivalent rotor maximum amplitudes may therefore be taken as conservative estimates of maximum whirl amplitude.

Two studies of overhung rotors were made, cases 5 and 10. In both instances the results observed were thought to be unproductive because the overhung model did not match the end bearing model. Earlier it was assumed that with flexible bearings the free-free mode would dominate the response, and the useful comparison would result. It is shown in section 6 that most rotors appear to function as overhung rotors, due largely to their overhung coupling sections. Care is therefore necessary in interpreting the results any rotor in terms of an equivalent end bearing rotor.

An attempt was made to correlate higher modes and to develop amplitude ratios for these modes. The results were not considered sufficiently successful to report here and the results are not included. Basically, the modeling procedure appears to suffer wherever the system model departs from mid-span symmetry. For symmetrical systems only odd-order modes were excited, whereas for unsymmetrical systems the even and odd modes were excited. This made comparison difficult.

6. BALANCING STUDY OF SIX ROTORS.

6.1 Procedure

Six practical rotor systems for which geometry, operating data and unbalance response data is available were examined to provide information on the following questions:

a) How readily can the response results computed in the present study be used to predict practical rotor whirl amplitudes?
b) How suitable are the flexible rotor balance criteria in DP 5343 when applied to specific practical rotor cases?
c) How suitable are the criteria parameters presently in use for rotor balancing, i.e. journal velocity, pedestal velocity?

Where possible, the practical rotor cases chosen had both test data and calculated results data available. Rotor system details are given in table 3. Results are compared with existing balance criteria in table 4. Additional details used in the calculations reported in these tables were obtained from references cited herein unless otherwise stated.

6.2 Case 1. Lund-Orcutt Rotor. Figure 46.

Lund and Orcutt [5] have described the calculation and testing of a multi-disk rotor in tilting-pad bearings. The correlation shown between their test data and their calculated rotor response vs speed data is close. The results of the Lund-Orcutt study were subsequently confirmed by Thomas [6]. The Lund-Orcutt rotor had a single central disk weighing 36.0 lb mounted on a uniform shaft weighing 88 lb. The rotor system critical speed is given as 12,800 rpm. System dimensions and operating details are quoted from ref. [5]. The stiffness parameter C/δ is found as follows:

1. Bearing clearance, C

For preload, $m = 0.5$ $C = 3.75 \cdot 10^{-3}$
Operating eccentricity at 12,800 rpm: $\varepsilon = 0.2$

TABLE 3. DETAILS OF SIX PRACTICAL ROTORS FROM LITERATURE

Case	Rotor	Bearing	Stiffness Ratio c/δ	Critical Speed ($\times 10^{-3}$ rpm)	Weight (lb.)	Unbalance (oz.in.)	c.g. Eccentricities (10^{-6}) in.	Critical Whirl Radius in. ($\times 10^{-3}$)	$\frac{r}{a}$	Equivalent Rotor r/a	Bearing Whir Radius Rati r/a	
											Test	Cal
1	Lund-Orcutt	Tilting Pad	9.47	12.8	124.0	1.0	500.	2.2 brg.	4.365	1.6	1.164	0.42
								2.6 cent.	5.158	1.4	1.375	0.37
2	Rieger-Badgley	Tilting Pad (Gas Bearing)	150	72.2	30.0	0.24	500.	45.0 brg	.90(47.2)	25.0	(10.5) 20.0	5.56
				86.5	30.0	0.24	500.	12.5 cent.	.25(6.55)	25.0	(1.46) 5.56	5.56
3	Lund-Tonneson	Ext.Pres. Plain Cylindrical Gas Brgs.	2.26	7.85	36.7	0.095	161.7	0.36 brg.	2.24	1.30	0.23	.13
								1.0 cent.	6.18	13.0	0.64	1.34
4	Gas Turbine	Tilting Pad	2.03	7.5	32	0.26	500.	0.2 brg.	0.4	1.4	.125	0.44
								0.5 cent.	1.0	3.9	.313	1.22
5	Kendig Gas Turbine	Tilting Pad Gas Bearing	10.5	10.0	50	3.0	3750	70.0 comp.	18.7	1.4	93	.7
								90.0 brg.	24.0	5.3	120	26.5
								25.0 turb.	6.67	1.4	33	.7
				24.95				45.0 brg.	12.0	5.3	60	26.5
6	Kendig Steam Turbine	Tilting Pad	14.5	2.3	5000	12.5 oz.in.	156	0.6 brg.	3.85	1.4	.13	.05
				12.0				26 brg.	167	10.0	5.78	.20

Table 4. Interpretation of rotor whirl using ISO balance and vibration criteria.

Case	ISO Rotor Category	Rigid Rotor Quality Grade	ISO Permissible Journal Velocity in/sec RMS	Corresponding Journal Amplitude ins. ($x10^3$) rms	Implied c.g. Eccentricity ins. ($x10^6$)	Permissible Bearing Whirl Radius Ratio $\frac{n}{c}$	Comments
1	II	G 6.3	0.283 Brg	0.21	48	0.11	
			0.567 Center	0.42	81	0.22	
2	IV	G 6.3	0.331 Brg	0.044	1.7	0.03	
			1.102 Center	0.146	5.8	0.09	
3	II	—	0.47 Brg	0.58	366.2	0.52	
			0.89 Center	1.08	247.1	0.97	
4	IV	G 2.5	0.33 Brg	0.42	1485	0.37	
			1.10 Center	1.40	2008	1.24	
5	IV	G 2.5	0.331 Brg	1.37	103.6 15.3	2.58 0.49	
			1.102 Center	0.26	957. 106.	86.7 1.7	
6	III	G 2.5	0.551 Brg	4.60	841.	0.72	
				0.90	162.	0.14	

2. Mid-span Deflection, δ

For a rigid-bearing uniform rotor $\delta = \frac{5}{384} \cdot \frac{wL^4}{EI}$

For N_c = 12,800 rpm, $\delta = 3.96 \cdot 10^{-4}$

3. Stiffness Ratio C/δ

$C/\delta = 9.47$

4. C. G. Eccentricity $a = 500 \times 10^{-6}$ in (given)

Figure 22 applies for a uniform rotor in tilting-pad bearings operating at journal eccentricity $\varepsilon = 0.2$. The stiffness curve $C/\delta = 10$ may thus be used for comparison with the Lund-Orcutt results for this case. This indicates a whirl radius $r = 2.2 \times 10^{-3}$ in at the bearings and $r = 2.6 \times 10^{-3}$ in at mid-span. Values of r/a are given below.

5. Whirl radius ratio (test)

Bearing $r/a = 2.2 \times 10^{-3}/0.5 \times 10^{-3} = 4.365$

Mid-span $r/a = 2.6 \times 10^{-3}/0.5 \times 10^{-3} = 5.158$

6. Whirl radius ratio (calculated)

Bearing. Figure 22.	$r/a = 1.6$
Mid-span. Figure 25.	$r/a = 1.4$

Calculated values of whirl radius ratio appear somewhat low for the rotor configuration involved. This may be due to the stiffness ratio $C/\delta = 9.74$ which corresponds to a stiff flexible rotor in damped flexible bearings. The response charts [5] for this case suggest a more flexible rotor in stiff low-damping bearings. Test values of C/δ appear to be correct. Similarity of response for the equivalent rotor and for the test rotor may be observed by

comparing figures 25 and 47.

A comparison of balancing criteria for the Lund-Orcutt rotor are shown in table 4. The Lund-Orcutt single disk rotor is a class 3, category II rotor. Rotor category data is given in table 5, from ISO DR 5343, Ref. [11]. These criteria values indicate the following conditions for the Lund-Orcutt rotor:

1. Rotor Quality Grade: Small turbine rotor G 6.3

2. Permissible Vibration Velocity (table 5)

   Journal: V = 0.283 in/sec r.m.s.
   Mid-span: V = 0.567 in/sec r.m.s.

3. Corresponding Whirl Amplitude at 12,800 rpm

   Journal: $r = 0.21 \times 10^{-3}$ in r.m.s.
   Mid-span: $r = 0.42 \times 10^{-3}$ in r.m.s.

4. Corresponding C. G. Eccentricity (implied by whirl radius)

   Journal: $a = r \cdot \frac{a}{r} = 0.21$ $= 48 \times 10^{-6}$ in
   Mid-span: $a = 0.42 \times$ $= 81 \times 10^{-6}$ in

5. Permissible Whirl Radius/Clearance Ratio

   Journal: $r/c = 0.21 \times 10^{-3} / \times 10^{-3} = 0.11$
   Mid-span: $r/c = 0.42 \times 10^{-3} / \times 10^{-3} = 0.22$

The required residual C.G. runout implied by the above results is consistent with practical balance quality for this type of rotor. The importance of relating balance criteria to measurement location on the shaft is clearly demonstrated by the differing values of whirl radius at the journal

and at mid-span. It is also apparent that observed whirl values depend on the rotor mode shape. Coupling mass causes a rotor to whirl more in a free-free mode, whereas mid-span mass tends to cause half-sine modes.

The implied (whirl radius/clearance) ratio values derived from the DR 5343 criteria would be consistent with stringent balance criteria, considering that they apply to resonant conditions with a sharp peak, figure 47. The observed values of r/c in table 5 appear to be more reasonable for this condition.

6.3 Case 2. Rieger-Badgley Rotor. Figure 48. Reference [15].

This rotor has a non-uniform distribution of mass and stiffness and operates in two tilting-pad gas bearings close to its ends. Two critical speeds exist within the range tested at 72,200 rpm and at 86,500 rpm. The same free-free rotor mode is involved in each instance, and the difference is due to bearing properties in the horizontal and vertical directions.

The stiffness ratio is high because of the high critical speed. This value corresponds to a stiff rotor in flexible bearings. This rotor whirls in a free-free mode, and this is confirmed by the critical speed ratio (ω/ω_n) of 2.25 in figure 22 for a corresponding C/δ value of 150. The rotor has an unbalance of 500 microinches at each disk, oriented in a planar manner which tends to induce the observed free-free whirl mode. Critical whirl radii of 45.0×10^{-3} in (bearing) and 12.5×10^{-3} in (mid-span) correspond to whirl ratios (r/a) of 90.0 and 25.0 respectively. The calculated (r/a) ratios obtained from figures 49 and 50 are 25.0 and 25.0. These values also include the effect of higher damping (and stiffness) present in the oil film bearings for which the charts were developed. Adjusted values of (r/a) which allow for the influence of bearing film compressibility are 47.3 and 6.55, respectively. Whirl radius/clearance ratio values corresponding to these results are high: (10.5, 1.46) for rotor results and (5.56, 5.56) from chart results, at resonance. These high values are due to the high unbalance (500 microinches) the prescribed distributions of which couples strongly with the free-free mode, as indicated above.

The balance criteria conditions indicate that this is a class 3, category IV rotor for which the permissible r.m.s. velocity levels are 0.331 in/sec (bearing) and 1.102 in/sec (center). The implied residual c.g. eccentricity to achieve these levels based on the corresponding r/a values given in table 5 are 1.7 microinches and 5.8 microinches. With these c.g. eccentricity values the whirl radius/clearance values are 0.03 (bearing) and 0.09 (mid-span).

It is apparent that the DIS 5343 balance criteria appear to be excessive in this instance. If resonant r/c values of 0.5 (bearing) was permitted, the c.g. eccentricity would be 24 microinches. This is still stringent, but attainable.

6.4 Case 3. Lund-Tonneson Rotor. Figure 50. Reference [16].

This rotor system consists of several disks on a flexible shaft, mounted in externally-pressurized gas bearings near its ends. The performance of this system has been described by Lund and Tonneson [16].

The first critical speed occurs at 7850 rpm. The mode shape is not shown in ref. [16], but may be expected to be a free-free mode similar to that of the Rieger-Badgley rotor. The corresponding system ratio is 2.26, which indicates that the rotor is flexible and operates in rigid bearings.

The stated residual unbalance is 0.095 oz. in, or a c.g. eccentricity of 161.7 microinches for the rotor weight of 36.7 lb. At the critical speed the whirl radius is 0.36×10^{-3} in at the bearing, and 1.0×10^{-3} in at mid-span. These figures correspond to whirl ratios (r/a) of 2.24 at the bearing and 6.18 at mid-span. For comparison, plain cylindrical bearings operating at eccentricity $\varepsilon = 0.2$ with an equivalent rotor $C/\delta = 3.0$ the whirl ratio is 1.30 at the bearing and 13.0 at mid-span.

The test rotor resonant r/c values are 0.23 (bearing) and 0.64 (mid-span). The equivalent rotor values are 0.13 (bearing) and 1.34 (mid-span). Both conditions appear to correspond to a medium-unbalanced condition which the 161.7 microinch eccentricity would suggest.

The balance criteria in table 5 indicate that this is an ISO class 3 category II rotor for which the permissible r.m.s. velocities would be 0.47 (bearing) and 0.89 (mid-span). The corresponding r.m.s. whirl amplitudes at 7850 rpm would be 0.58×10^{-3} in (bearing) and 1.08×10^{-3} in (mid-span). Using the whirl ratio, these amplitudes imply C.G. eccentricities of 366.2 microinches (bearing) and 247.1 microinches (mid-span), respectively. The corresponding whirl radius/clearance values are 0.52 (bearing) and 0.97 (mid-span).

The results show that the ISO DR 5343 criteria values are fully met with the rotor balance stated in table 5. For gas bearing rotors stringent balance control is necessary, which may account for the low residual unbalance observed.

6.5 Case 4. Gas Turbine Rotor. Figure 52.

This rotor weighs 32.0 pounds and is mounted in fluid-film tilting pad bearings. The first bending critical speed occurs at 7500 rpm though the operating speed range extends through 52000 rpm, and includes several higher critical speeds. The mode shape is again a free-free mode.

The c.g. eccentricity of 500 micro inches causes a critical whirl radius 0.2×10^{-3} in at the bearing and 0.5×10^{-3} in. at midspan. These values correspond to whirl ratios r/a of 0.4 (bearing) and 1.0 (bearing). The corresponding clearance ratios r/c are 0.125 (bearings) and 0.313 (midspan).

The stiffness ratio for this rotor system, based on the bending critical speed of 7500 rpm, is 2.03. This indicates a flexible rotor in stiff bearings. From figures 22 and 25 for tilting-pad bearings the response of the equivalent rotor at resonance is r/a = 1.4 (bearings) and 3.9 (midspan). The corresponding clearance ratios r/c are 0.44 (bearings) and 1.22 (midspan).

The balance criteria in table 5 indicate that this is a Class 3, Category IV rotor for which the permissible rms velocities are 0.33 in/sec (bearing)

and 1.10 in/sec (midspan). The corresponding rms critical speed amplitudes are 0.42×10^{-3} in (bearing) and 1.4×10^{-3} in (midspan). The implied c.g. eccentricity which would cause these whirl amplitudes are 1485 micro inches (bearing) and 2008 (midspan).

From this is appears that the existing balance condition of 500 micro-inches is adequate, both from existing criteria and from the clearance whirl ratio values.

6.6 Case 5. Kendig Gas Turbine Rotor. Figure 53. Reference [17].

This is a small gas turbine rotor weighing 50 pounds and operating in tilting-pad gas bearings. The service speed is 66,000 rpm. There is a damped rigid body composite critical speed at 10,000 rpm and a bending critical speed at 24,950 rpm. Modes for both these critical speeds are shown in figure 54. The stiffness ratio $c/\delta = 10.5$ is based on the bending critical speed and indicates a flexible rotor in flexible bearings at this speed equivalent rotor response chart for this stiffness ratio shows a damped critical speed peak at approximately 40 percent of the free-free critical speed. This result supports the equivalent rotor model for this case.

Calculations were made to determine the response of this rotor system to a residual inbalance of 0.3 oz. in or 375 microinches c.g. eccentricity. Whirl radius of 7.0×10^{-3} in (compressor bearing) and 9.0×10^{-3} in (turbine bearing) were indicated at the bending critical speed, and lower whirl amplitudes at the rigid body critical speed. These values correspond to whirl radius ratio values of 24.0 and 12.0 respectively. The equivalent rotor whirl ratio values are 5.3 (compressor) and 5.3 (turbine). The corresponding critical speed clearance ratios r/c are 12.0 and 6.0 for the calculated rotor and 26.5 and 26.5 for the equivalent rotor.

The criteria table shows this rotor to be a Class 3 Category IV rotor for which the permissible rms velocities are 0.331 in/sec (journal) and

1.102 in/sec (midspan). Permissible critical whirl amplitudes are 0.26×10^{-3} in/sec and 0.90×10^{-3} in/sec. These amplitudes imply c.g. eccentricities of 15.3 microinches and 106 microinches. The corresponding clearance ratios are 0.49 and 1.7.

Practical considerations require clearance ratios of 0.5 at the bearings. This corresponds to a c.g. eccentricity of 15 microinches. This fine balance is consistent with operation through a bending critical speed with gas-bearing turbomachinery.

6.7 Case 6. Kendig Steam Turbine Rotor. Figure 55. Reference [17].

This rotor system consists of a 5000 lb. medium power steam turbine rotor in end bearings. Critical speeds exist at 2300 rpm (rigid body) and at 12,000 rpm (free-free bending). The stiffness ratio $c/\delta = 14.5$ is based on the bending critical speed. Reference to figure 22 for an equivalent rotor in tilting pad bearings shows a rigid body critical speed around $\omega/\omega_n = 0.5$ and a free-free mode at 2.25.

7. COMMENTS ON FLEXIBLE ROTOR BALANCING CRITERIA

Details of the specific rotors studies are given in Table 3. Details of the comparison with ISO Draft flexible rotor balance criteria are given in Table 4. The criteria numbers are obtained from the ISO documents indicated. All rotors are flexible (Class 3) rotors. The ISO rotor category refers to the type of machine in which each rotor is used, as indicated in Table 4 of ISO DR 5343.

The balance criteria values given in ISO DR 5343 are based on VDI criteria, which are compatible with criteria for vibration in rotating machinery given in ISO DR 2372. The permissible journal rms velocity values in Table 4 apply to each rotor. Values are given for the journal, and at midspan using the correction factors in Table 4 of ISO 5343. Permissible amplitude values were obtained by using $v = \omega r$ where v is the rms velocity, ω the rotor speed in rad/sec and r is the permissible rms amplitude. Using the uniform rotor response charts allowed the implied c.g. eccentricity to be deduced corresponding permissible values of (whirl radius/bearing clearance) were then obtained for each bearing.

Table 4 shows that using the ISO criteria with the response charts gives permissible resonant whirl radius ratios (r/c) between 0.03 and 0.72 at the journals of these six rotors. The exception to this is case 5. The small gas turbine rotor, which shows excessive values at both its critical speeds. This discrepancy is due to excessive rotor unbalance. Good balancing could reduce the c.g. eccentricity to 25×10^{-6} in, which would in turn reduce the r/c values to 0.6 and 2.0 respectively. The latter value is still large, possibly due to inaccuracy in defining the peak accurately in the calculations.

Table 3 shows results for critical whirl radius r at the journals and at midspan obtained from the results of several authors, under critical speed conditions. These values range from 0.2 in to 70.0, depending on the amount of residual unbalance present. Normalizing these results with c.g. eccentricity, a, gives (r/a) values between 0.4 and 24.0 (journal) and 1.0 and 167 (midspan). Comparable results obtained from the equivalent rotor calculations show values between 1.3 to 25.0 (journal) and 1.4 to 25.0 (midspan). In general, the rotor r/a values may be up to four times larger at the bearings than the values of r/a determined by the equivalent rotor method. As these are resonant r/a results, it is possible (perhaps likely) that peak r/a values in practice would be smaller than indicated in the actual rotor results, due to non-linear effects in the bearings. At midspan, the correlation is again similar with the actual r/a values

exceeding the equivalent rotor r/a values by about 4:1.

During the analysis of results it was noted that most actual rotors behaved more like free-free beams in their bending modes than like pinned-pinned beams. This is apparent when it is observed that most rotors have overhung end drive sections carrying couplings. It is felt that if the equivalent rotor method were based on results from overhung rotors, closer correlation could have been obtained in all results. The extension of the equivalent rotor method to include a free-free beam analysis is recommended for further study.

The accuracy of results obtained in this study was also affected by the impreciseness of the resonant amplitude values both in the actual rotors and in the equivalent rotor calculations. As the final results are strongly dependant on both peak values it is evident that discrepancies and some randomness will occur in the correlation of results. As a present guideline, if the equivalent rotor method described herein is used, and the results for r/a are multiplied by a factor of 4, this appears to allow sufficiently consistent resonant r/a values to be defined for use in practice. When these values are then utilized with the r/c values at the bearings, a decision on the quality of balance required can be made.

The final conclusion is that the proposal equivalent rotor method appears to offer good promise as a simple procedure for deciding the quality of balance required in a given rotor, but that the procedure should more likely be based on the lowest free-free mode of a uniform flexible rotor in bearings rather than on end-bearing rotor modes, as was done herein. When this is done the method could represent a consistent basis for balance quality selection.

8. CONCLUSIONS

1. The equivalent rotor method represents a practical procedure for selection of flexible rotor balance criteria, based on the uniform rotor/specified bearing charts presented in this report.

2. General unbalance response charts for uniform rotors in specified fluid-film end bearings have been developed. Data is available for rotor response at mid-span and at journals for each bearing type. These charts are suitable for specifying balance criteria for flexible end-bearing rotors.

3. Use of these general response charts should extend to end-bearing rotors only. Application of the charts to rotors with end overhangs may give results which are in error.

4. The charts apply best to end-bearing rotors with mid-span symmetry. Where system symmetry decreases for any reason, the correlation between actual response amplitude and equivalent rotor response amplitude also decreases.

5. Difficulty arises in specifying general balance criteria for flexible rotors which operate through more than one critical speed because one mode may not be excited as strongly as another mode by the rotor residual unbalance distribution.

9. RECOMMENDATIONS

1. Similar response charts should be developed for a uniform rotor with overhangs. This would provide general response data for the two main classes of flexible rotor systems.

2. Practical data should be obtained from flexible rotors operating in the field unbalance to demonstrate the suitability of specifying balance criteria based on the equivalent rotor procedure.

10. REFERENCES

1. International Standards Organization Document 1940 (1973) "Balancing of Rigid Rotors."

2. Muster D, Flores, B., "Balancing Criteria and Their Relationship to Current American Practice," Univ. of Houston, Tech. Report No. 3, (1967).

3. Lund, J.W., Sternlicht, B., "Rotor-Bearing Dynamics with Emphasis on Attenuation," Trans. ASME, Jnl. Basic Eng., Vol. 84, (1962).

4. Warner, P.C., Thoman, R.J., "Effect of the 150-Degree Partial Bearing on Rotor-Unbalance Vibration," ASME paper No. 63-LUB-36, (1963).

5. Lund, J.W., Orcutt, F.K., "Calculations and Experiments on the Unbalance Response of a Flexible Rotor," Trans. ASME, Jnl. Eng. for Ind., vol. 89, (1967).

6. Thomas, C.B., "A Unified Matrix Formulation for the Unbalance Response of a Flexible Rotor in Fluid-Film Bearings," M.S. Thesis, Rochester Institute of Technology, Rochester, NY, (1974).

7. Rieger, N.F., "Unbalance Response of an Elastic Rotor in Damped Flexible Bearings at Supercritical Speeds," Trans. ASME, Jnl. Eng. Pwr., vol. 93, (1971).

8. Feldman, S., "Unbalance Tolerances and Criteria," Proc. Balancing Seminar, Vol. IV, USN BuShips, Report No. 58GL122, (1958).

9. Federn, K., "Fundamentals of Systematic Vibration Elimination from Rotors with Elastic Shafts," VDI Berichte Bd., Berlin, (1957).

10. Rathbone, T.C., "Vibration Tolerance," Power Plant Engineering, Vol. 43, No. 11, (1939).

11. International Standards Organization. "Draft International Standard 5343 (1976)."

12. Giers, A., "Comparison of the Balancing of Flexible Rotors Following the Methods of Federn-Kellenberger and Moore," VDI-Berichte Nr, vol. 161, (1971).

13. International Standards Organization. "Draft International Standard 2905 (1978)."

14. McCallion, H., Rieger, N.F., "Moment and Shear Equations for Bar Vibration Analysis," The Structural Eng., Vol. 43, No 7, (1965).

15. Rieger, N.F., Badgley, R.H., "Flexible Rotor Balancing of a High-Speed Gas Turbine Engine," S.A.E. paper No 720741, (1972).

16. Lund, J.W., Tonneson, J., "Analysis and Experiments on Multi-Plane Balancing of a Flexible Rotor," Trans. ASME, Jnl. Eng. for Ind., vol. 94, No. 1, (1972).

17. Kendig, J.R., "Comparison of Current Flexible Rotor-Bearing System Balancing Techniques Using Computer Simulation," M.S. Thesis, Rochester Institute of Technology, Rochester, NY, (1975).

11. APPENDIX - COMPUTER PROGRAM ROTOR

11.1 Program Capabilities and Limitations

ROTOR is a general purpose computer program for the unbalance response analysis of a uniform elastic rotor supported in fluid-film bearings. The program is capable of assembling a rotor with any or all of the following basic components.

1. Beam elements- having distributed mass and elastic properties and constant E, A and I throughout the length.
2. Disks- with concentrated mass MD, polar and transverse mass moments of inertia I_p and I_t respectively.
3. Fluid-film bearings- described by eight speed dependent dynamic stiffness and damping properties K_{xx}, K_{xy},.... D_{xx}, D_{xy},....
4. Unbalance forces- represented by the real and imaginary components of a rotating force vector at each node.

The maximum number of elements are 7 thus fixing the maximum number of nodes at 8. At each speed increment the complex nodal displacements and rotations are calculated and used in formulating the major and minor ellipse radii and the ellipse angle from the positive x axis to the major axis of the ellipse and the program gives this information as output.

Limitations of the program are:

1. Only two identical bearings may be accurately represented. For multibearing use, the statically indeterminate support problem must be solved first.
2. Short stubby sections heavily loaded in shear may not be accurately represented.
3. The same weight density and Young's Modulus is used for each beam section.
4. Static deflection due to gravity is not taken into concideration thus limiting the analysis to the classical "vertical rotor" problem.
5. Steady state response is only concidered.

11.2 General Programing Information

ROTOR is written in Fortran IV and was developed using a Xerox Sigma 6 computer. Data input is from a card reader whose device unit no. is (105) and output is to a line printer whose device unit no. is (108). All computations are executed using complex double precision arithmatic. The main program plus eleven subroutines contained 475 Fortran statements. The program requires 15.8 K words of main computer core.

The functions of the main program and of the subroutines are as follows.

1. MAIN program - array declarations, reads in and writes out data input for checking, acts as an executive routine for calling subroutines, assembles the structural stiffness matrix, generates the force vector and solves for the major and minor whirl ellipse axis.
2. ELEM - sets up an 8x8 dynamic stiffness matrix for a single beam element, all terms in the matrix are real double precision.
3. EDISKL - sets up an 8x8 complex double precision matrix which reflects the effects of the addition of a disk to the left end of the element.
4. EDISKR - same as 3 except for a disk added to the right end of the element.

5. EBEARL - sets up an 8x8 complex double precision matrix which reflects the effects of a fluid-film bearing added to the left end of the element.
6. EBEARR - same as 5 except for a fluid film bearing added to the right end of the element.
7. ZEROM - initializes a real matrix to zero.
8. ZEROMC - initializes a complex matrix to zero.
9. CADDM1 - adds a real matrix to a complex matrix.
10. CADDM2 - adds two complex matrices.
11. CMULTM - multiplies two complex matrices
12. CINV - inverts a complex double precision matrix using the Gauss Elimination with partial pivoting.

11.3 Input Data Format

Data input to ROTOR is in the form of punched cards. Seven sets of data (1-7) are required, with the number of input cards per set depending on the particular problem being solved. The definition of the input parameters, the order in which they should appear and their format is as follows.

DATA SET 1 - General element information

One card (2I5,3F20.3)

NELEM - total no. of elements used (max. 7)

NODES - no. of nodes (max. 8)

EMOD - Young's Modulus lb/in^2

ERHO - weight desity lb/in^3

DATA SET 2 - Speed information

One card (3F20.3)

BSPEED - begining speed rpm.

SPEEDI - speed increment rpm.

FSPEED - final speed rpm.

DATA SET 3 - Unbalance forces

One card for each node (3F20.3)

CUBALF - cos component of unbalance oz-in.

SUBALF - sin component of unbalance oz-in.

DATA SET 4 - Control cards and specific element information

Two cards for each element, a total of 2xNELEM cards

card 1 (5I5)

IELEM - 1 if element exists

0 if element does not exist

IDISKL - 1 if left end disk is present

0 if no left end disk

IDISKR - 1 if right end disk is present

0 if no right end disk

IBEARL - 1 if left end bearing is present

0 if no left end bearing

IBEARR - 1 if right end bearing is present

0 if no right end bearing

card 2 (2I5,3F20.3)

NA - left end node of element being specified

NB - right end node of element being specified

EINER - element inertia in^4.

EAREA - element area in^2.

ELEN - element lenght in.

DATA SET 5 - Disk information

One card for each node, (3F20.3)

DW - disk weight lb.

DRAD - disk radius in.

DLEN - disk lenght in.

DATA SET 6 - Bearing locations

One card (5I5)

NBL - left end bearing node

NBR - right end bearing node

DATA SET 7 - Bearing properties

Two cards for each speed increment (4F20.3)

card 1

SXX - bearing stiffness in load direction lb/in.

SXY - cross coupled stiffness lb/in.

SYX - cross coupled stiffness lb/in.

SYY - bearing stiffness perpendicular to load direction lb/in.

card 2

DXX - bearing damping in load direction lb. sec./in.

DXY - cross coupled damping lb. sec./in.

DYX - cross coupled damping lb. sec./in.

DYY - bearing damping perpendicular to load direction lb sec/in.

11.4 Sample Input-Output Problem for ROTOR

```
RUN

 NO. ELEMENTS     NO. NODES     YOUNGS MOD      WEIGHT DENSITY      FIRST SPEED      SPEED INCREMENT      FINAL SPEED
     2              3          .30000D 08          .283              1000.0             500.0              1500.0

 ELEMENT NO.     NODE A     NODE B     ELEMENT INERTIA      ELEMENT AREA     ELEMENT LENGTH
     1             1          2          .30000D 01           .70700D 01         .2500D 02
     2             2          3          .30000D 01           .70700D 01         .2500D 02

 UNBALANCE FORCE     NODE NO.      COS COMPONENT     SIN COMPONENT
                        1              .000              .000
                        2             1.000              .000
                        3              .000              .000

 DISK INFORMATION    NODE NO.      DISK WEIGHT      DISK RAD.      DISK LENGTH
                        1             .0000            .0000          .0000
                        2             .0000            .0000          .0000
                        3             .0000            .0000          .0000

 LEFT END BEARING NODE:    1      RIGHT END BEARING NODE:    3

 ROTOR SPEED=  1000.0

 BEARING INFORMATION      KYY=  216000.0      KYX=  -83000.0      KXY=  400000.0      KXX=  283300.0
                          DYY=    2364.8      DYX=    2167.7      DXY=    2167.7      DXX=    6283.4

 UNBAL ORBIT      NODE NO.      MAJOR ELLIPSE RAD      MINOR ELLIPSE RAD.      ELLIPSE ANGLE
                     1             .58009548D-05          .28400346D-05            33.234

 UNBAL ORBIT      NODE NO.      MAJOR ELLIPSE RAD      MINOR ELLIPSE RAD.      ELLIPSE ANGLE
                     2             .45670856D-04          .41391615D-04            -39.734

 UNBAL ORBIT      NODE NO.      MAJOR ELLIPSE RAD      MINOR ELLIPSE RAD.      ELLIPSE ANGLE
                     3             .58009548D-05          .28400346D-05            33.234

 ROTOR SPEED=  1500.0

 BEARING INFORMATION      KYY=  216000.0      KYX=  -83000.0      KXY=  400000.0      KXX=  283300.0
                          DYY=    1909.9      DYX=    1445.1      DXY=    1445.1      DXX=    4189.0

 UNBAL ORBIT      NODE NO.      MAJOR ELLIPSE RAD      MINOR ELLIPSE RAD.      ELLIPSE ANGLE
                     1             .13039730D-04          .67713567D-05            33.303

 UNBAL ORBIT      NODE NO.      MAJOR ELLIPSE RAD      MINOR ELLIPSE RAD.      ELLIPSE ANGLE
                     2             .10635079D-03          .98623609D-04            -39.003

 UNBAL ORBIT      NODE NO.      MAJOR ELLIPSE RAD      MINOR ELLIPSE RAD.      ELLIPSE ANGLE
                     3             .13039730D-04          .67713567D-05            33.303
```

```
C*****************************************************
C   COMPUTER PROGRAM ROTOR.....
C   FOR THE STEADY STATE UNBALANCE RESPONSE ANALYSIS
C   OF ROTORS IN FLUID-FILM BEARINGS. UP TO (7) ROTOR
C   ELEMENTS MAY BE AXIALLY ASSEMBLED.  THE  ROTOR
C   ELEMENT MASS AND ELASTIC PROPERTIES ARE DISTRIBUTED
C   UNIFORMLY ALONG THE LENGTH OF THE ELEMENT.
C   UNBALANCE FORCES, FLUID-FILM BEARINGS AND DISKS
C   ARE ALLOWED AT EACH NODAL POINT. AT EACH SPEED THE
C   DYNAMIC STIFFNESS MATRIX IS FORMED AND INVERTED BY
C   GAUSS ELIMINATION WITH PARTIAL PIVOTING. AT EACH
C   NODAL POINT THE STEADY STATE WHIRL ORBIT IS
C   CALCULATED DUE TO SPECIFIED UNBALANCE IN THE SYSTEM.
C   THE UNBALANCE FORCES ARE REPRESENTED BY A ROTATING
C   VECTOR. THE FLUID-FILM BEARINGS ARE REPRESENTED BY
C   EIGHT SPEED DEPENDENT DYNAMIC STIFFNESS AND DAMPING
C   COEFFICIENTS. THE DISKS POSSESS MASS AND GYROSCOPIC
C   COUPLING PROPERTIES. COMPUTATIONS ARE PERFORMED IN
C   COMPLEX DOUBLE PRECISION ARITHMATIC.
C*****************************************************
C   C.B. THOMAS, N.F. RIEGER, A. ARSLANCAN
C   ROCHESTER INSTITUTE OF TECHNOLOGY JUNE, 1974
C*****************************************************
C   MAIN PROGRAM
C*****************************************************
      IMPLICIT REAL*8 (A-H,O-Z)
      REAL*8 EELK(8,8),CUBALF(8),SUBALF(8),CENTFC(8),CENTFS(8)
      REAL*8 DRAD(8),DLEN(8),DW(8),EINER(7),EAREA(7),ELEN(7)
      COMPLEX*16 EDKL(8,8),EDKR(8,8),EBKL(8,8),EBKR(8,8)
      COMPLEX*16 SDK(32,32),SDKI(32,32),FVEC(32,1),XX(32,1)
      DIMENSION IELEM(7),IDISKL(7),IDISKR(7),IBEARL(7),IBEARR(7)
      DIMENSION NA(7),NB(7)
      COMMON EMOD,EINER,EAREA,ELEN,ERHO
      COMMON EELK,EDKL,EDKR,EBKL,EBKR
      COMMON DW,DRAD,DLEN
      COMMON SXXL,SXYL,SYXL,SYYL,DXXL,DXYL,DYXL,DYYL
      COMMON SXXR,SXYR,SYXR,SYYR,DXXR,DXYR,DYXR,DYYR
C*****************************************************
C   READ IN AND WRITE OUT INPUT DATA
C*****************************************************
      READ(105,1) NELEM,NODES,EMOD,ERHO
      READ(105,2) BSPEED,SPEEDI,FSPEED
      DO 1000 I=1,NODES
 1000 READ(105,2) CUBALF(I),SUBALF(I)
      DO 1050 I=1,NELEM
      READ(105,3) IELEM(I),IDISKL(I),IDISKR(I),IBEARL(I),IBEARR(I)
 1050 READ(105,1) NA(I),NB(I),EINER(I),EAREA(I),ELEN(I)
      DO 2000 I=1,NODES
 2000 READ(105,2) DW(I),DRAD(I),DLEN(I)
      READ(105,3) NBL,NBR
      NSIZE=4*(NELEM+1)
      WRITE(108,10)
   10 FORMAT(//,1X,'NO. ELEMENTS',5X,'NO. NODES',5X,'YOUNGS MOD',
     15X,'WEIGHT DENSITY',5X,'FIRST SPEED',5X,'SPEED INCREMENT',
     25X,'FINAL SPEED')
      WRITE(108,15) NELEM,NODES,EMOD,ERHO,BSPEED,SPEEDI,FSPEED
   15 FORMAT(/,2X,I5,10X,I5,8X,D11.5,9X,F5.3,12X,F7.1,10X,
     1F7.1,12X,F7.1)
      WRITE(108,20)
   20 FORMAT(//,1X,'ELEMENT NO.',5X,'NODE A',5X,'NODE B',5X,
     1'ELEMENT INERTIA',5X,'ELEMENT AREA',5X,'ELEMENT LENGTH')
      DO 2050 I=1,NELEM
 2050 WRITE(108,25) I,NA(I),NB(I),EINER(I),EAREA(I),ELEN(I)
   25 FORMAT(/,5X,I2,12X,I2,9X,I2,9X,D10.4,9X,D10.4,9X,D10.4)
      WRITE(108,30)
   30 FORMAT(//,1X,'UNBALANCE FORCE',5X,'NODE NO.',5X,
     1'COS COMPONENT',5X,'SIN COMPONENT')
      DO 3000 I=1,NODES
 3000 WRITE(108,35) I,CUBALF(I),SUBALF(I)
   35 FORMAT(/,23X,I2,12X,F7.3,12X,F7.3)
      WRITE(108,37)
   37 FORMAT(//,1X,'DISK INFORMATION',3X,'NODE NO.',5X,
     1'DISK WEIGHT',5X,'DISK RAD.',5X,'DISK LENGTH')
      DO 3010 I=1,NODES
```

```
 3010 WRITE(108,38) I,DW(I),DRAD(I),DLEN(I)
   38 FORMAT(/,23X,I2,10X,F8.3,6X,F8.4,7X,F8.4)
      WRITE(108,40) NBL,NBR
   40 FORMAT(//,1X,'LEFT END BEARING NODE:',I5,5X,
     1'RIGHT END BEARING NODE:',I5)
C*****************************************
C  BEGINNING OF SPEED LOOP
C*****************************************
  444 ROMEGA=RSPEED*2.0D0*3.14159265D0/60.0D0
      READ(105,4) SXXL,SXYL,SYXL,SYYL
      READ(105,4) DXXL,DXYL,DYXL,DYYL
      READ(105,4) SXXR,SXYR,SYXR,SYYR
      READ(105,4) DXXR,DXYR,DYXR,DYYR
      WRITE(108,45) RSPEED
   45 FORMAT(///,1X,'ROTOR SPEED=',F8.1)
      WRITE(108,50) SXXL,SXYL,SYXL,SYYL
   50 FORMAT(//,1X,'LEFT BEARING INFORMATION',5X,'KXXL=',F10.1,5X,
     1 'KXYL=',F10.1,5X,'KYXL=',F10.1,5X,'KYYL=',F10.1)
      WRITE(108,55) DXXL,DXYL,DYXL,DYYL
   55 FORMAT(/,30X,'DXXL=',F10.1,5X,'DXYL=',F10.1,5X,'DYXL=',F10.1,
     1 5X,'DYYL=',F10.1)
      WRITE(108,51) SXXR,SXYR,SYXR,SYYR
   51 FORMAT(/,1X,'RIGHT BEARING INFORMATION',4X,'KXXR=',F10.1,5X,
     1 'KXYR=',F10.1,5X,'KYXR=',F10.1,5X,'KYYR=',F10.1)
      WRITE(108,52) DXXR,DXYR,DYXR,DYYR
   52 FORMAT(/,30X,'DXXR=',F10.1,5X,'DXYR=',F10.1,5X,'DYXR=',F10.1,
     1 5X,'DYYR=',F10.1)
C*****************************************
C  INDIVIDUAL ELEMENT SET UP FOR DYNAMIC STIFFNESS
C  MATRIX USING INPUT CONTROL
C*****************************************
      DO 3050 J=1,NELEM
      IF(IELEM(J)) 200,200,100
  100 CONTINUE
      CALL ELEM(J,ROMEGA)
      GO TO 201
  200 CONTINUE
      CALL ZEROM(EELK,8,8)
  201 IF(IDISKL(J)) 400,400,300
  300 CONTINUE
      CALL EDISKL(J,ROMEGA)
      GO TO 401
  400 CONTINUE
      CALL ZEROMC(EDKL,8,8)
  401 IF(IDISKR(J)) 600,600,500
  500 CONTINUE
      CALL EDISKR(J,ROMEGA)
      GO TO 601
  600 CONTINUE
      CALL ZEROMC(EDKR,8,8)
  601 IF(IBEARL(J)) 800,800,700
  700 CONTINUE
      CALL EBEARL(ROMEGA)
      GO TO 801
  800 CONTINUE
      CALL ZEROMC(EBKL,8,8)
  801 IF(IBEARR(J)) 900,900,850
  850 CONTINUE
      CALL EBEARR(ROMEGA)
      GO TO 901
  900 CONTINUE
      CALL ZEROMC(EBKR,8,8)
  901 CONTINUE
      CALL CADDM1(EELK,EDKL,8,8)
      CALL CADDM2(EDKL,EDKR,8,8)
      CALL CADDM2(EDKR,EBKL,8,8)
      CALL CADDM2(EBKL,EBKR,8,8)
      IF(J.GT.1) GO TO 902
C*****************************************
C  INITIALIZE THE STRUCTURAL DYNAMIC STIFFNESS MATRIX
C  TO ZERO AND FIT IN THE INDIVIDUAL ELEMENT MATRICES
C*****************************************
      CALL ZEROMC(SDK,32,32)
```

```
  902 II=4*NA(J)-3
      II=II
      JJ=II
      DO 4000 K=1,8
      DO 4050 L=1,8
      SDK(II,JJ)=SDK(II,JJ)+FBKR(K,L)
 4050 JJ=JJ+1
      JJ=II
 4000 II=II+1
 3050 CONTINUE
      CALL ZEROMC(FVEC,32,1)
C*****************************************
CC   BUILD THE PARTICULAR FORCE VECTOR ASSOCIATED
CC   WITH THE PROBLEM
C*****************************************
      DO 5000 J=1,NODES
      CENTFC(J)=CUBALF(J)*ROMEGA**2/(386.4D0*16.0D0)
      CENTFS(J)=SUBALF(J)*ROMEGA**2/(386.4D0*16.0D0)
      FVEC(4*J-3,1)=DCMPLX(CENTFS(J),-CENTFC(J))
 5000 FVEC(4*J-1,1)=DCMPLX(CENTFC(J),CENTFS(J))
C*****************************************
CC   INVERSION OF THE STRUCTURAL DYNAMIC STIFFNESS
CC   MATRIX AND SOLUTION FOR THE NODAL DISPLACEMENTS
C    AND ROTATIONS
      CALL CINV(NSIZE,SDK,SDKI)
      CALL CMULTM(SDKI,NSIZE,NSIZE,FVEC,1,XX)
C*****************************************
CC   CALCULATION OF THE MAJOR AND MINOR AXIS OF THE
CC   WHIRL ORBIT AND ANGLE ALPHA FROM THE POSITIVE
CC   X AXIS TO THE MAJOR AXIS OF THE ELLIPSE IN THE
CC   DIRECTION OF ROTATION
C*****************************************
      DO 5050 K=1,NODES
      A=DREAL(XX(4*K-3,1))
      B=DIMAG(XX(4*K-3,1))
      E=DREAL(XX(4*K-1,1))
      F=DIMAG(XX(4*K-1,1))
      A1=A**2+B**2+E**2+F**2
      A2=A1**2
      A3=-4.0*(-A*F+B*E)**2
      IF((A2+A3).LT.0.0) GO TO 880
      A4=0.5*DSQRT(A2+A3)
      GO TO 881
  880 A4=0.0
  881 AM=DSQRT(0.5*A1+A4)
      AMM=DSQRT(0.5*A1-A4)
      ALPHA=57.2957E0*ATAN(2.0E0*(A*E+B*F)/(E*E+F*F-A*A-B*B))/2.0E0
      WRITE(108,60)
   60 FORMAT(//,1X,'WHIRL ORBIT',5X,'NODE NO.',5X,'MAJOR ELLIPSE RAD',
     15X,'MINOR ELLIPSE RAD.',5X,'ELLIPSE  ANGLE')
      WRITE(108,65) K,AM,AMM,ALPHA
   65 FORMAT(/,19X,I2,10X,D15.8,9X,D15.8,9X,F8.3)
 5050 CONTINUE
      BSPEED=BSPEED+SPEEDI
      IF(BSPEED.GT.FSPEED) GO TO 9999
      GO TO 444
C*****************************************
C    END OF SPEED LOOP
C*****************************************
    1 FORMAT(2I5,3F20.3)
    2 FORMAT(3F20.3)
    3 FORMAT(5I5)
    4 FORMAT(4F20.3)
 9999 STOP
      END
```

```
C*************************************************
C   SUBROUTINE ELEM.... SETS UP THE REAL DOUBLE PRECISION
C   8X8 DYNAMIC STIFFNESS MATRIX FOR AN ELEMENT
C*************************************************
      SUBROUTINE ELEM(J,ROMEGA)
      IMPLICIT REAL*8(A-H,O-Z)
C     BAR DYNAMIC STIFFNESS MATRIX 8X8 REAL
      REAL*8 EINER(7),EAREA(7),ELEN(7)
      REAL*8 EELK(8,8),DW(8),DRAD(8),DLEN(8)
      COMPLEX*16 EDKL(8,8),EDKR(8,8),EBKL(8,8),EBKR(8,8)
      COMMON EMOD,EINER,EAREA,ELEN,ERHO
      COMMON EELK,EDKL,EDKR,EBKL,EBKR
      COMMON DW,DRAD,DLEN
      COMMON SXXL,SXYL,SYXL,SYYL,DXXL,DXYL,DYXL,DYYL
      COMMON SXXR,SXYR,SYXR,SYYR,DXXR,DXYR,DYXR,DYYR
      ELAM4=(ERHO*EAREA(J)*(ROMEGA**2))/(EMOD*EINER(J)*386.0D0)
      ELAM2=DSQRT(ELAM4)
      ELAM=DSQRT(ELAM2)
      ELL=ELAM*ELEN(J)
      SELL=DSIN(ELL)
      CELL=DCOS(ELL)
      SHELL=DSINH(ELL)
      CHELL=DCOSH(ELL)
      F1=SELL*SHELL
      F3=CELL*CHELL-1.0D0
      F5=CELL*SHELL-SELL*CHELL
      F6=CELL*SHELL+SELL*CHELL
      F7=SELL+SHELL
      F8=SELL-SHELL
      F10=CELL-CHELL
      ECOM=EMOD*EINER(J)*ELAM**2/F3
      CALL ZEROM(EELK,8,8)
      EELK(1,1)=ECOM*(-ELAM*F6)
      EELK(1,2)=ECOM*(-F1)
      EELK(1,5)=ECOM*(ELAM*F7)
      EELK(1,6)=ECOM*(F10)
      EELK(2,1)=EELK(1,2)
      EELK(2,2)=ECOM*(F5/ELAM)
      EELK(2,5)=-EELK(1,6)
      EELK(2,6)=ECOM*(F8/ELAM)
      EELK(3,3)=EELK(1,1)
      EELK(3,4)=EELK(1,2)
      EELK(3,7)=EELK(1,5)
      EELK(3,8)=EELK(1,6)
      EELK(4,3)=EELK(2,1)
      EELK(4,4)=EELK(2,2)
      EELK(4,7)=EELK(2,5)
      EELK(4,8)=EELK(2,6)
      EELK(5,1)=EELK(1,5)
      EELK(5,2)=EELK(2,5)
      EELK(5,5)=EELK(3,3)
      EELK(5,6)=-EELK(3,4)
      EELK(6,1)=EELK(1,6)
      EELK(6,2)=EELK(2,6)
      EELK(6,5)=EELK(5,6)
      EELK(6,6)=EELK(4,4)
      EELK(7,3)=EELK(3,7)
      EELK(7,4)=EELK(4,7)
      EELK(7,7)=EELK(5,5)
      EELK(7,8)=EELK(5,6)
      EELK(8,3)=EELK(3,8)
      EELK(8,4)=EELK(4,8)
      EELK(8,7)=EELK(7,8)
      EELK(8,8)=EELK(6,6)
      RETURN
      END
```

```
C*************************************************
C  LEFT END DISK EFFECTS 8X8 COMPLEX DOUBLE PRECISION
C*************************************************
      SUBROUTINE EDISKL(J,ROMEGA)
      IMPLICIT REAL*8 (A-H,O-Z)
      REAL*8 EINER(7),EAREA(7),ELEN(7)
      REAL*8 EELK(8,8),DW(8),DRAD(8),DLEN(8)
      COMPLEX*16 EDKL(8,8),EDKR(8,8),EBKL(8,8),EBKR(8,8),DCMPLX
      COMMON EMOD,EINER,EAREA,ELEN,ERHO
      COMMON EELK,EDKL,EDKR,EBKL,EBKR
      COMMON DW,DRAD,DLEN
      COMMON SXXL,SXYL,SYXL,SYYL,DXXL,DXYL,DYXL,DYYL
      COMMON SXXR,SXYR,SYXR,SYYR,DXXR,DXYR,DYXR,DYYR
      DMASS=DW(J)/386.4D0
      TINER=(DMASS/12.0D0)*(3.0D0*DRAD(J)**2+DLEN(J)**2)
      PINER=(DMASS/2.0D0)*(DRAD(J)**2)
      CALL ZEROMC(EDKL,8,8)
      EDKL(1,1)=DCMPLX(-DMASS*ROMEGA**2,0.0)
      EDKL(3,3)=EDKL(1,1)
      EDKL(2,2)=DCMPLX(-TINER*ROMEGA**2,0.0)
      EDKL(4,4)=EDKL(2,2)
      EDKL(2,4)=DCMPLX(0.0,-PINER*ROMEGA**2)
      EDKL(4,2)=DCMPLX(0.0,PINER*ROMEGA**2)
      RETURN
      END
```

```
C*************************************************
C  RIGHT END DISK EFFECTS 8X8 COMPLEX DOUBLE PRECESION
C*************************************************
      SUBROUTINE EDISKR(J,ROMEGA)
      IMPLICIT REAL*8 (A-H,O-Z)
      REAL*8 EINER(7),EAREA(7),ELEN(7)
      REAL*8 EELK(8,8),DW(8),DRAD(8),DLEN(8)
      COMPLEX*16 EDKL(8,8),EDKR(8,8),EBKL(8,8),EBKR(8,8),DCMPLX
      COMMON EMOD,EINER,EAREA,ELEN,ERHO
      COMMON EELK,EDKL,EDKR,EBKL,EBKR
      COMMON DW,DRAD,DLEN
      COMMON SXXL,SXYL,SYXL,SYYL,DXXL,DXYL,DYXL,DYYL
      COMMON SXXR,SXYR,SYXR,SYYR,DXXR,DXYR,DYXR,DYYR
      DMASS=DW(J+1)/386.4D0
      TINER=(DMASS/12.0D0)*(3.0D0*DRAD(J+1)**2+DLEN(J+1)**2)
      PINER=(DMASS/2.0D0)*(DRAD(J+1)**2)
      CALL ZEROMC(EDKR,8,8)
      EDKR(5,5)=DCMPLX(-DMASS*ROMEGA**2,0.0)
      EDKR(7,7)=EDKR(5,5)
      EDKR(6,6)=DCMPLX(-TINER*ROMEGA**2,0.0)
      EDKR(8,8)=EDKR(6,6)
      EDKR(6,8)=DCMPLX(0.0,-PINER*ROMEGA**2)
      EDKR(8,6)=DCMPLX(0.0,PINER*ROMEGA**2)
      RETURN
      END
```

```
C*************************************************
C  LEFT END BEARING EFFECTS 8X8 COMPLEX DOUBLE PRECESION
C*************************************************
      SUBROUTINE EBEARL(ROMEGA)
      IMPLICIT REAL*8(A-H,O-Z)
      REAL*8 EINER(7),EAREA(7),ELEN(7)
      REAL*8 EELK(8,8),DW(8),DRAD(8),DLEN(8)
      COMPLEX*16 EDKL(8,8),EDKR(8,8),EBKL(8,8),EBKR(8,8),DCMPLX
      COMMON EMOD,EINER,EAREA,ELEN,ERHO
      COMMON EELK,EDKL,EDKR,EBKL,EBKR
      COMMON DW,DRAD,DLEN
      COMMON SXXL,SXYL,SYXL,SYYL,DXXL,DXYL,DYXL,DYYL
      COMMON SXXR,SXYR,SYXR,SYYR,DXXR,DXYR,DYXR,DYYR
      CALL ZEROMC(EBKL,8,8)
      EBKL(1,1)=DCMPLX(SXXL,ROMEGA*DXXL)
      EBKL(1,3)=DCMPLX(SXYL,ROMEGA*DXYL)
      EBKL(3,1)=DCMPLX(SYXL,ROMEGA*DYXL)
      EBKL(3,3)=DCMPLX(SYYL,ROMEGA*DYYL)
      RETURN
      END
```

```
C*************************************************
C  RIGHT END BEARING EFFECTS 8X8 COMPLEX DOUBLE PRECESION
C*************************************************
      SUBROUTINE EBEARR(ROMEGA)
      IMPLICIT REAL*8(A-H,O-Z)
C     RIGHT END BEARING EFFECTS 8X8 COMPLEX
      REAL*8 EINER(7),EAREA(7),ELEN(7)
      REAL*8 EELK(8,8),DW(8),DRAD(8),DLEN(8)
      COMPLEX*16 EDKL(8,8),EDKR(8,8),EBKL(8,8),EBKR(8,8),DCMPLX
      COMMON EMOD,EINER,EAREA,ELEN,ERHO
      COMMON EELK,EDKL,EDKR,EBKL,EBKR
      COMMON DW,DRAD,DLEN
      COMMON SXXL,SXYL,SYXL,SYYL,DXXL,DXYL,DYXL,DYYL
      COMMON SXXR,SXYR,SYXR,SYYR,DXXR,DXYR,DYXR,DYYR
      CALL ZEROMC(EBKR,8,8)
      EBKR(5,5)=DCMPLX(SXXR,ROMEGA*DXXR)
      EBKR(5,7)=DCMPLX(SXYR,ROMEGA*DXYR)
      EBKR(7,5)=DCMPLX(SYXR,ROMEGA*DYXR)
      EBKR(7,7)=DCMPLX(SYYR,ROMEGA*DYYR)
      RETURN
      END
```

```
C*****************************************************
C  LEFT END DISK EFFECTS 8X8 COMPLEX COUBLE PRECISION
C*****************************************************
      SUBROUTINE EDISKL(J,ROMEGA)
      IMPLICIT REAL*8 (A-H,O-Z)
      REAL*8 EINER(7),EAREA(7),ELEN(7)
      REAL*8 EELK(8,8),DW(8),DRAD(8),DLEN(8)
      COMPLEX*16 EDKL(8,8),EDKR(8,8),EBKL(8,8),EBKR(8,8),DCMPLX
      COMMON EMOD,EINER,EAREA,ELEN,ERHO
      COMMON EELK,EDKL,EDKR,EBKL,EBKR
      COMMON DW,DRAD,DLEN
      COMMON SXXL,SXYL,SYXL,SYYL,DXXL,DXYL,DYXL,DYYL
      COMMON SXXR,SXYR,SYXR,SYYR,DXXR,DXYR,DYXR,DYYR
      DMASS=DW(J)/386.4D0
      TINER=(DMASS/12.0D0)*(3.0D0*DRAD(J)**2+DLEN(J)**2)
      PINER=(DMASS/2.0D0)*(DRAD(J)**2)
      CALL ZEROMC(EDKL,8,8)
      EDKL(1,1)=DCMPLX(-DMASS*ROMEGA**2,0.0)
      EDKL(3,3)=EDKL(1,1)
      EDKL(2,2)=DCMPLX(-TINER*ROMEGA**2,0.0)
      EDKL(4,4)=EDKL(2,2)
      EDKL(2,4)=DCMPLX(0.0,-PINER*ROMEGA**2)
      EDKL(4,2)=DCMPLX(0.0,PINER*ROMEGA**2)
      RETURN
      END
```

```
C*****************************************************
C  RIGHT END DISK EFFECTS 8X8 COMPLEX DOUBLE PRECESION
C*****************************************************
      SUBROUTINE EDISKR(J,ROMEGA)
      IMPLICIT REAL*8 (A-H,O-Z)
      REAL*8 EINER(7),EAREA(7),ELEN(7)
      REAL*8 EELK(8,8),DW(8),DRAD(8),DLEN(8)
      COMPLEX*16 EDKL(8,8),EDKR(8,8),EBKL(8,8),EBKR(8,8),DCMPLX
      COMMON EMOD,EINER,EAREA,ELEN,ERHO
      COMMON EELK,EDKL,EDKR,EBKL,EBKR
      COMMON DW,DRAD,DLEN
      COMMON SXXL,SXYL,SYXL,SYYL,DXXL,DXYL,DYXL,DYYL
      COMMON SXXR,SXYR,SYXR,SYYR,DXXR,DXYR,DYXR,DYYR
      DMASS=DW(J+1)/386.4D0
      TINER=(DMASS/12.0D0)*(3.0D0*DRAD(J+1)**2+DLEN(J+1)**2)
      PINER=(DMASS/2.0D0)*(DRAD(J+1)**2)
      CALL ZEROMC(EDKR,8,8)
      EDKR(5,5)=DCMPLX(-DMASS*ROMEGA**2,0.0)
      EDKR(7,7)=EDKR(5,5)
      EDKR(6,6)=DCMPLX(-TINER*ROMEGA**2,0.0)
      EDKR(8,8)=EDKR(6,6)
      EDKR(6,8)=DCMPLX(0.0,-PINER*ROMEGA**2)
      EDKR(8,6)=DCMPLX(0.0,PINER*ROMEGA**2)
      RETURN
      END
```

```
C*************************************************
C  LEFT END BEARING EFFECTS 8X8 COMPLEX DOUBLE PRECESION
C*************************************************
      SUBROUTINE EBEARL(ROMEGA)
      IMPLICIT REAL*8(A-H,O-Z)
      REAL*8 EINER(7),EAREA(7),ELEN(7)
      REAL*8 EELK(8,8),DW(8),DRAD(8),DLEN(8)
      COMPLEX*16 EDKL(8,8),EDKR(8,8),EBKL(8,8),EBKR(8,8),DCMPLX
      COMMON EMOD,EINER,EAREA,ELEN,ERHO
      COMMON EELK,EDKL,EDKR,EBKL,EBKR
      COMMON DW,DRAD,DLEN
      COMMON SXXL,SXYL,SYXL,SYYL,DXXL,DXYL,DYXL,DYYL
      COMMON SXXR,SXYR,SYXR,SYYR,DXXR,DXYR,DYXR,DYYR
      CALL ZEROMC(EBKL,8,8)
      EBKL(1,1)=DCMPLX(SXXL,ROMEGA*DXXL)
      EBKL(1,3)=DCMPLX(SXYL,ROMEGA*DXYL)
      EBKL(3,1)=DCMPLX(SYXL,ROMEGA*DYXL)
      EBKL(3,3)=DCMPLX(SYYL,ROMEGA*DYYL)
      RETURN
      END
```

```
C*************************************************
C  RIGHT END BEARING EFFECTS 8X8 COMPLEX DOUBLE PRECESION
C*************************************************
      SUBROUTINE EBEARR(ROMEGA)
      IMPLICIT REAL*8(A-H,O-Z)
C     RIGHT END BEARING EFFECTS 8X8 COMPLEX
      REAL*8 EINER(7),EAREA(7),ELEN(7)
      REAL*8 EELK(8,8),DW(8),DRAD(8),DLEN(8)
      COMPLEX*16 EDKL(8,8),EDKR(8,8),EBKL(8,8),EBKR(8,8),DCMPLX
      COMMON EMOD,EINER,EAREA,ELEN,ERHO
      COMMON EELK,EDKL,EDKR,EBKL,EBKR
      COMMON DW,DRAD,DLEN
      COMMON SXXL,SXYL,SYXL,SYYL,DXXL,DXYL,DYXL,DYYL
      COMMON SXXR,SXYR,SYXR,SYYR,DXXR,DXYR,DYXR,DYYR
      CALL ZEROMC(EBKR,8,8)
      EBKR(5,5)=DCMPLX(SXXR,ROMEGA*DXXR)
      EBKR(5,7)=DCMPLX(SXYR,ROMEGA*DXYR)
      EBKR(7,5)=DCMPLX(SYXR,ROMEGA*DYXR)
      EBKR(7,7)=DCMPLX(SYYR,ROMEGA*DYYR)
      RETURN
      END
```

```
      SUBROUTINE ZEROM(A,I,J)
C  INITIALIZES A REAL MATRIX TO ZERO
      REAL*8 A(1)
      II=I*J
      DO 10 K=1,II
   10 A(K)=0.0D0
      RETURN
      END



      SUBROUTINE ZEROMC(A,I,J)
C  INITIALIZES A COMPLEX MATRIX TO ZERO
      COMPLEX*16 A(I,J)
      DO 10 K=1,I
      DO 10 L=1,J
   10 A(K,L)=(0.0D0,0.0D0)
      RETURN
      END



      SUBROUTINE CADDM1(A,B,I,J)
C  ADDS A REAL MATRIX TO A COMPLEX MATRIX
      REAL*8 A(I,J)
      COMPLEX*16 B(I,J)
      DO 10 K=1,I
      DO 10 L=1,J
   10 B(K,L)=A(K,L)+B(K,L)
  100 RETURN
      END



      SUBROUTINE CMULTM(A,K,I,B,J,C)
C  MULTIPLIES TWO COMPLEX MATRICES
      COMPLEX*16 A(32,32),B(32,1),C(32,1)
      DO 10 L=1,K
      DO 10 M=1,J
      C(L,M)=(0.0D0,0.0D0)
      DO 10 N=1,I
      C(L,M)=C(L,M)+A(L,N)*B(N,M)
   10 CONTINUE
  100 RETURN
      END



      SUBROUTINE CADDM2(A,B,I,J)
C  ADDS TWO COMPLEX MATRICES
      COMPLEX*16 A(I,J),B(I,J)
      DO 10 K=1,I
      DO 10 L=1,J
   10 B(K,L)=A(K,L)+B(K,L)
  100 RETURN
      END
```

```
      SUBROUTINE CINV(N,A,AI)
C*****************************************************
CCC   CINV...FINDS THE INVERSE OF THE COMPLEX DOUBLE
CCC   PRECESION MATRIX S BY GAUSS ELIMINATION WITH
CCC   PARTIAL PIVOTING. THE INVERSE OF MATRIX S IS
CCC   STORED TO AI
CCC   N= ORDER OF MATRIX TO BE INVERTED
C*****************************************************
      IMPLICIT COMPLEX*16 (A-H,O-Z)
      REAL*8 CDABS,SMAX
      COMPLEX*16 S(32,32),AI(32,32),A(32,32)
C
      DO 10 I=1,N
      DO 10 J=1,N
   10 S(I,J)=A(I,J)
CCC
CCC   INITIALIZE AI
CCC
      NM=N-1
      DO 100 I=1,NM
      AI(I,I)=(1.0D0,0.0D0)
      DO 100 J=I,NM
      AI(I,J+1)=(0.0D0,0.0D0)
      AI(J+1,I)=(0.0D0,0.0D0)
  100 CONTINUE
      AI(N,N)=(1.0D0,0.0D0)
      DO 430 K=2,N
CCC
CCC   SEARCH FOR LARGEST ENTRY IN (K-1)TH COLUMN OF S
CCC
      KM=K-1
      IMAX=KM
      SMAX=CDABS(S(KM,KM))
      DO 210 J=K,N
      IF(SMAX-CDABS(S(J,KM))) 200,210,210
  200 IMAX=J
      SMAX= CDABS(S(J,KM))
  210 CONTINUE
      IF(IMAX-KM) 300,400,300
CCC
CCC   SWITCH (K-1)TH AND IMAXTH EQUATIONS
CCC
  300 DO 310 J=KM,N
      TEMP=S(KM,J)
      S(KM,J)=S(IMAX,J)
  310 S(IMAX,J)=TEMP
      DO 320 J=1,N
      TEMP=AI(KM,J)
      AI(KM,J)=AI(IMAX,J)
      AI(IMAX,J)=TEMP
  320 CONTINUE
CCC
CCC   ELIMINATE X(K-1) FROM KTH THRU NTH EQUATIONS
CCC
  400 DO 420 I=K,N
      RS=S(I,KM)/S(KM,KM)
      DO 410 J=K,N
  410 S(I,J)=S(I,J)-RS*S(KM,J)
      DO 420 J=1,N
  420 AI(I,J)=AI(I,J)-RS*AI(KM,J)
  430 CONTINUE
C
CCC   BACK SUBSTITUTE
C
      DO 500 I=1,N
  500 AI(N,I)=AI(N,I)/S(N,N)
      DO 520 K=2,N
      NK=N+1-K
      DO 520 J=1,N
      DO 510 L=2,K
  510 AI(NK,J)=AI(NK,J)-S(NK,N+2-L)*AI(N+2-L,J)
      AI(NK,J)=AI(NK,J)/S(NK,NK)
  520 CONTINUE
      RETURN
      END
```

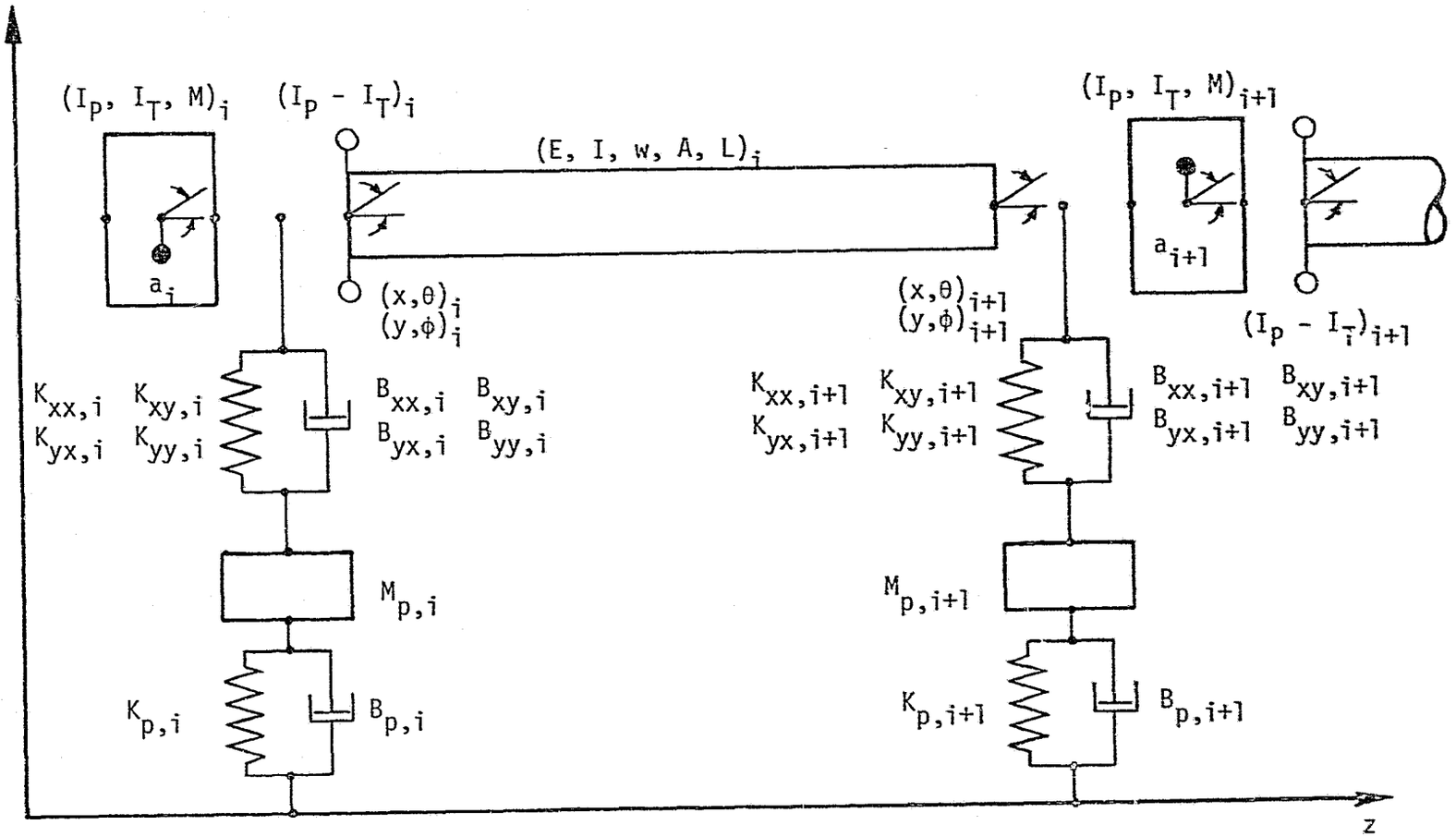

Figure 1. System Used in Rotor - Bearing Dynamic Analysis Program.

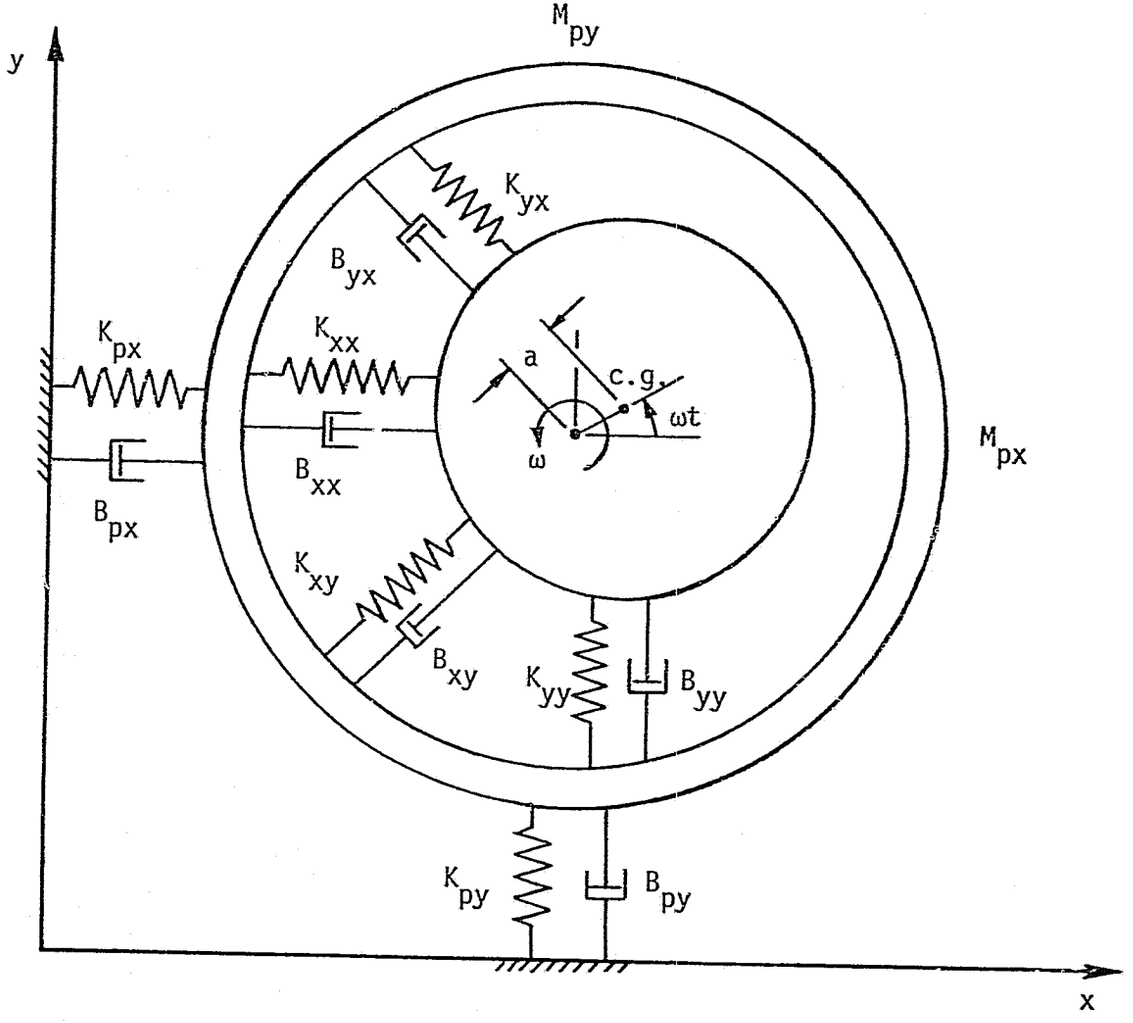

Figure 2. Bearing - Pedestal Representation in Rotor System Model.

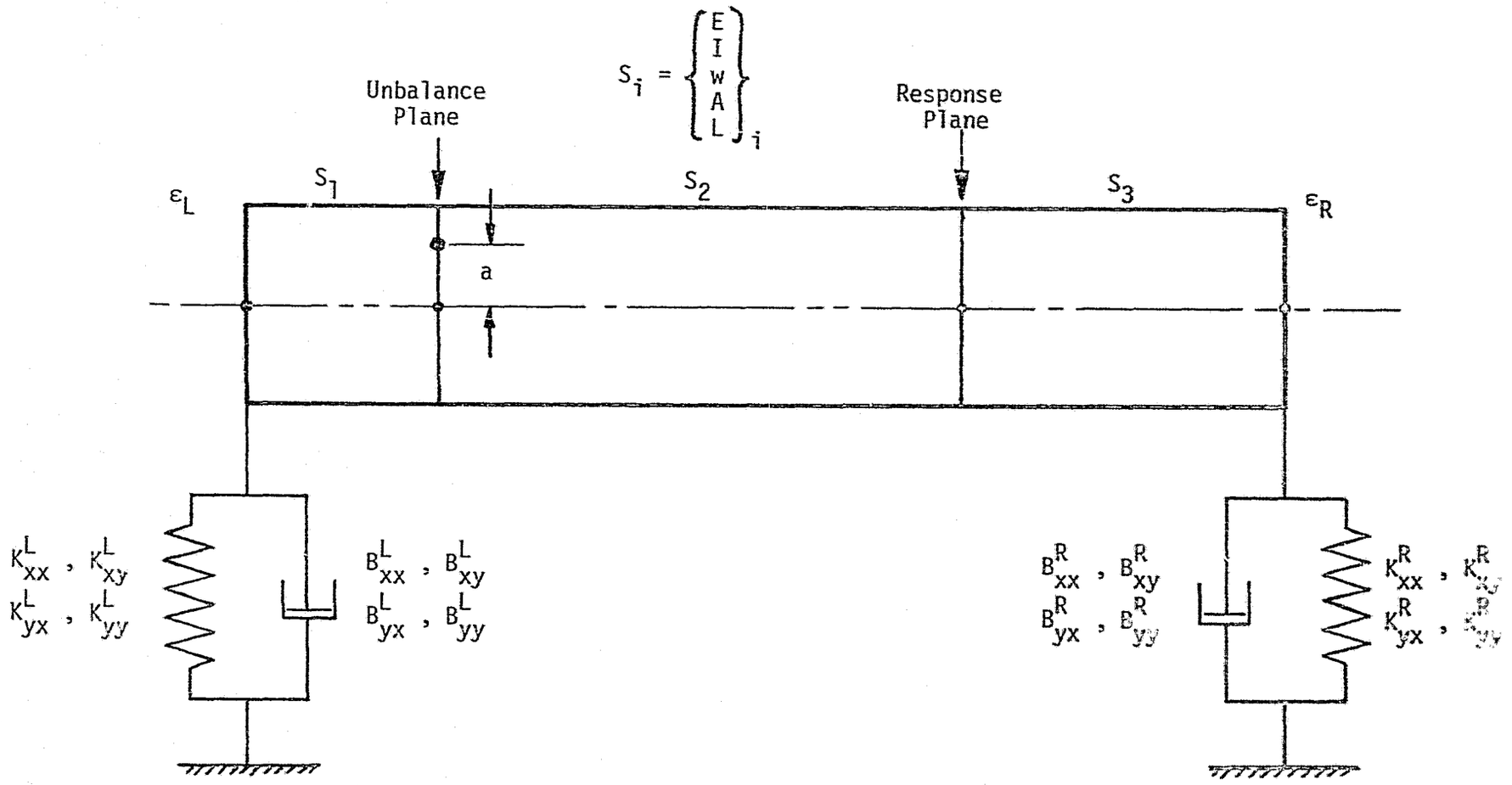

Figure 3. Representation of Rotor in Fluid-Film Bearings for Uniform Rotor Study.

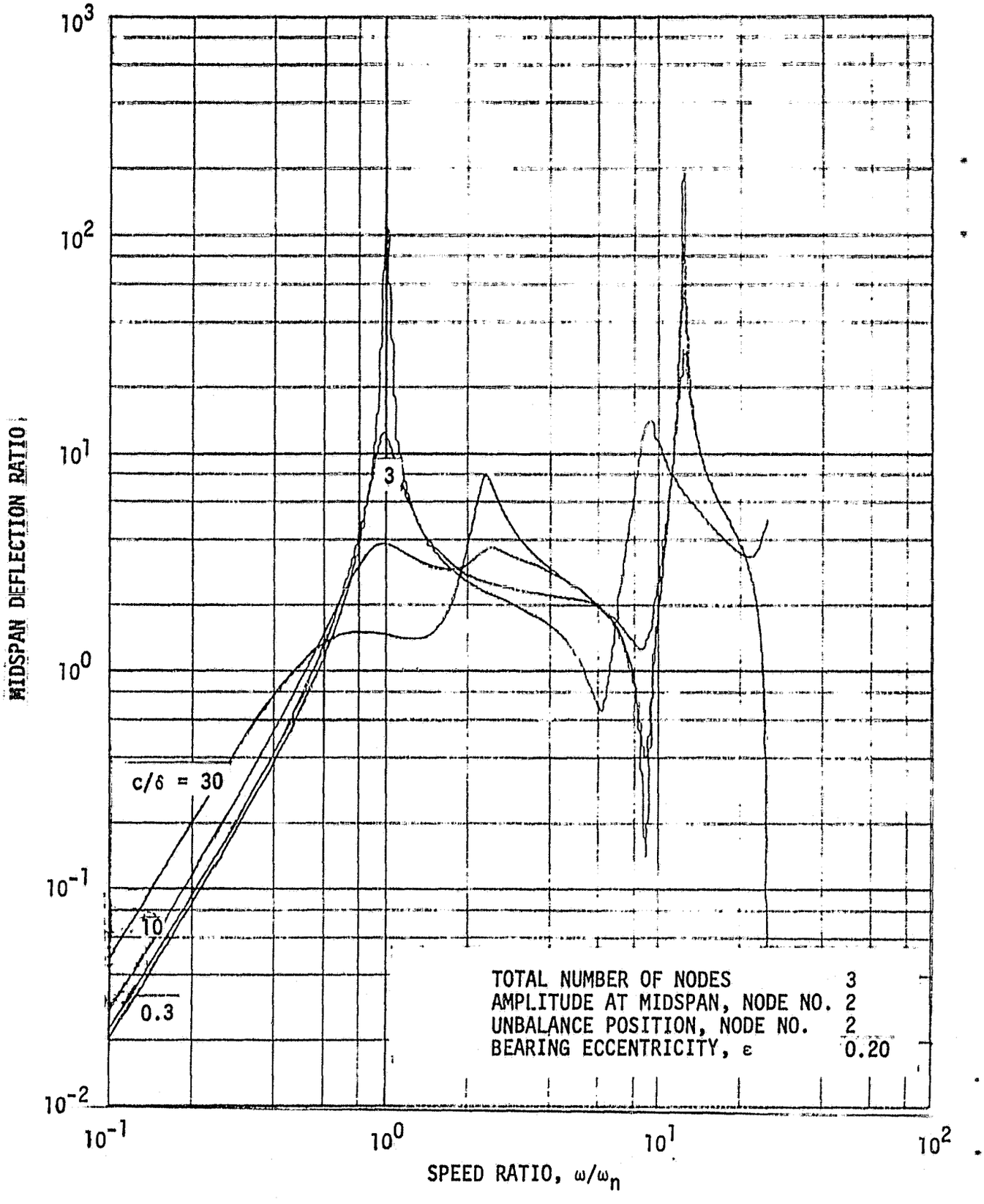

Figure 4. Midspan Unbalance Response of Uniform Rotor in End Bearings. Case B1. Plain Cylindrical Bearings. ε = 0.20.

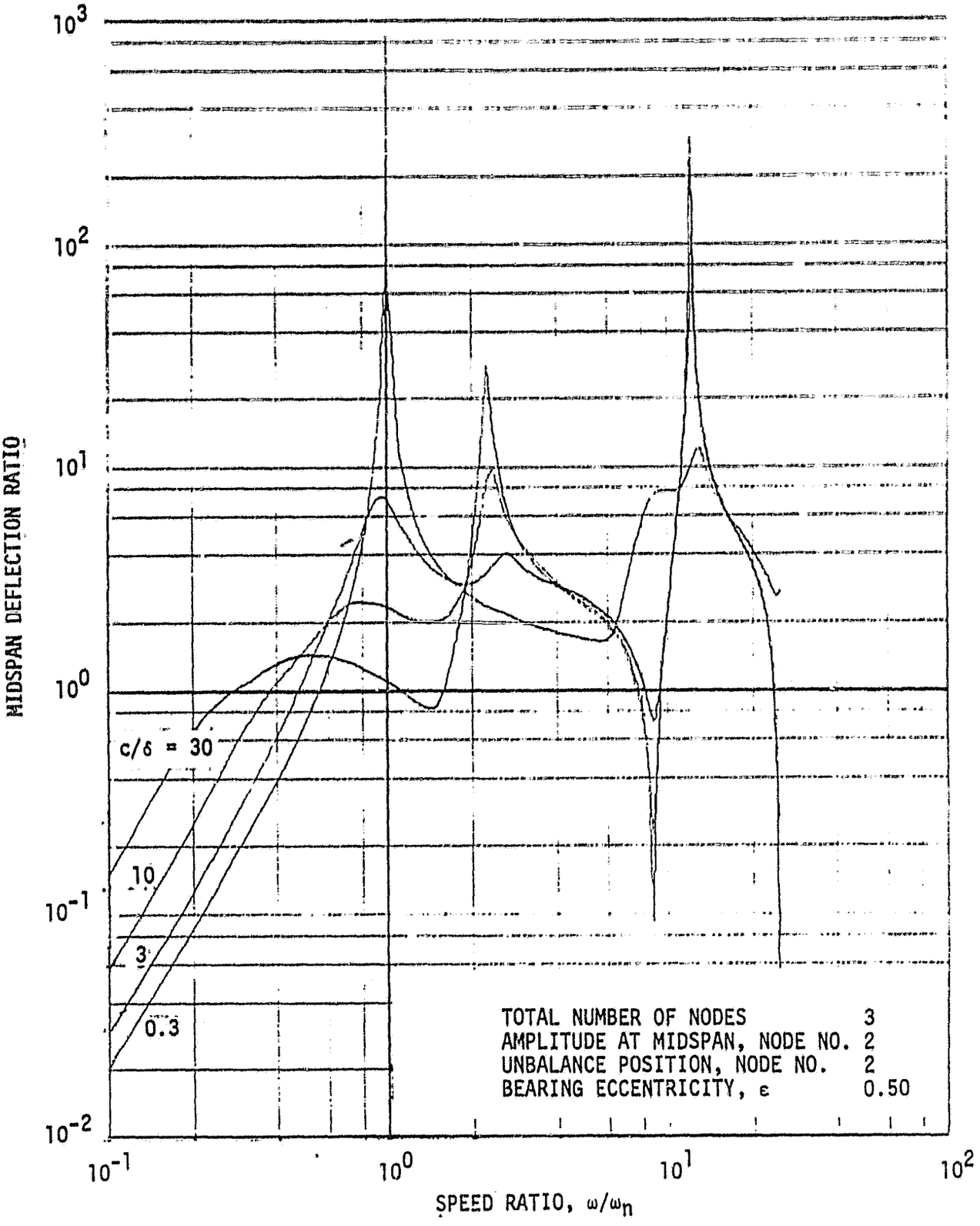

Figure 5. Midspan Unbalance Response of Uniform Rotor in End Bearings. Case B3. Plain Cylindrical Bearings. $\varepsilon = 0.50$.

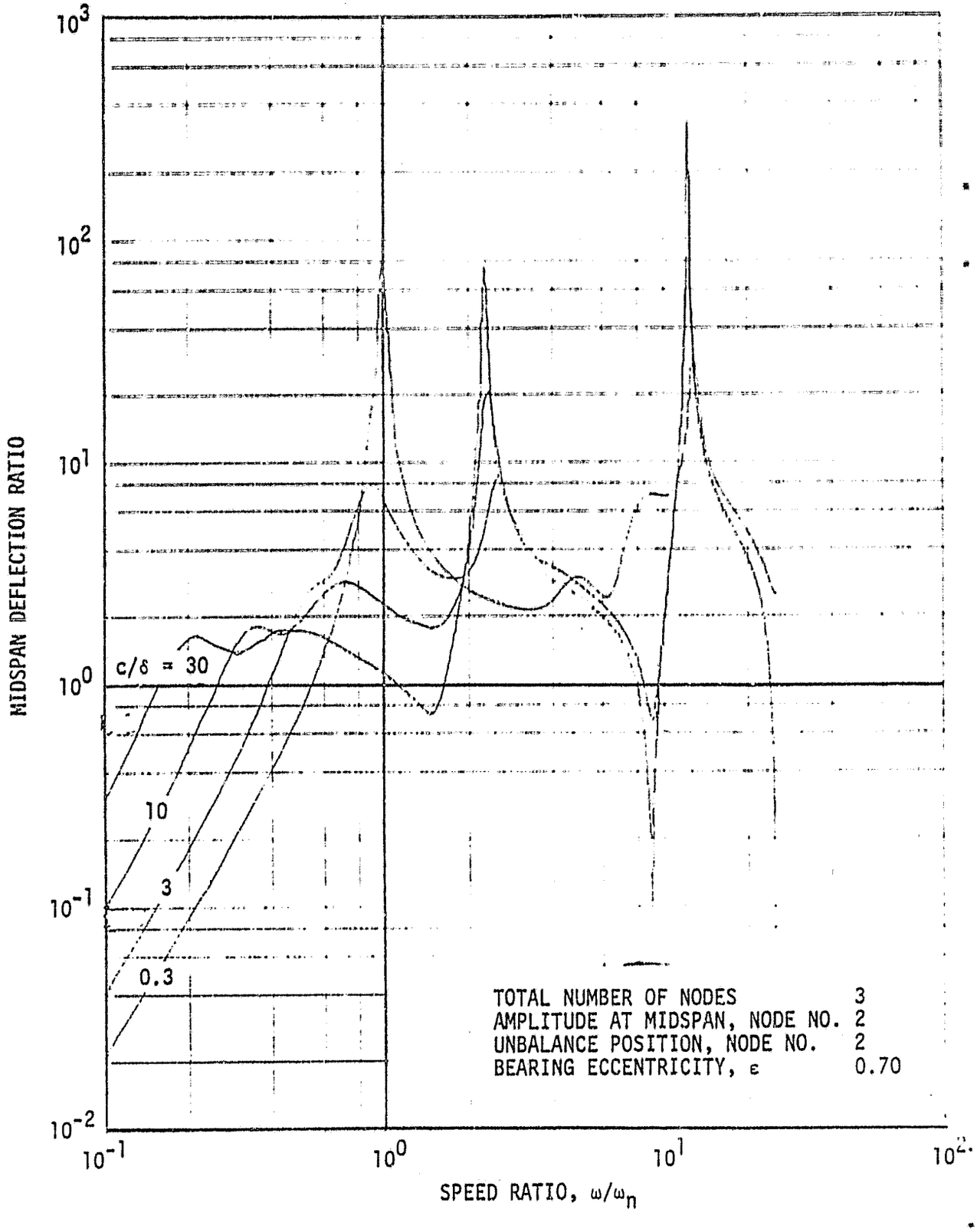

Figure 6. Midspan Unbalance Response of Uniform Rotor in End Bearings. Case B5. Plain Cylindrical Bearings. $\varepsilon = 0.70$.

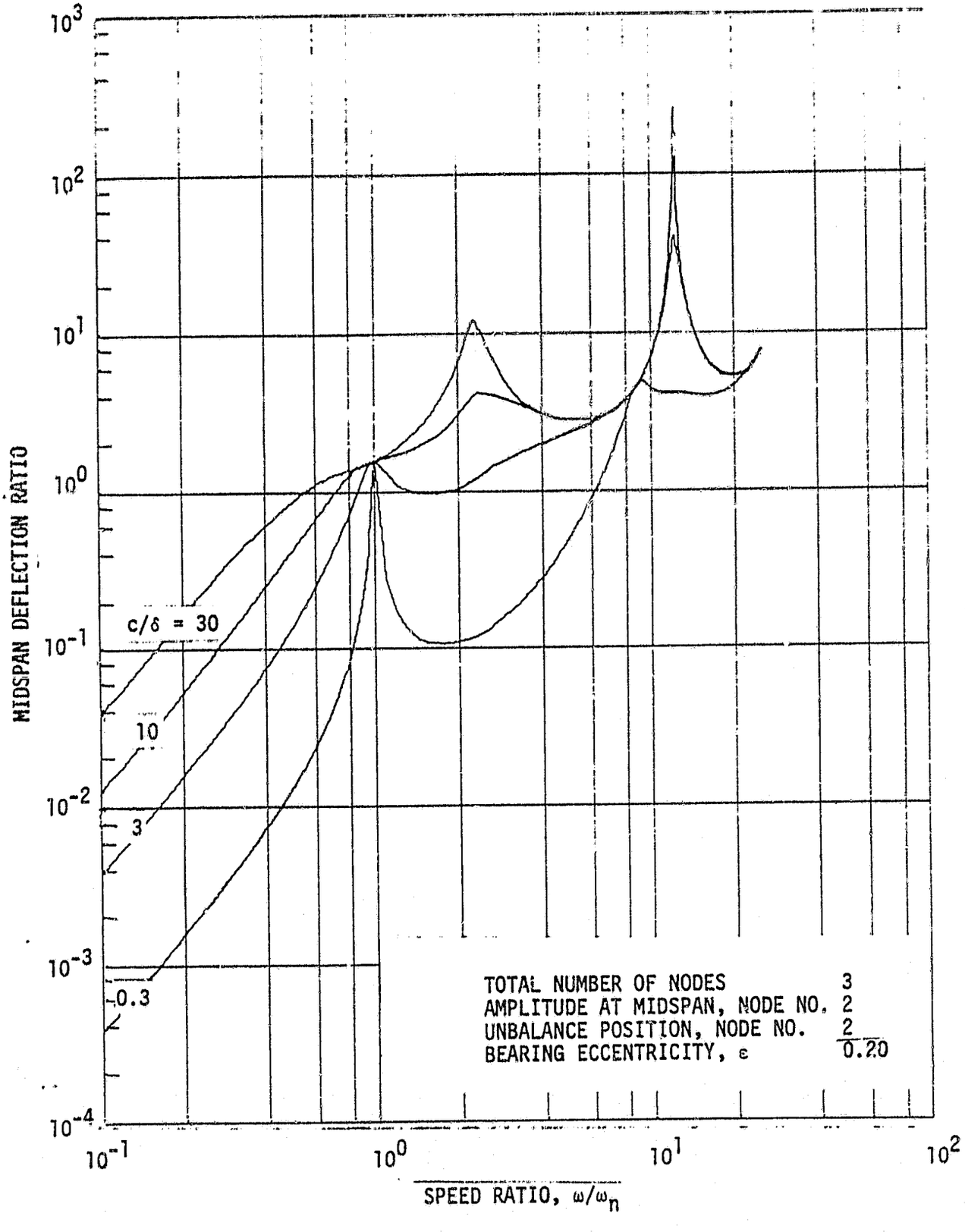

Figure 7. Journal Unbalance Response of Uniform Rotor in End Bearings. Case B7. Plain Cylindrical Bearings. $\varepsilon = 0.20$.

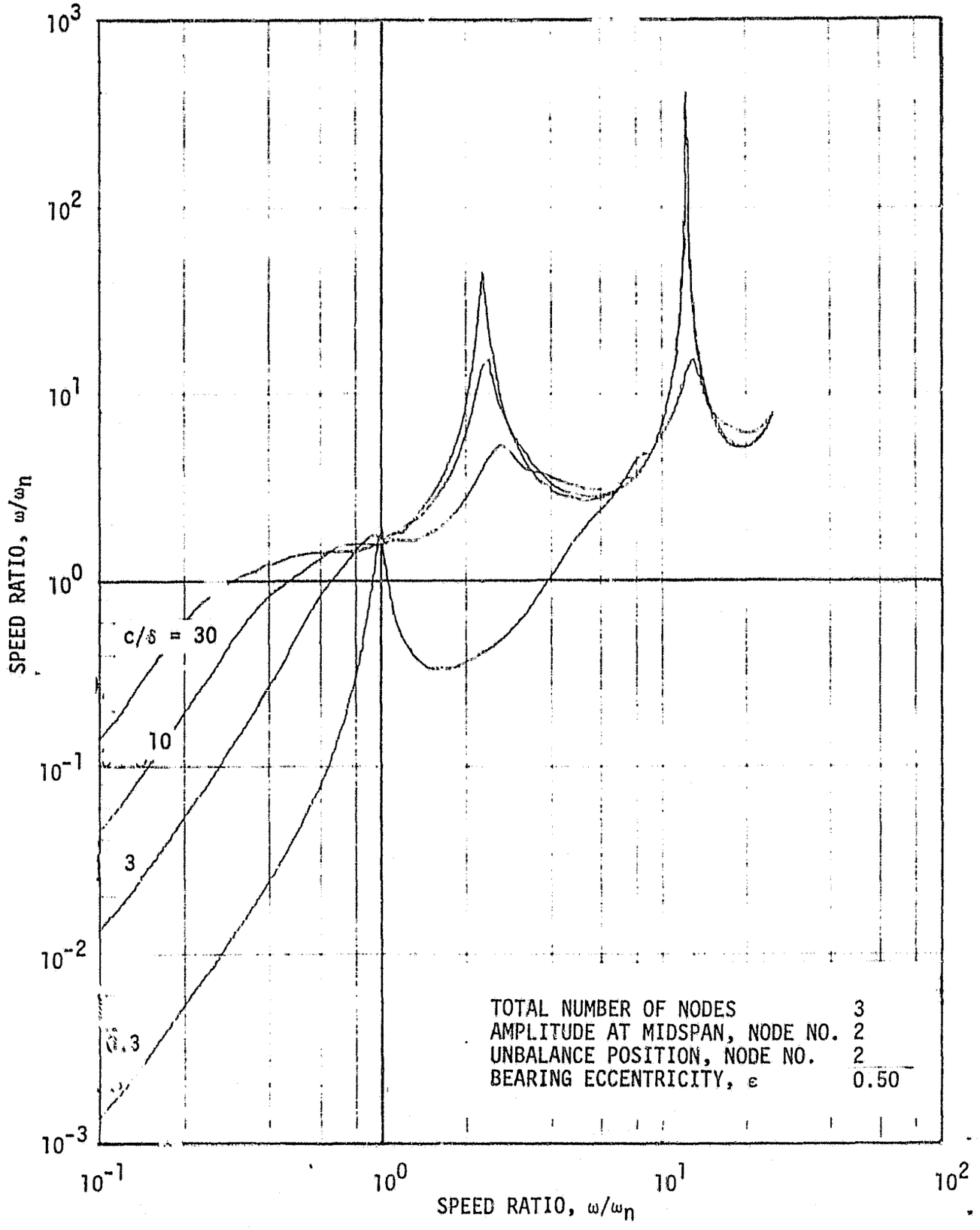

Figure 8. Journal Unbalance Response of Uniform Rotor in End Bearings. Case b) Plain Cylindrical Bearings. $\varepsilon = 0.50$.

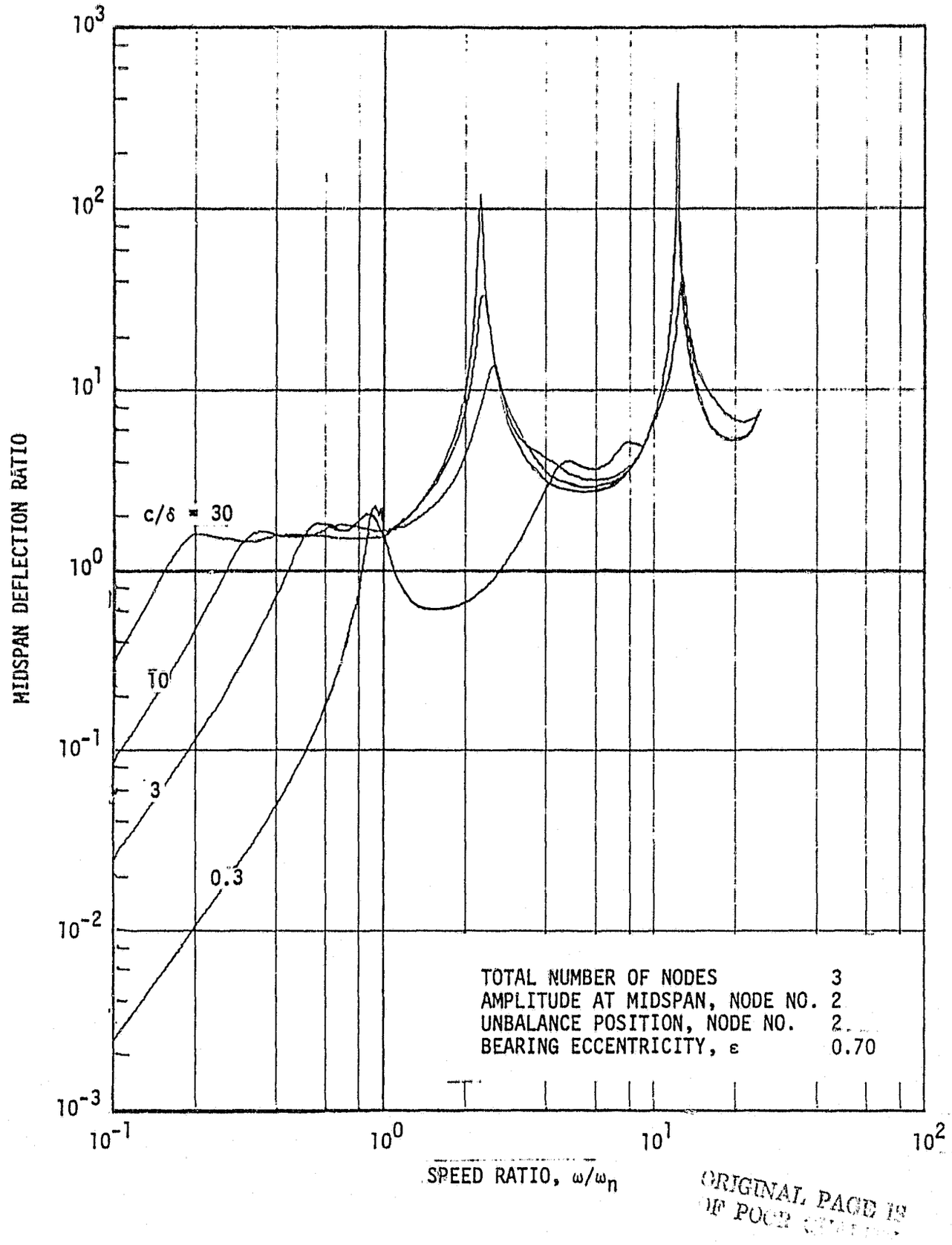

Figure 9. Journal Unbalance Response of Uniform Rotor in End Bearings. Case B11. Plain Cylindrical Bearings. $\varepsilon = 0.70$.

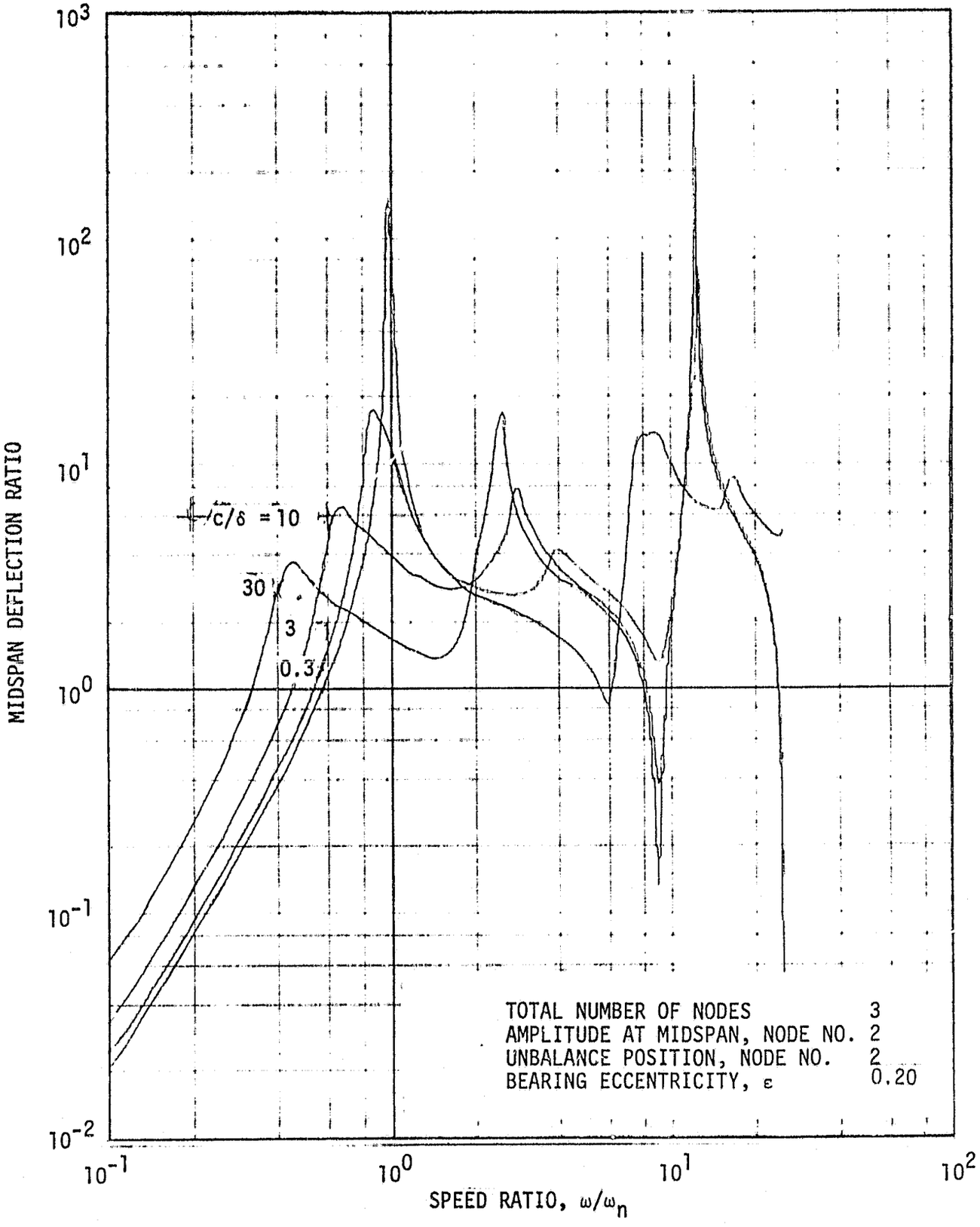

Figure 10. Midspan Unbalance Response of Uniform Rotor in End Bearings. Case B13. Axial Groove Bearings. $\varepsilon = 0.20$.

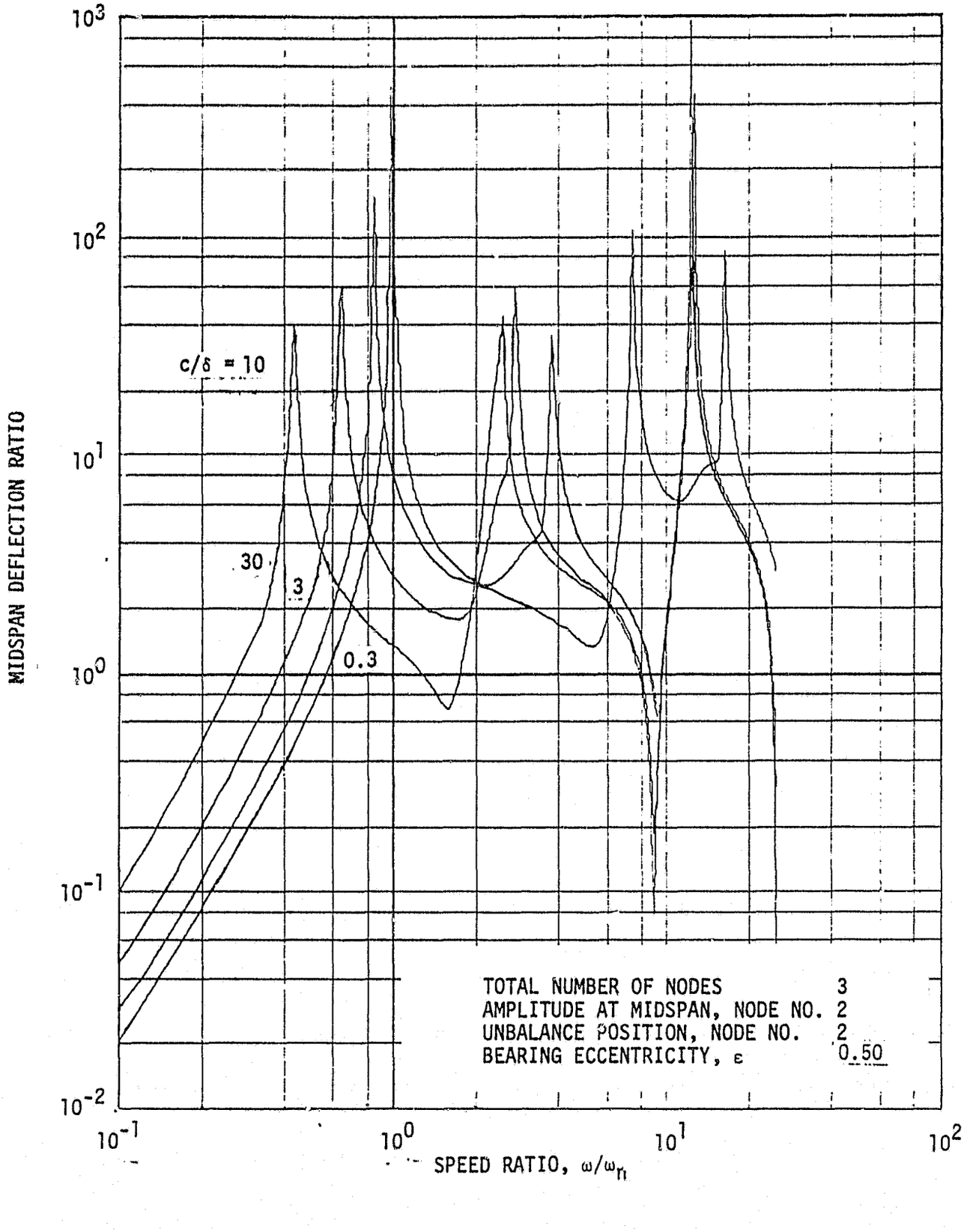

Figure 11. Midspan Unbalance Response of Uniform Rotor in End Bearings.. Case B15. Axial Groove Bearings. $\varepsilon = 0.50$.

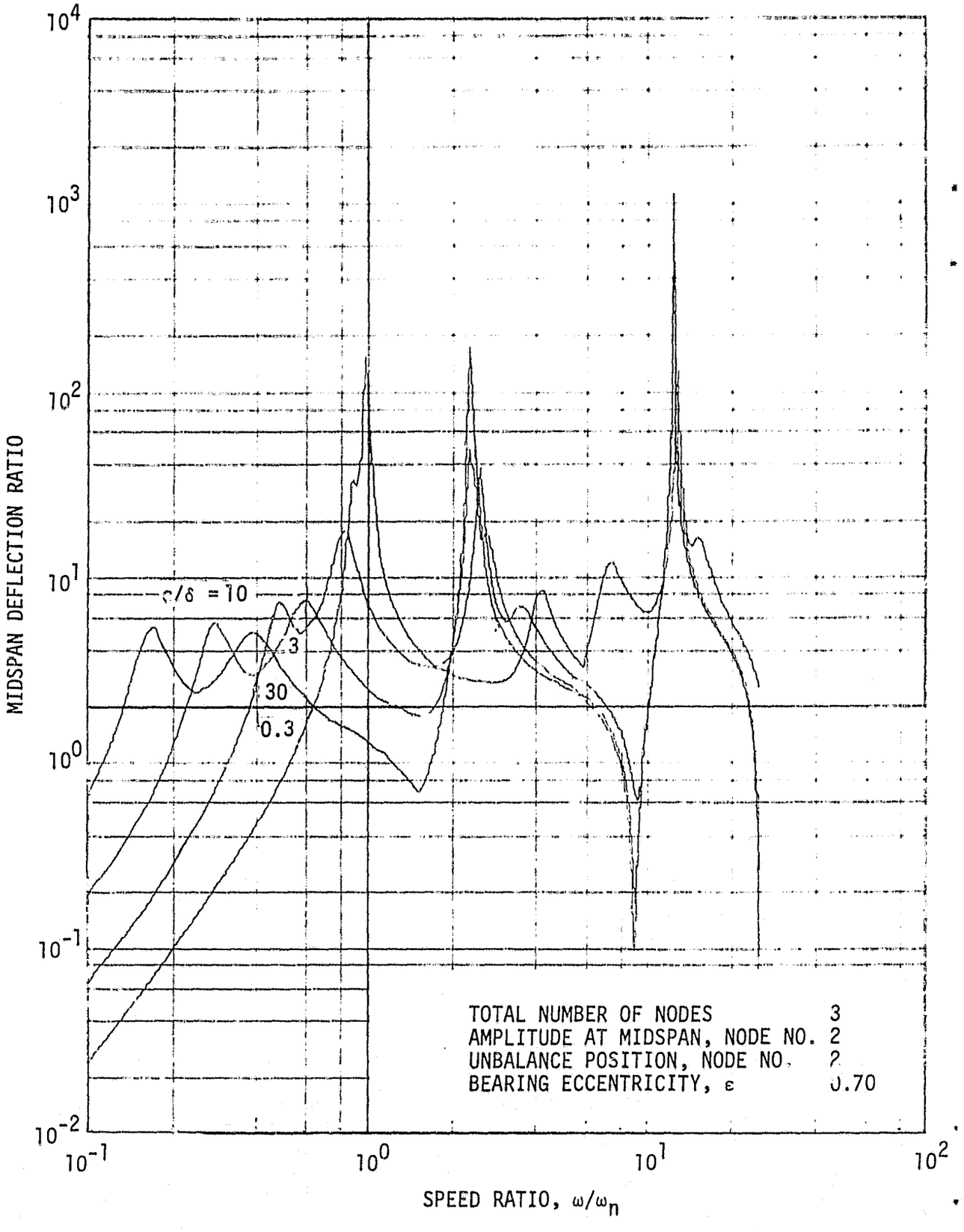

Figure 12. Midspan Unbalance Response of Uniform Rotor in End Bearings. Case B17. Axial Groove Bearings. $\varepsilon = 0.70$.

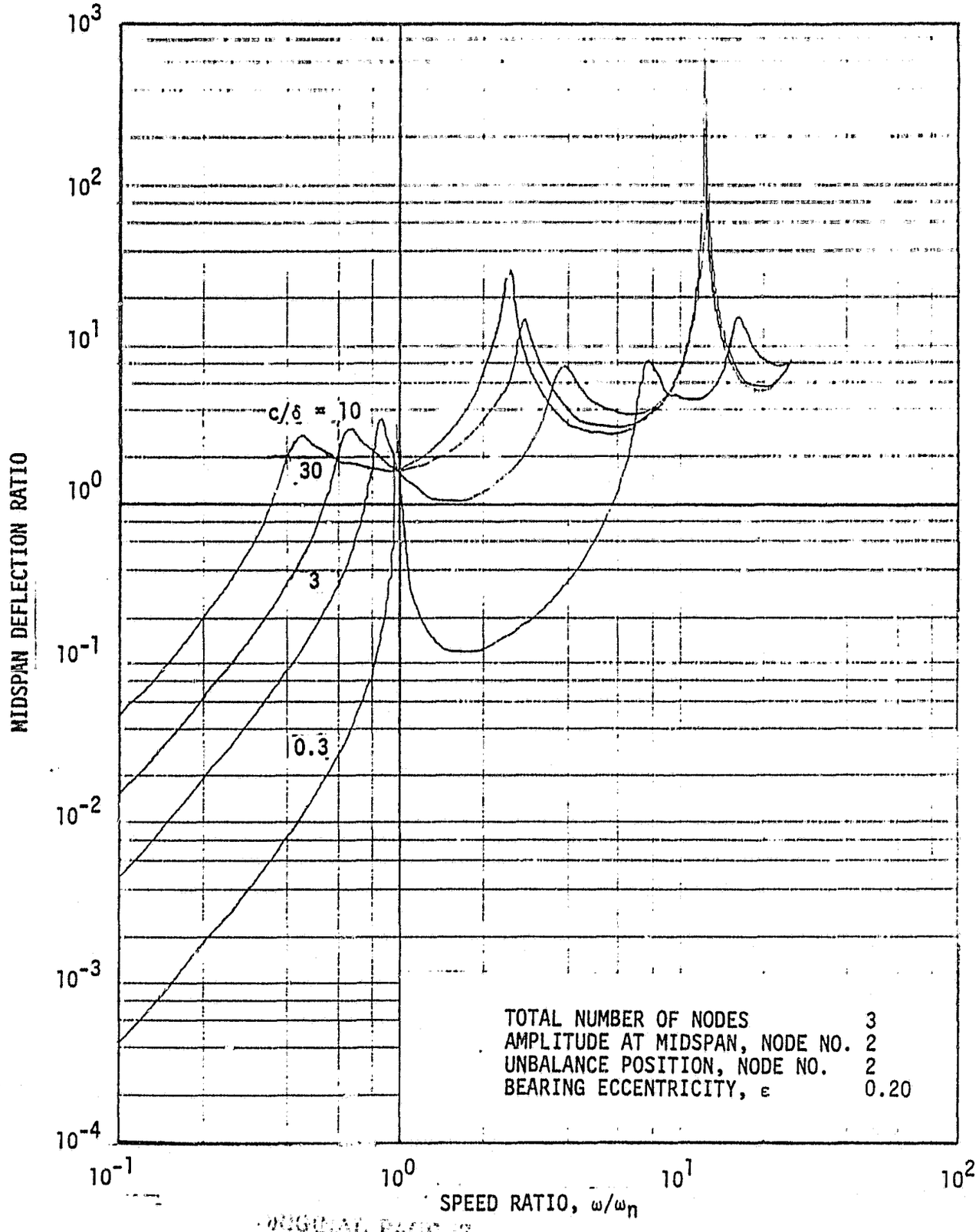

Figure 13. Journal Unbalance Response of Uniform Rotor in End Bearings. Case B19. Axial Groove Bearings. $\varepsilon = 0.20$.

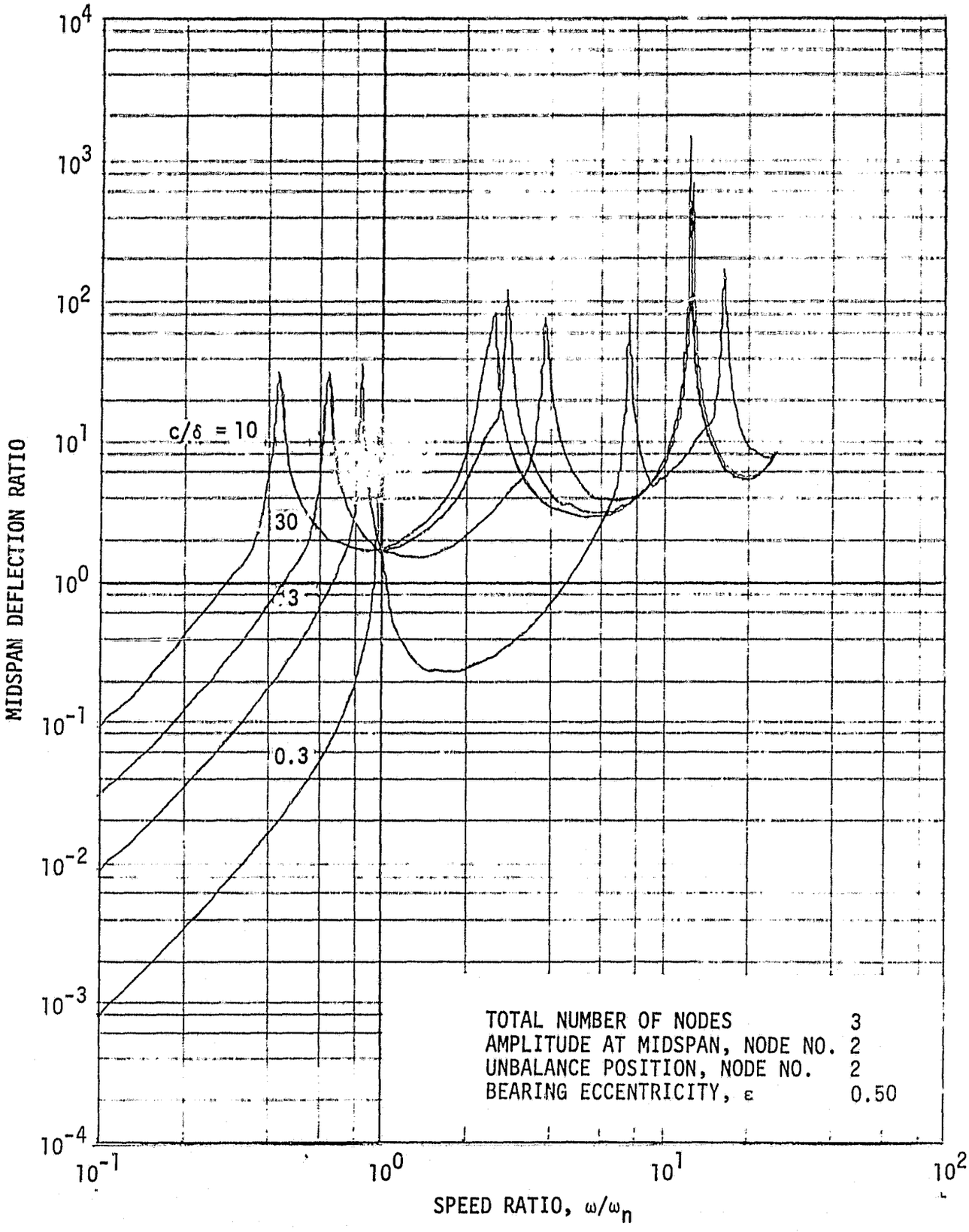

Figure 14. Journal Unbalance Response of Uniform Rotor in End Bearings. Case B21. Axial Groove Bearings. $\varepsilon = 0.50$.

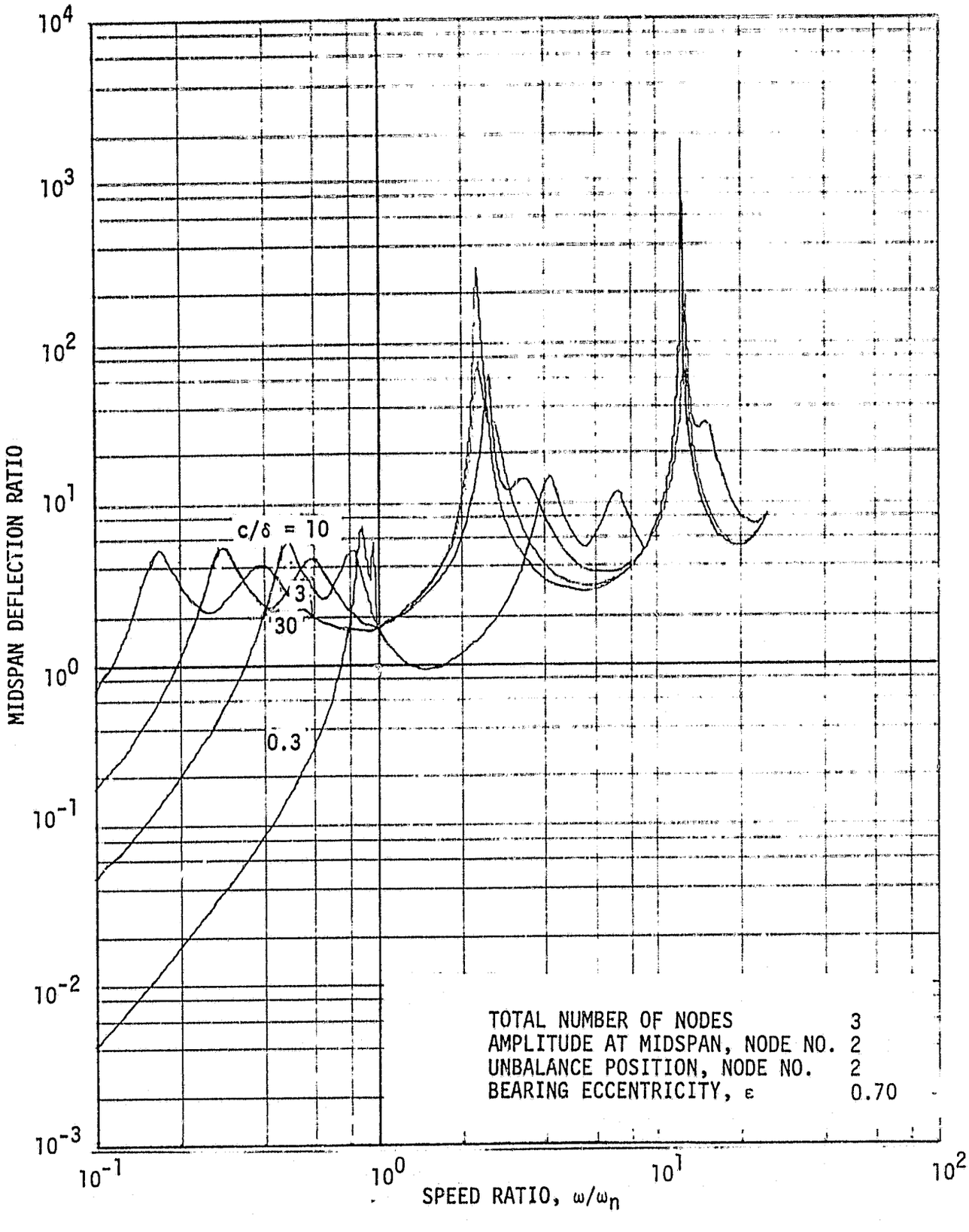

Figure 15. Journal Unbalance Response of Uniform Rotor in End Bearings. Case B23. Axial Groove Bearings. $\varepsilon = 0.70$.

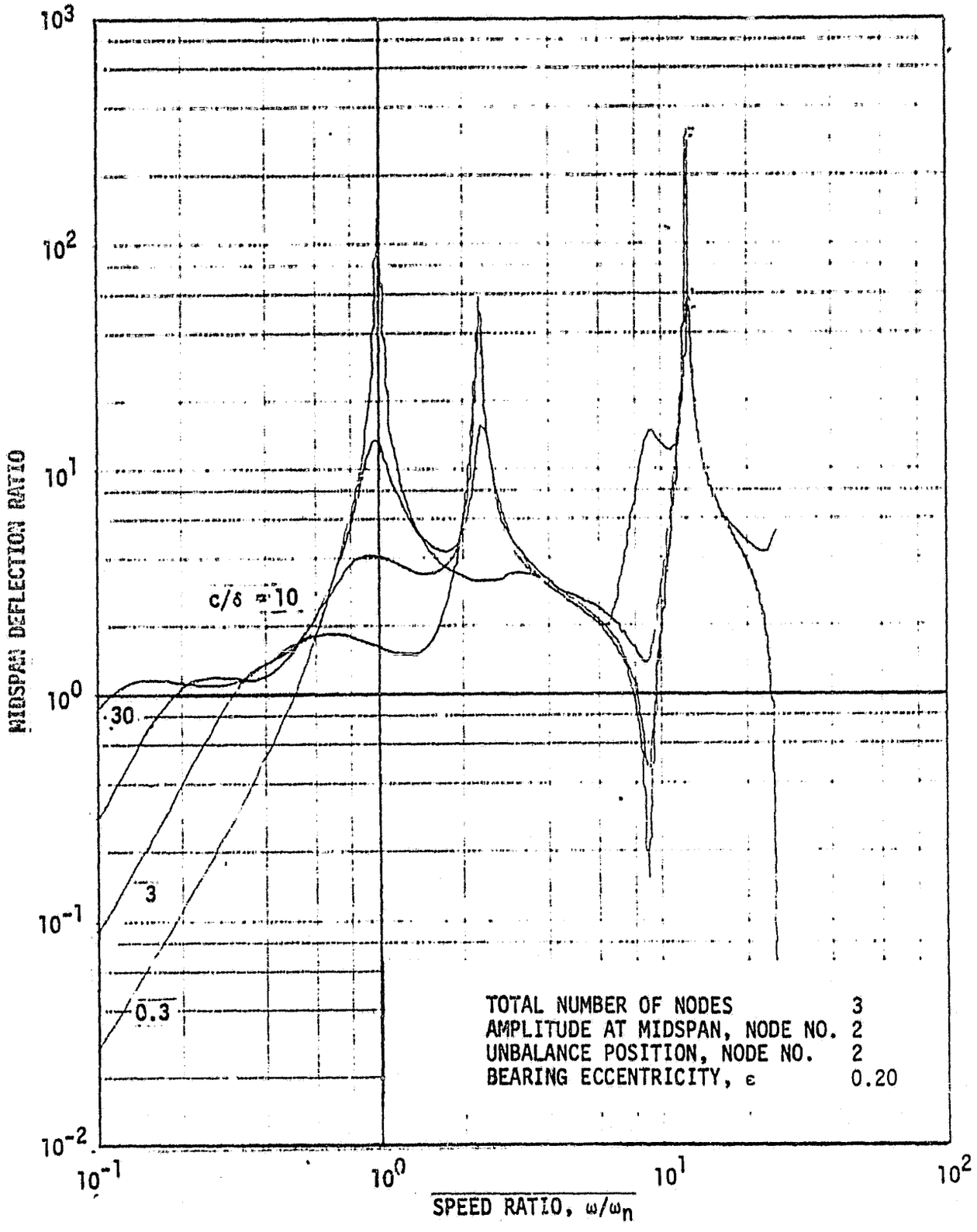

Figure 16. Midspan Unbalance Response of Uniform Rotor in End Bearings. Case B25. Partial Arc Bearings. $\varepsilon = 0.20$.

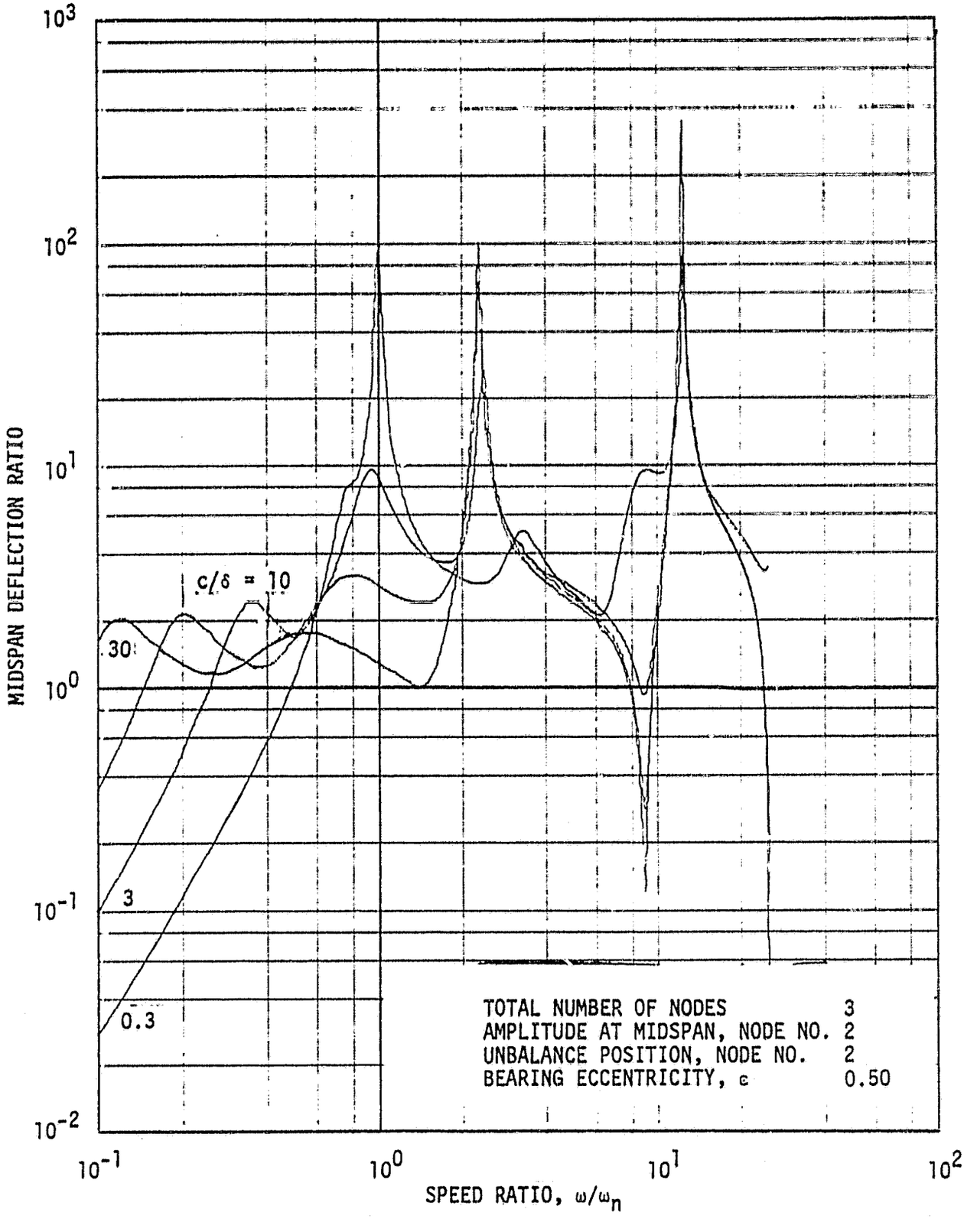

Figure 17. Midspan Unbalance Response of Uniform Rotor in End Bearings. Case B27. Partial Arc Bearings. $\varepsilon = 0.50$.

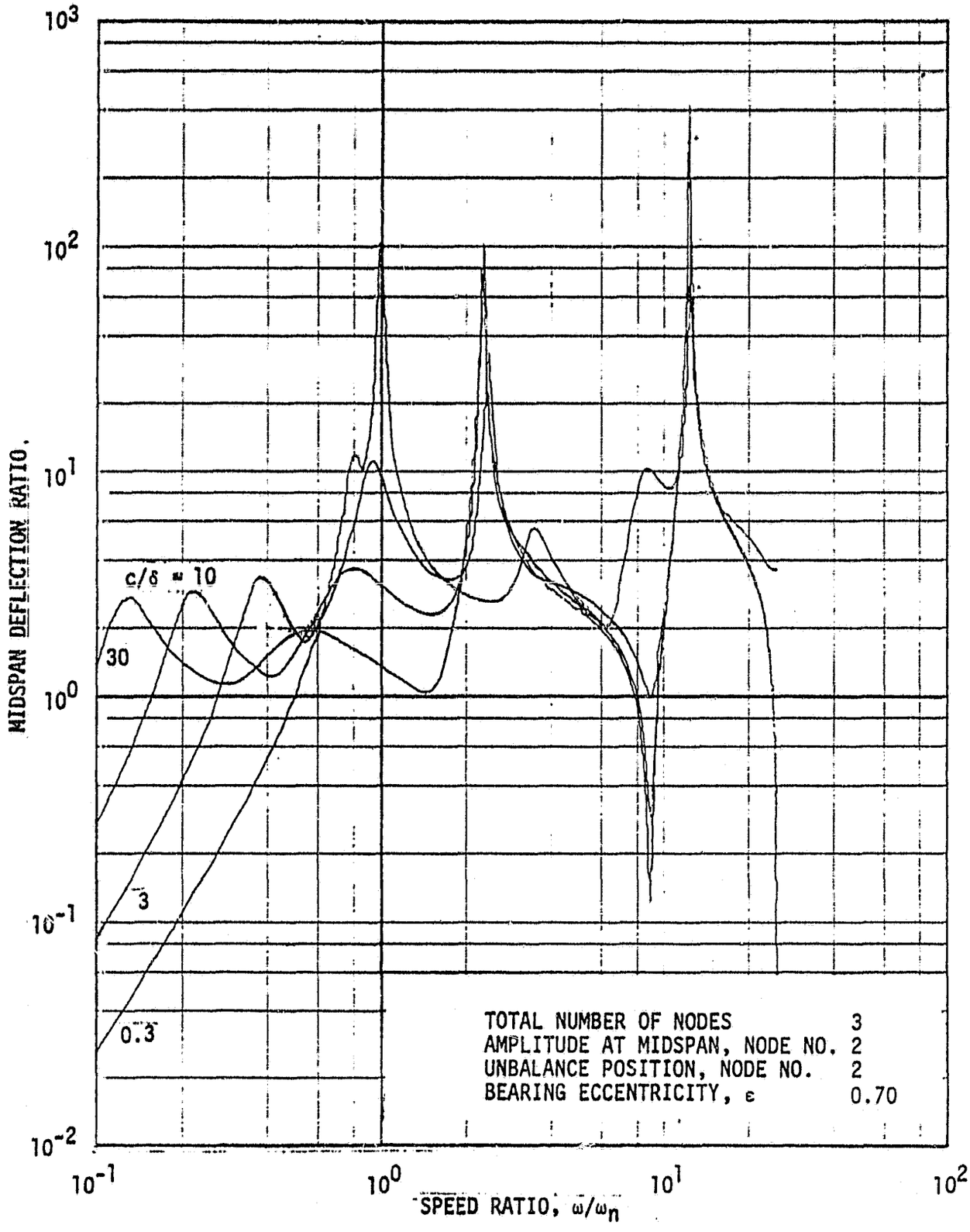

Figure 18. Midspan Unbalance Response of Uniform Rotor in End Bearings. Case B29. Partial Arc Bearings. $\varepsilon = \overline{0.70}$.

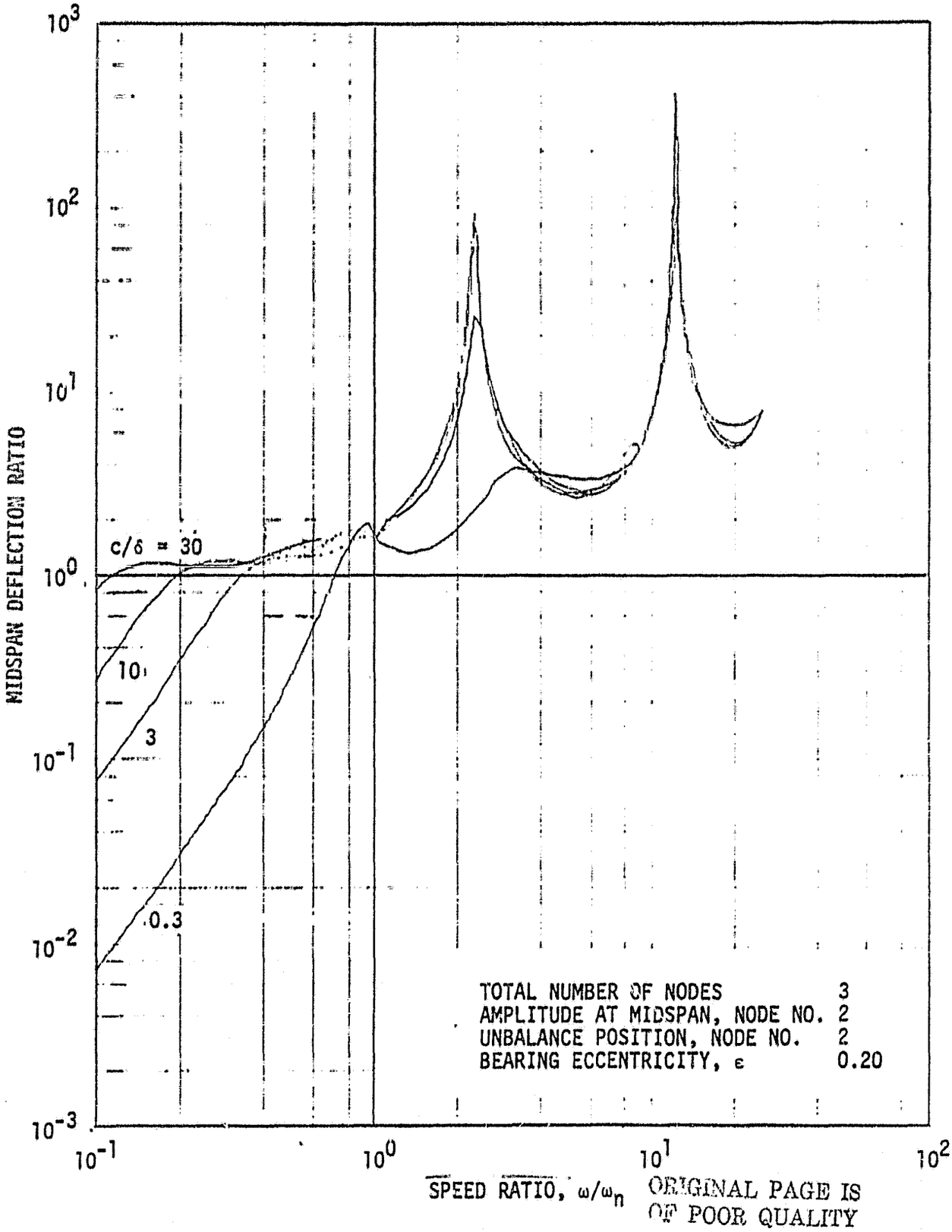

Figure 19. Journal Unbalance Response of Uniform Rotor in End Bearings. Case B31. Partial Arc Bearings. $\varepsilon = 0.20$.

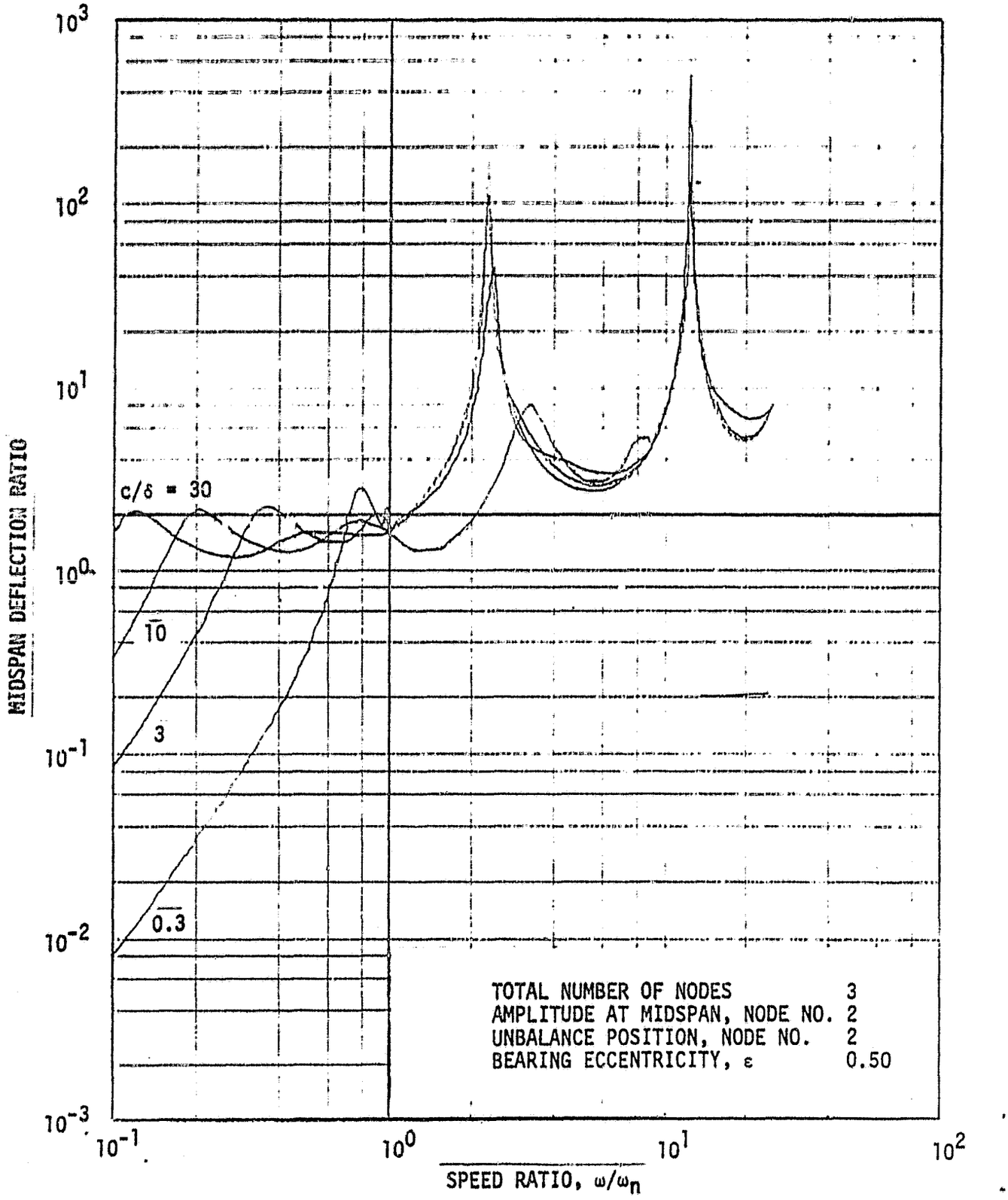

Figure 20. Journal Unbalance Response of Uniform Rotor in End Bearings. Case B33. Partial Arc Bearings. $\varepsilon = 0.50$.

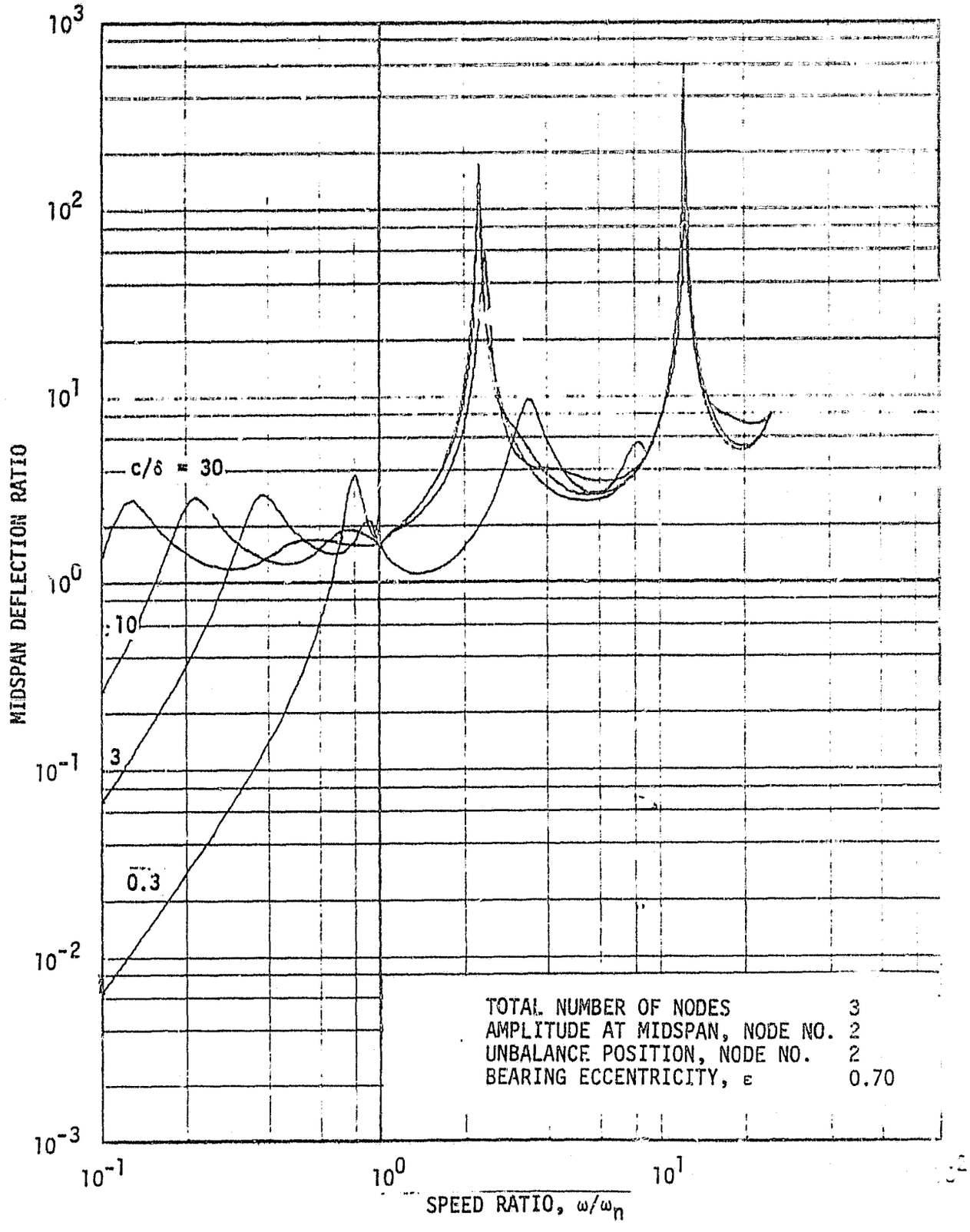

Figure 21. Journal Unbalance Response of Uniform Rotor in End Bear... Case B35. Partial Arc Bearings. $\varepsilon = 0.70$.

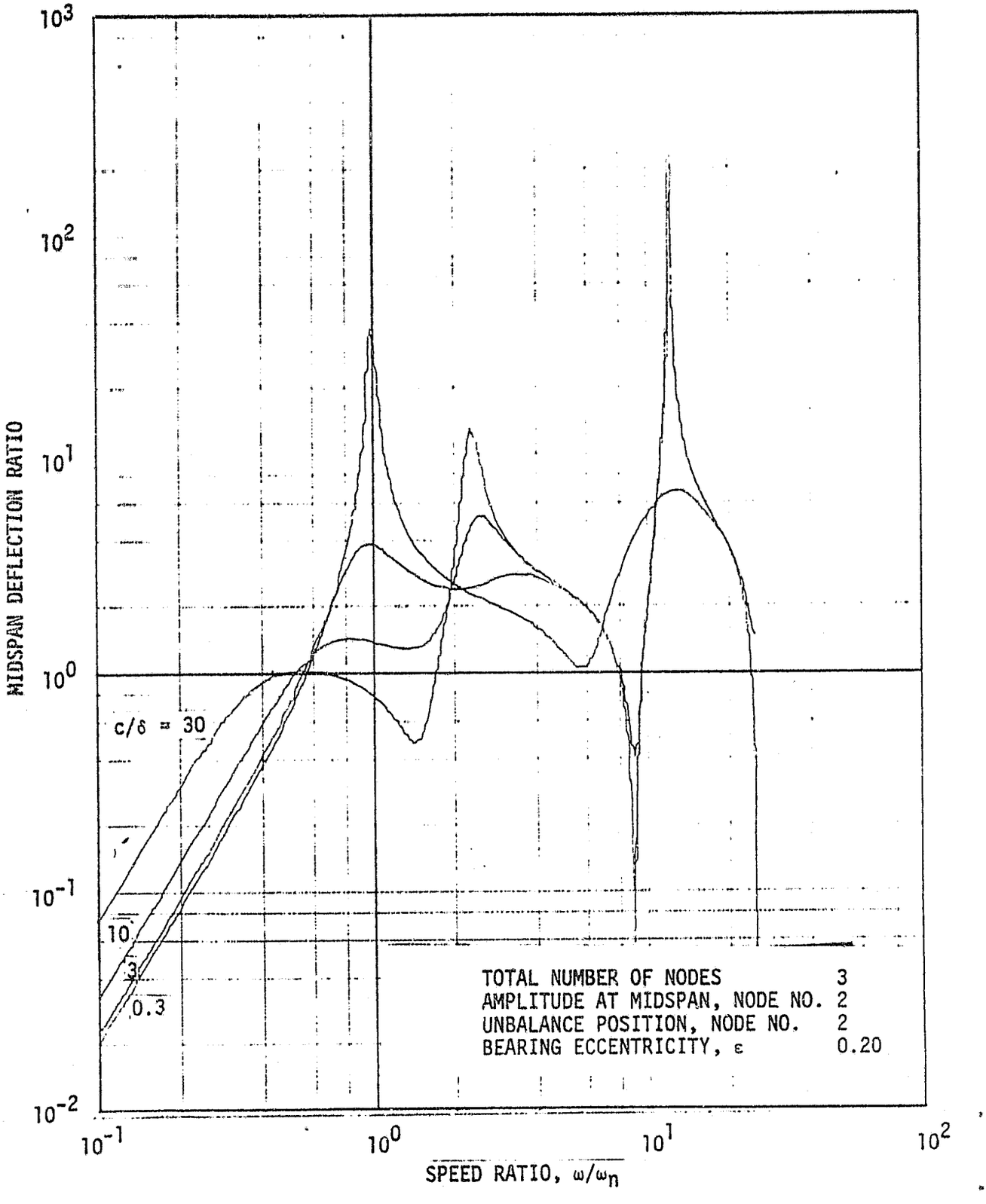

Figure 22. Midspan Unbalance Response of Uniform Rotor in End Bearings. Case B37. Tilting Pad Bearings. $\varepsilon = 0.20$.

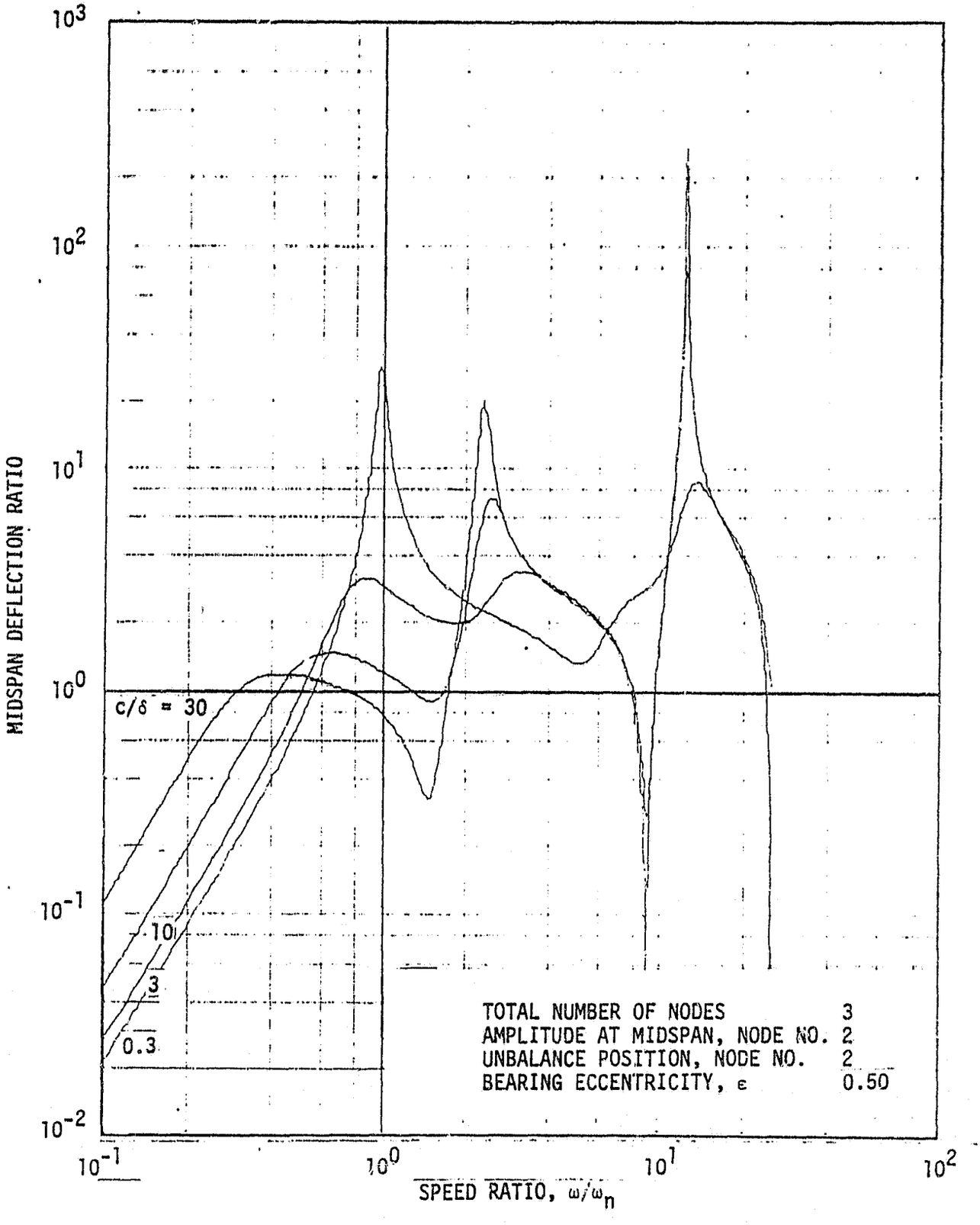

Figure 23. Midspan Unbalance Response of Uniform Rotor in End Bearings. Case B39. Tilting Pad Bearings. $\varepsilon = 0.50$.

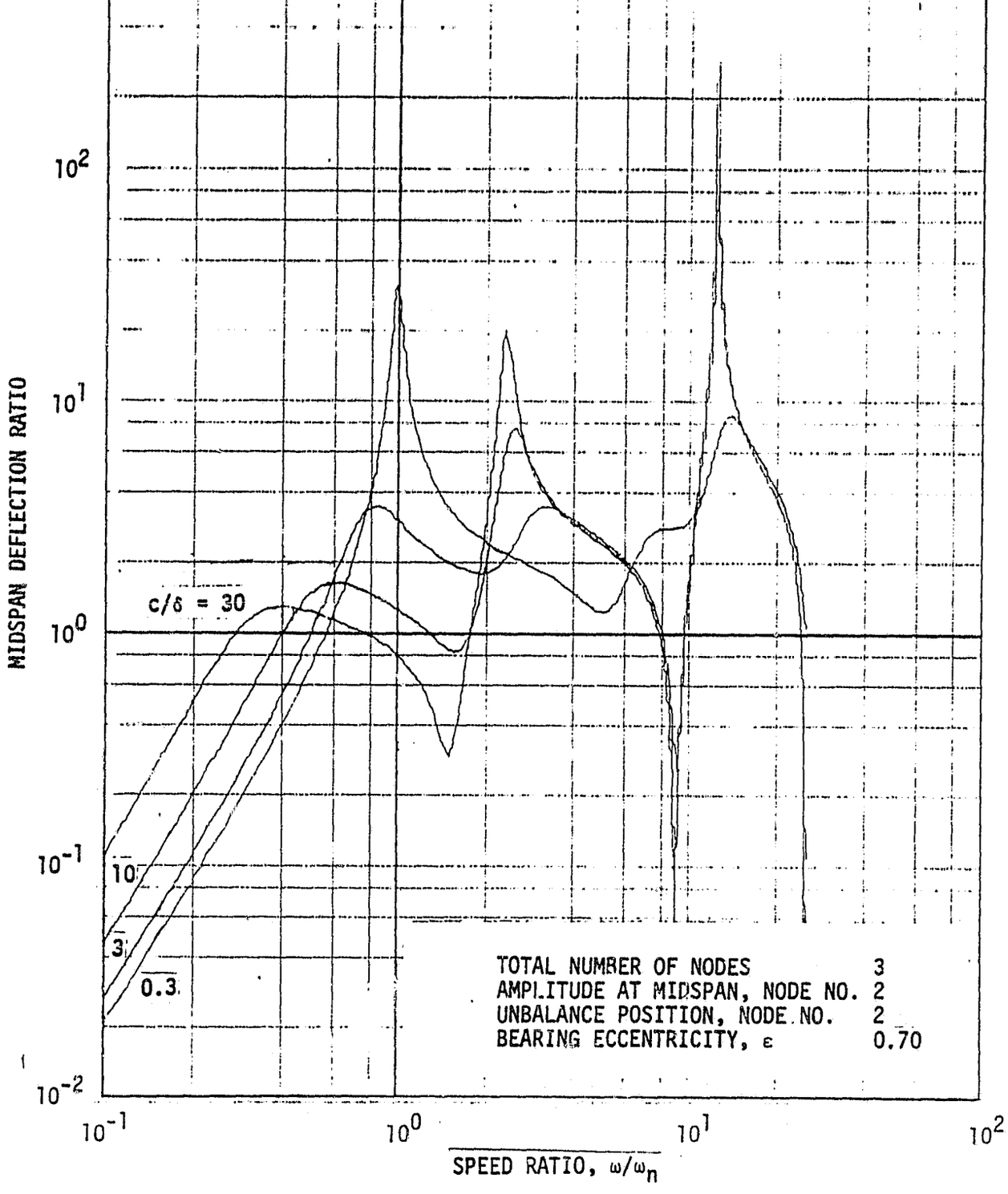

Figure 24. Midspan Unbalance Response of Uniform Rotor in End Bearings. Case B41. Tilting Pad Bearings. $\varepsilon = 0.70$.

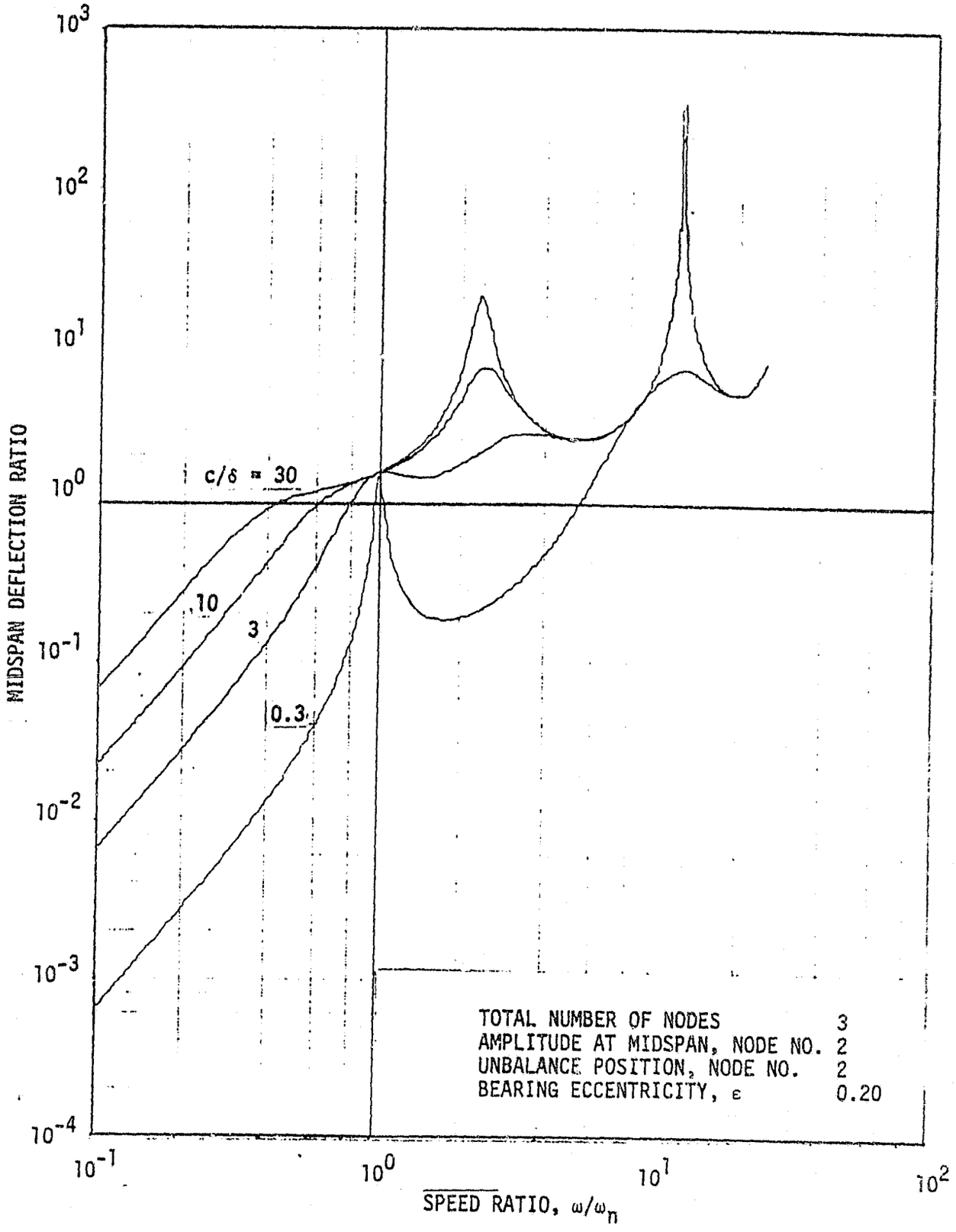

Figure 25. Journal Unbalance Response of Uniform Rotor in End Bearings. Case B43. Tilting Pad Bearings. $\varepsilon = 0.20$.

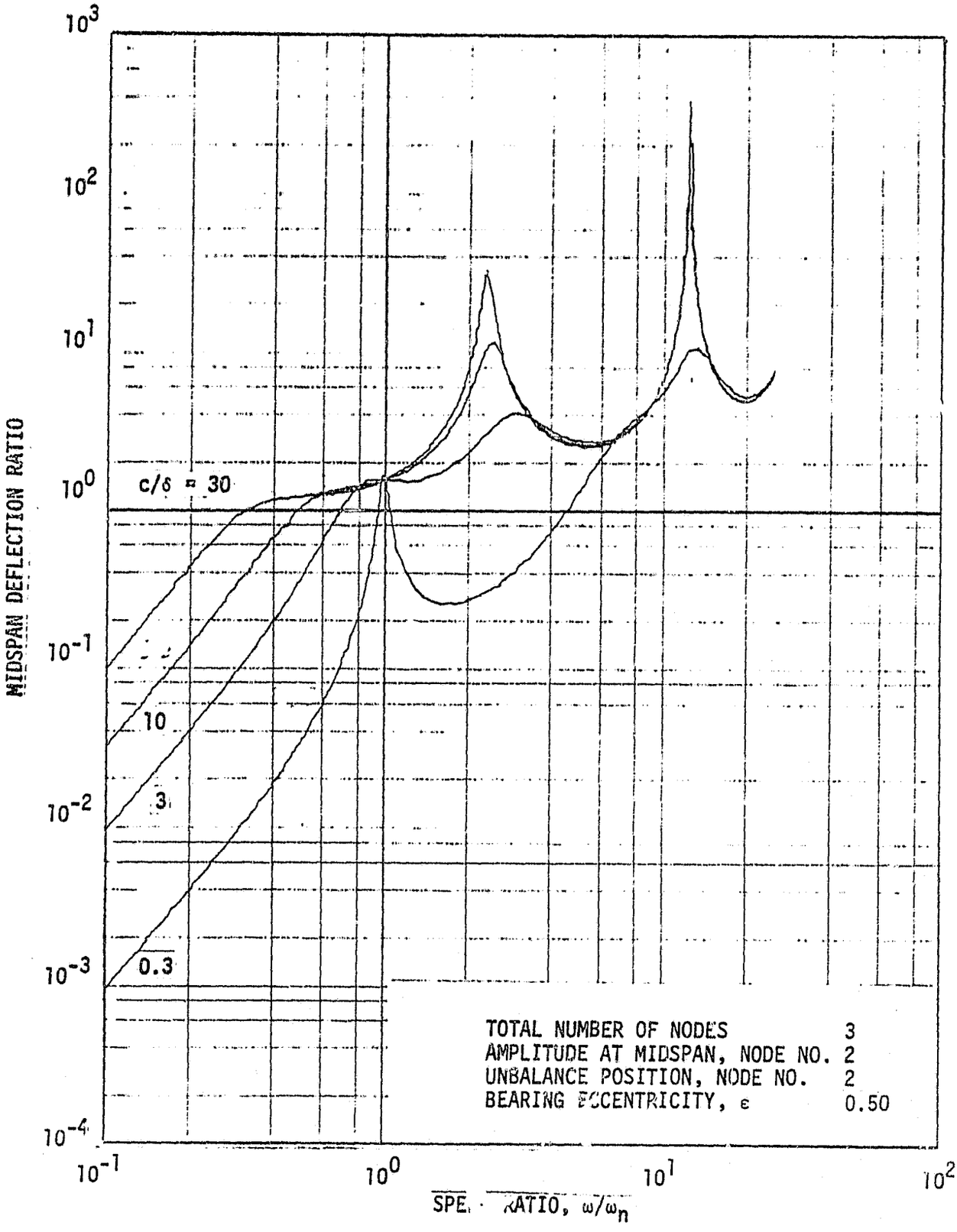

Figure 26. Journal Unbalance Response of Uniform Rotor in End Bearings. Case B45. Tilting Pad Bearings. $\varepsilon = 0.50$.

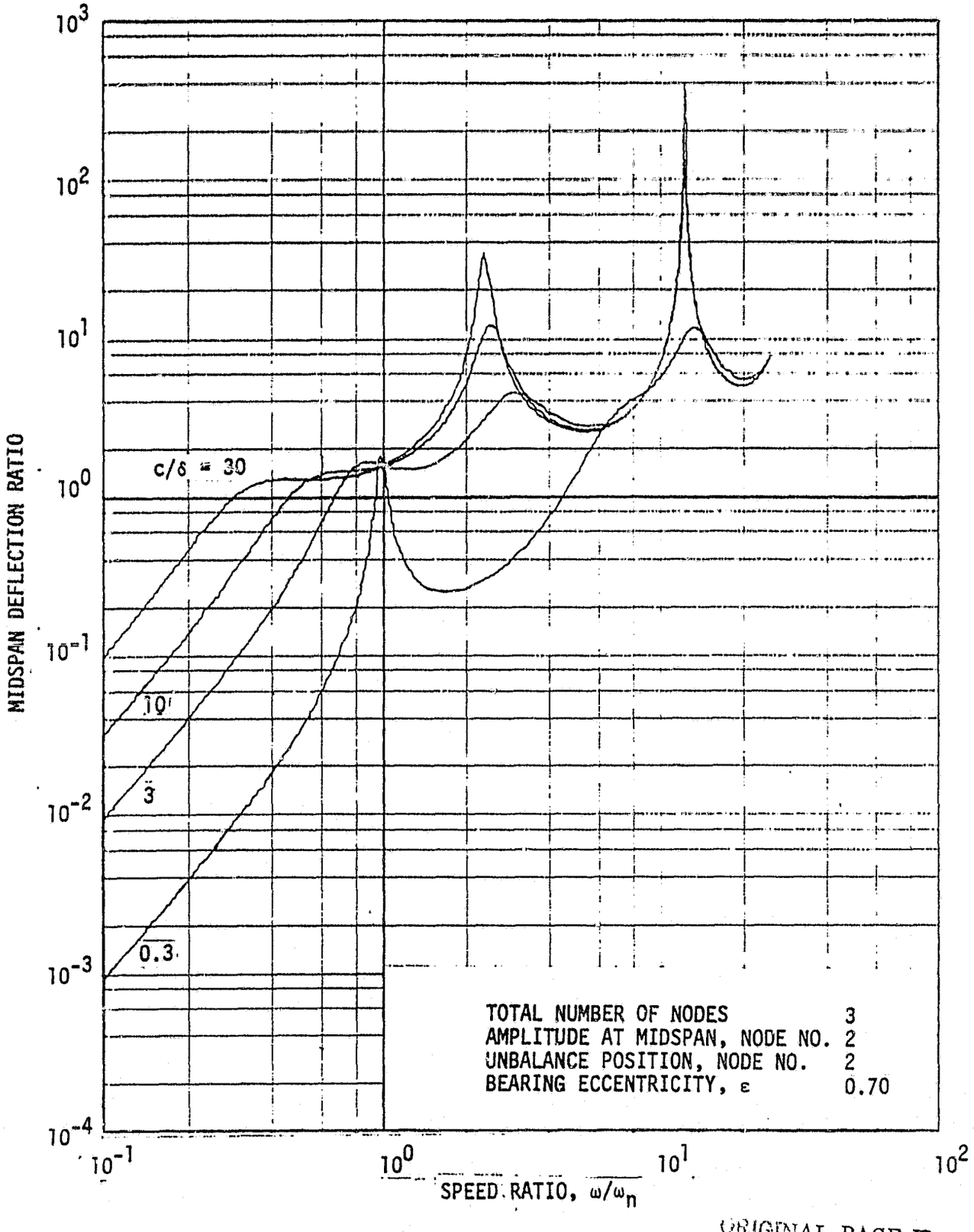

Figure 27. Journal Unbalance Response of Uniform Rotor in End Bearings. Case B47. Tilting Pad Bearings. $\varepsilon = 0.70$.

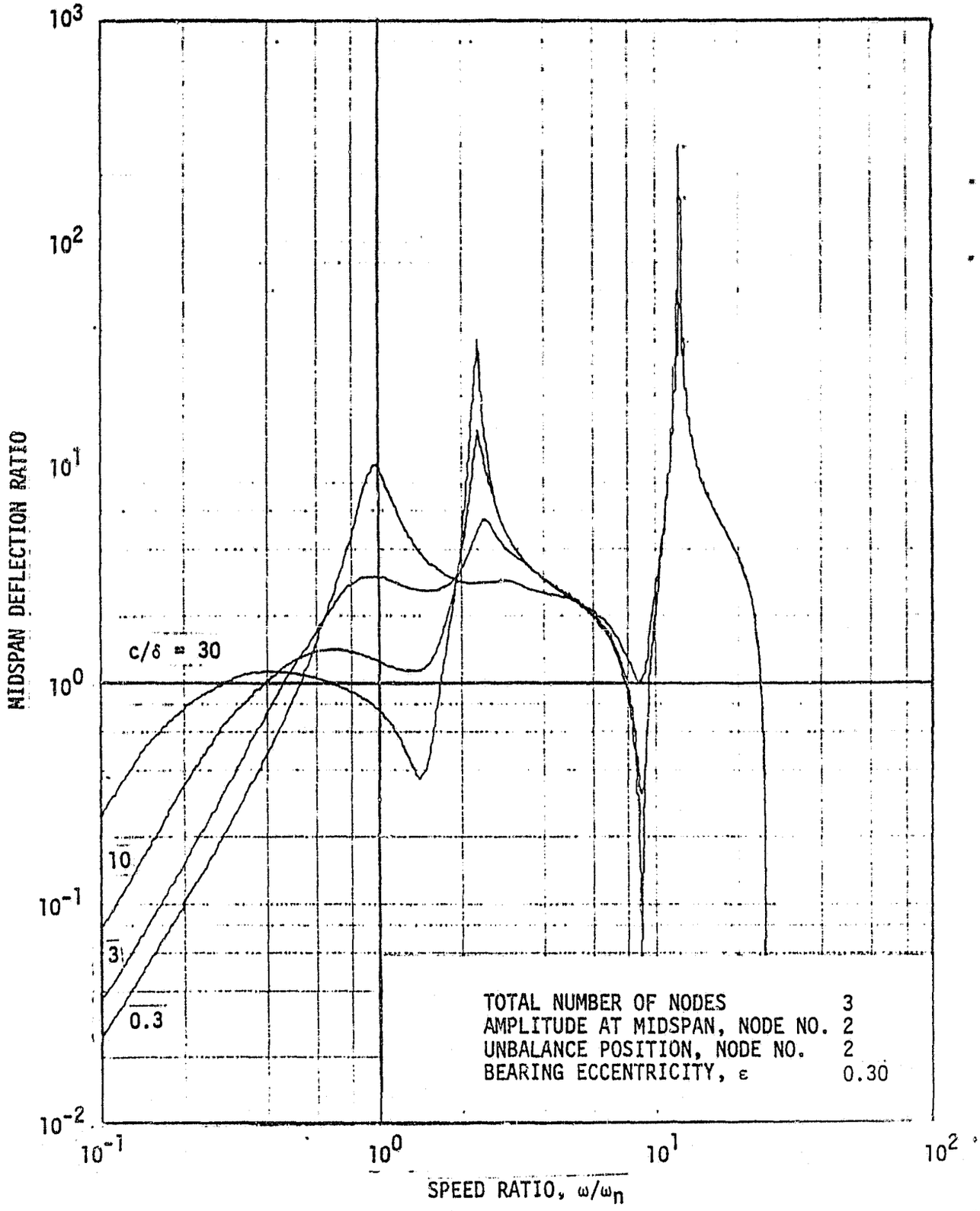

Figure 28. Midspan Unbalance Response of Uniform Rotor in End Bearings. Case B49. Plain Cylindrical Bearings. $\varepsilon = 0.30$.

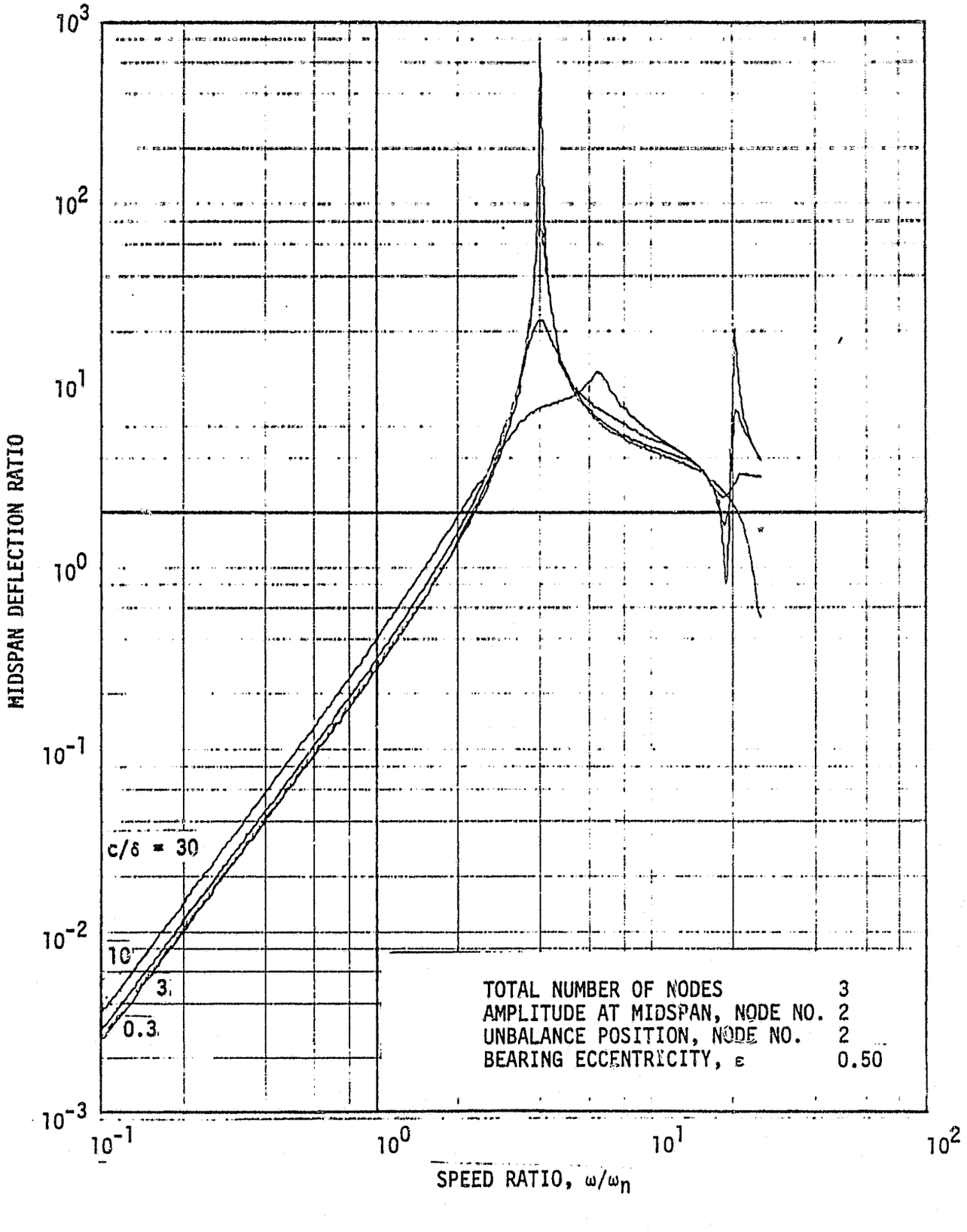

Figure 29. Quarter Span Unbalance Response of Uniform Rotor in End Bearings. Case B50. Plain Cylindrical Bearings: $\varepsilon = 0.50$.

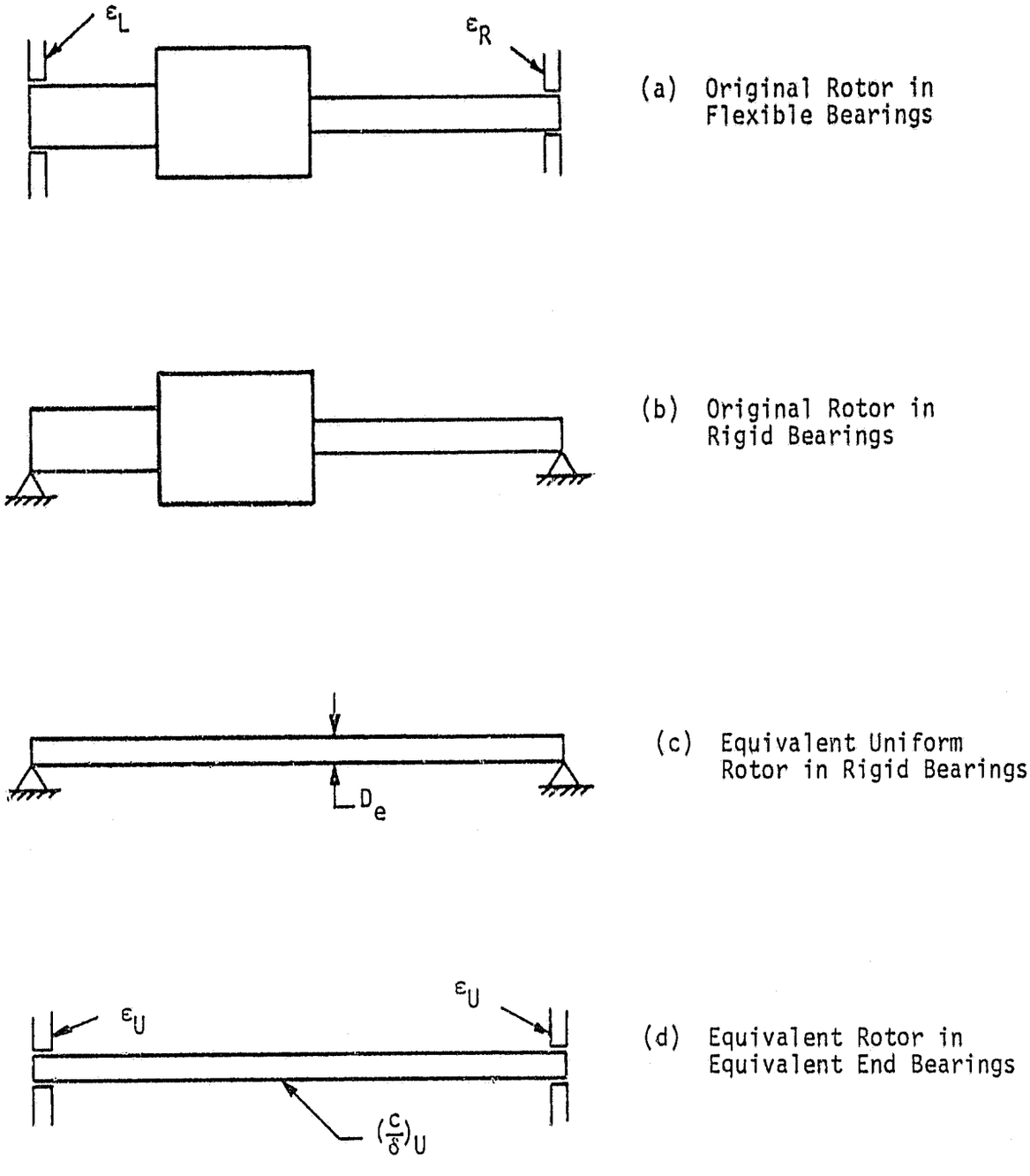

Figure 30. Procedure for Finding an Equivalent Rotor

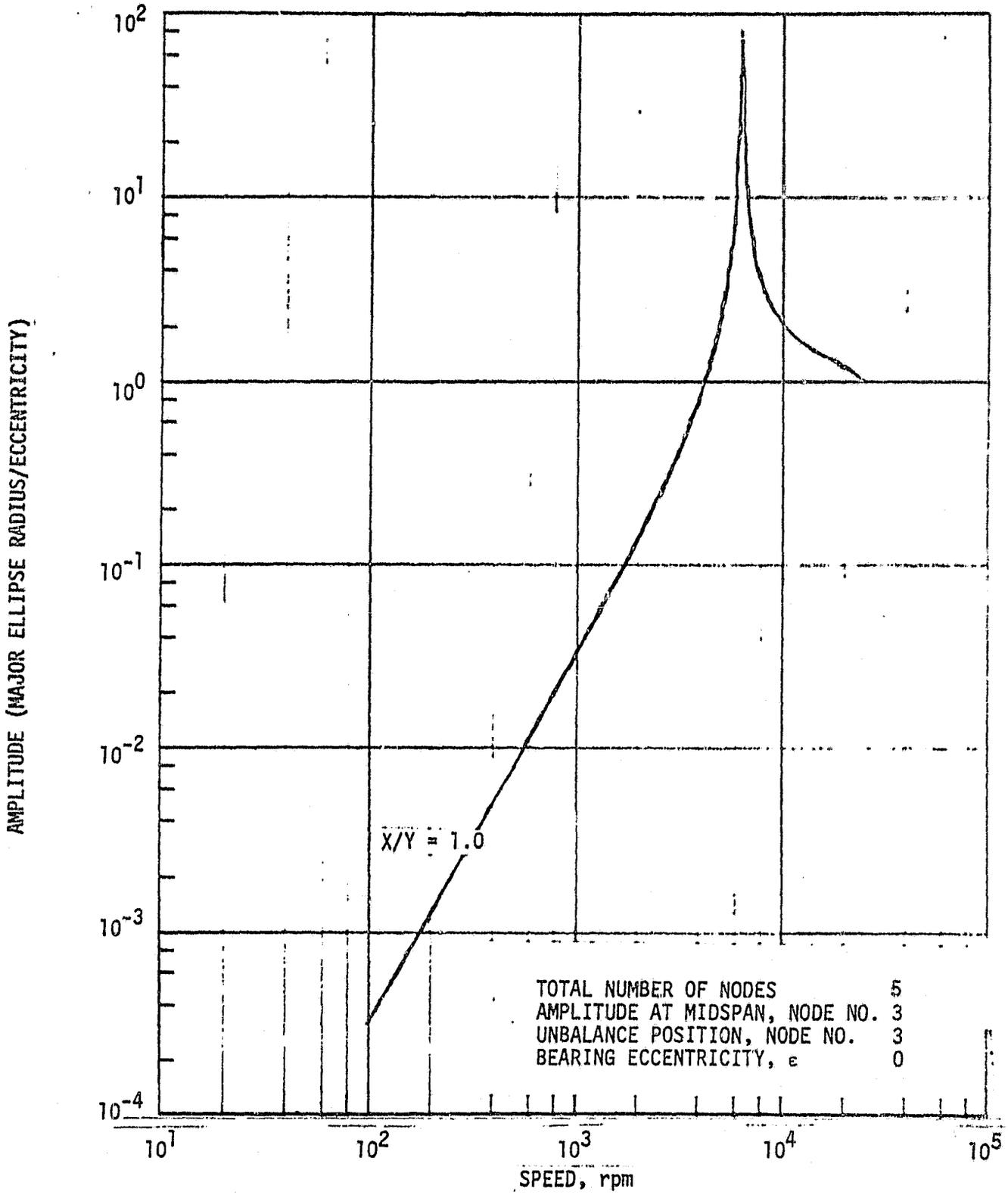

Figure 31. Response of Stepped Rotor. Case 1. Rigid Bearings.

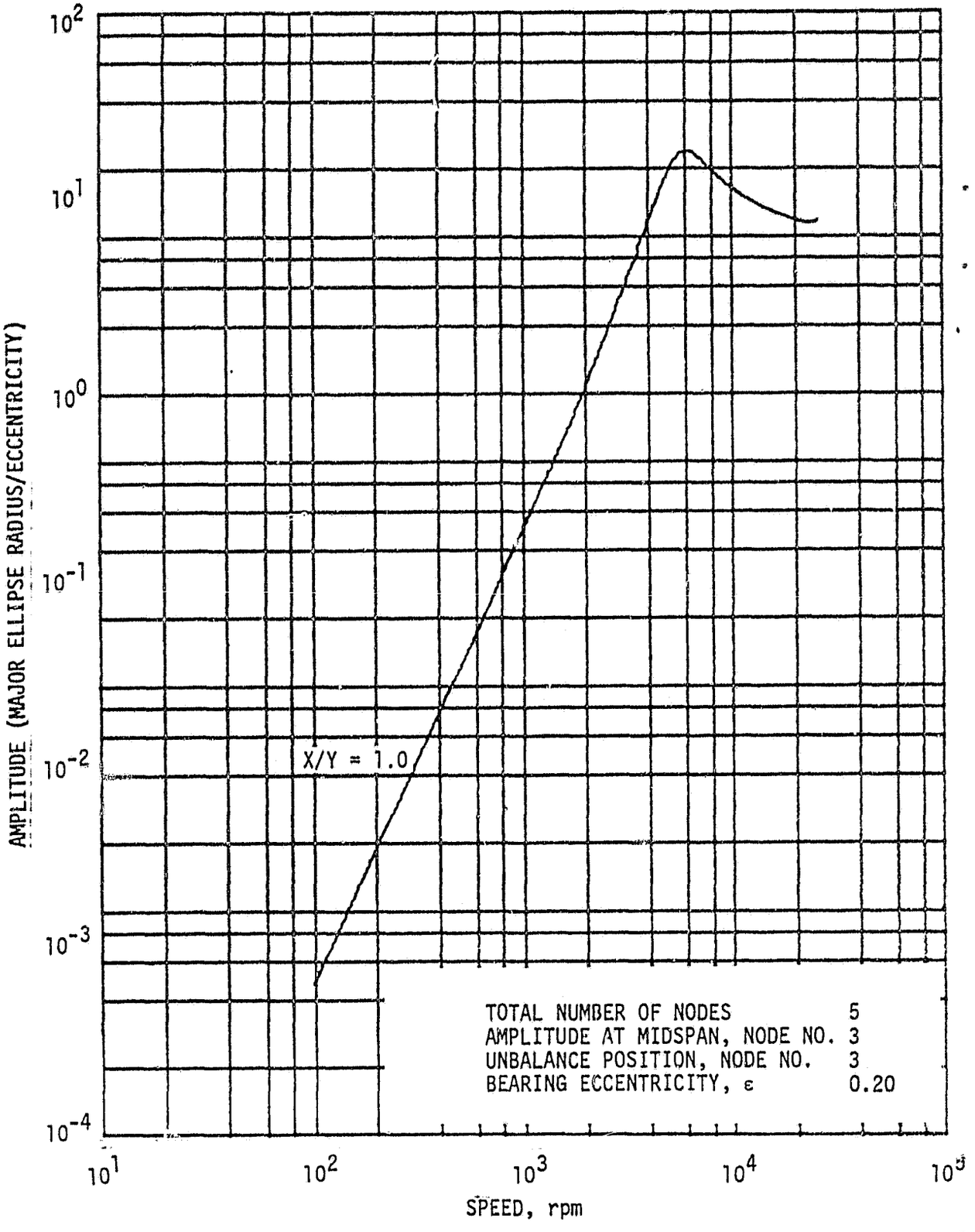

Figure 32. Stepped Rotor Response. Case 1. Plain Cylindrical Bearings.

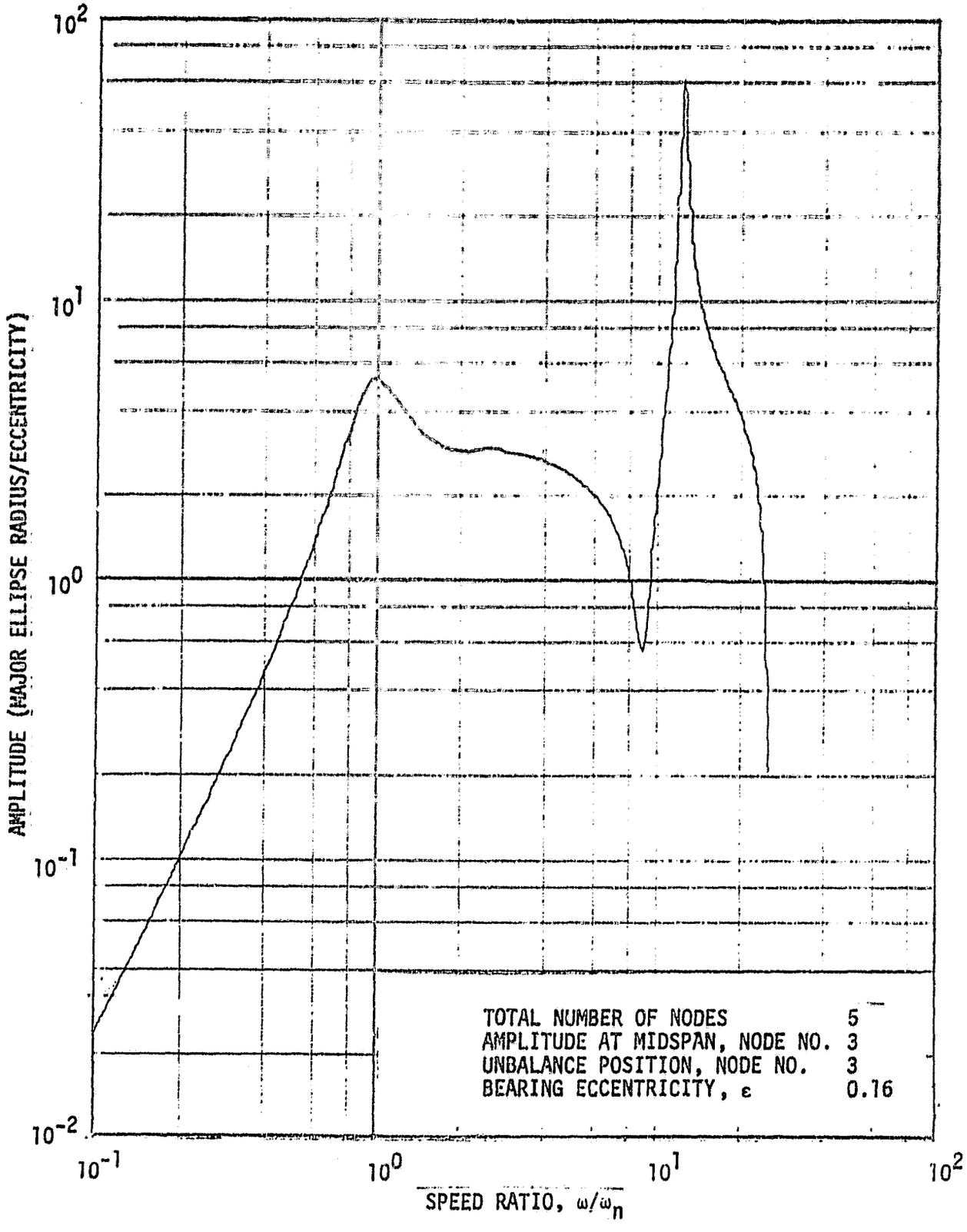

Figure 33. Equivalent Rotor Response. Case 1. Plain Cylindrical Bearings.

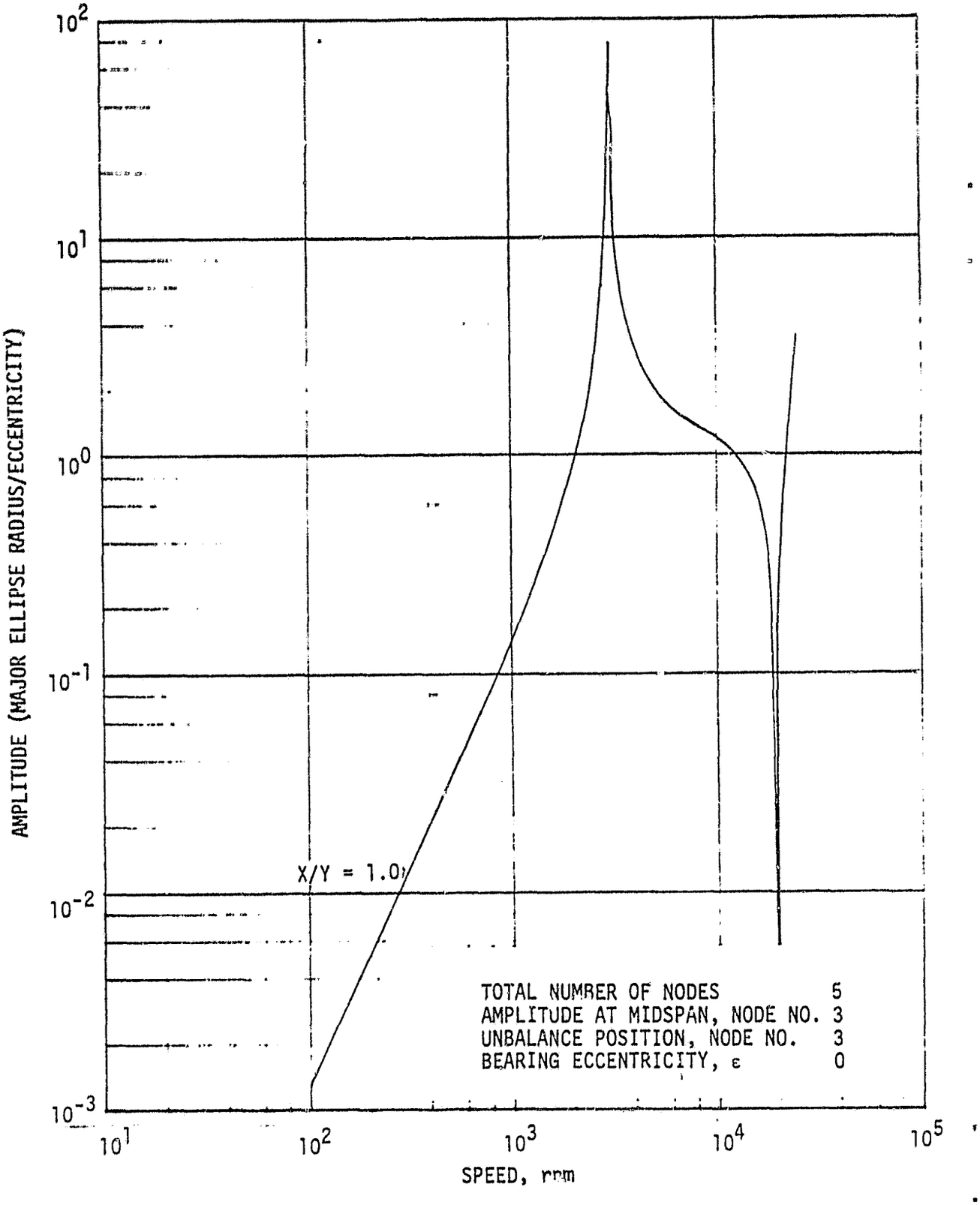

Figure 34. Response of Stepped Rotor. Case 2. Rigid Bearings.

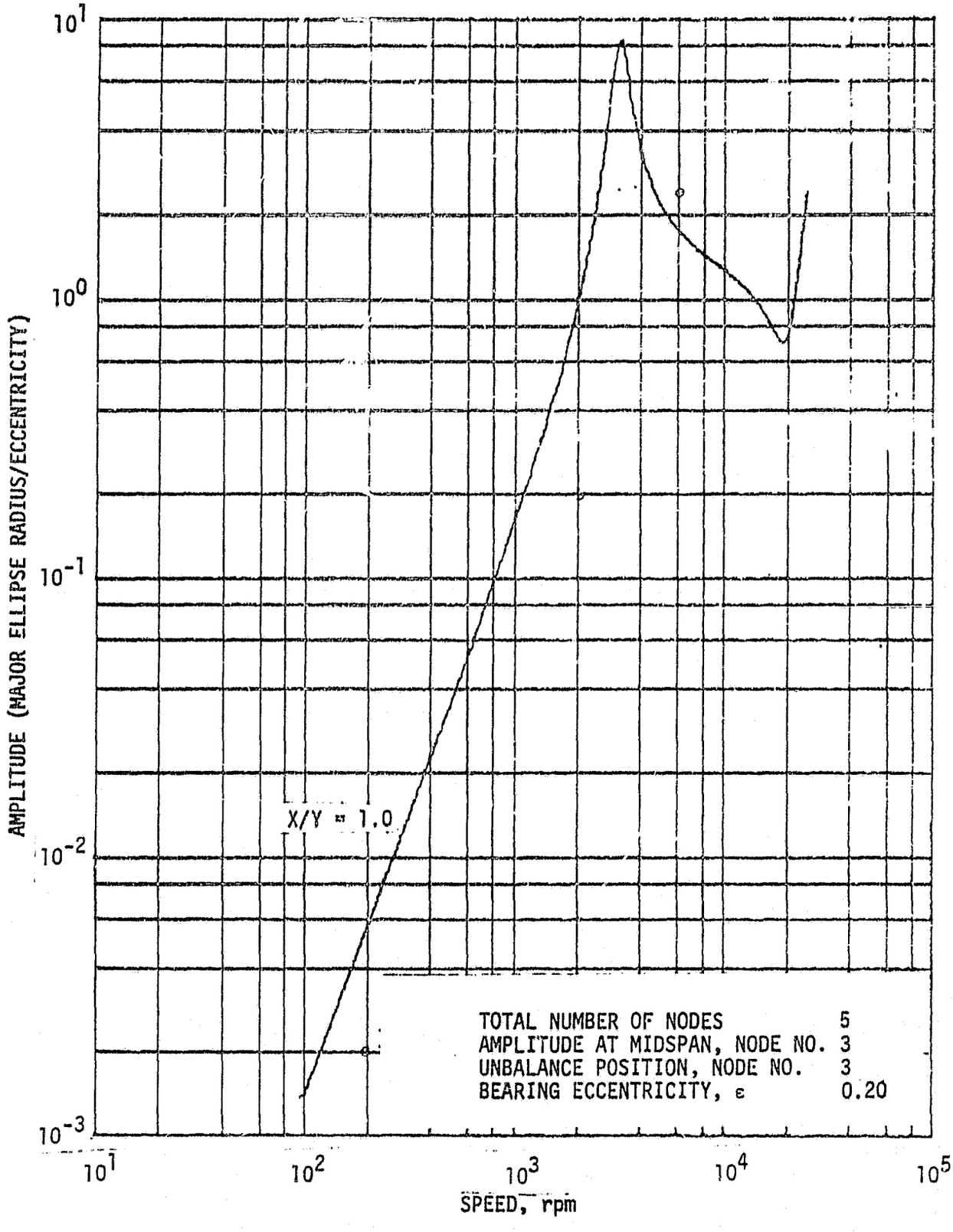

C-2

Figure 35. Response of Stepped Rotor. Case 2. Flexible Bearings.

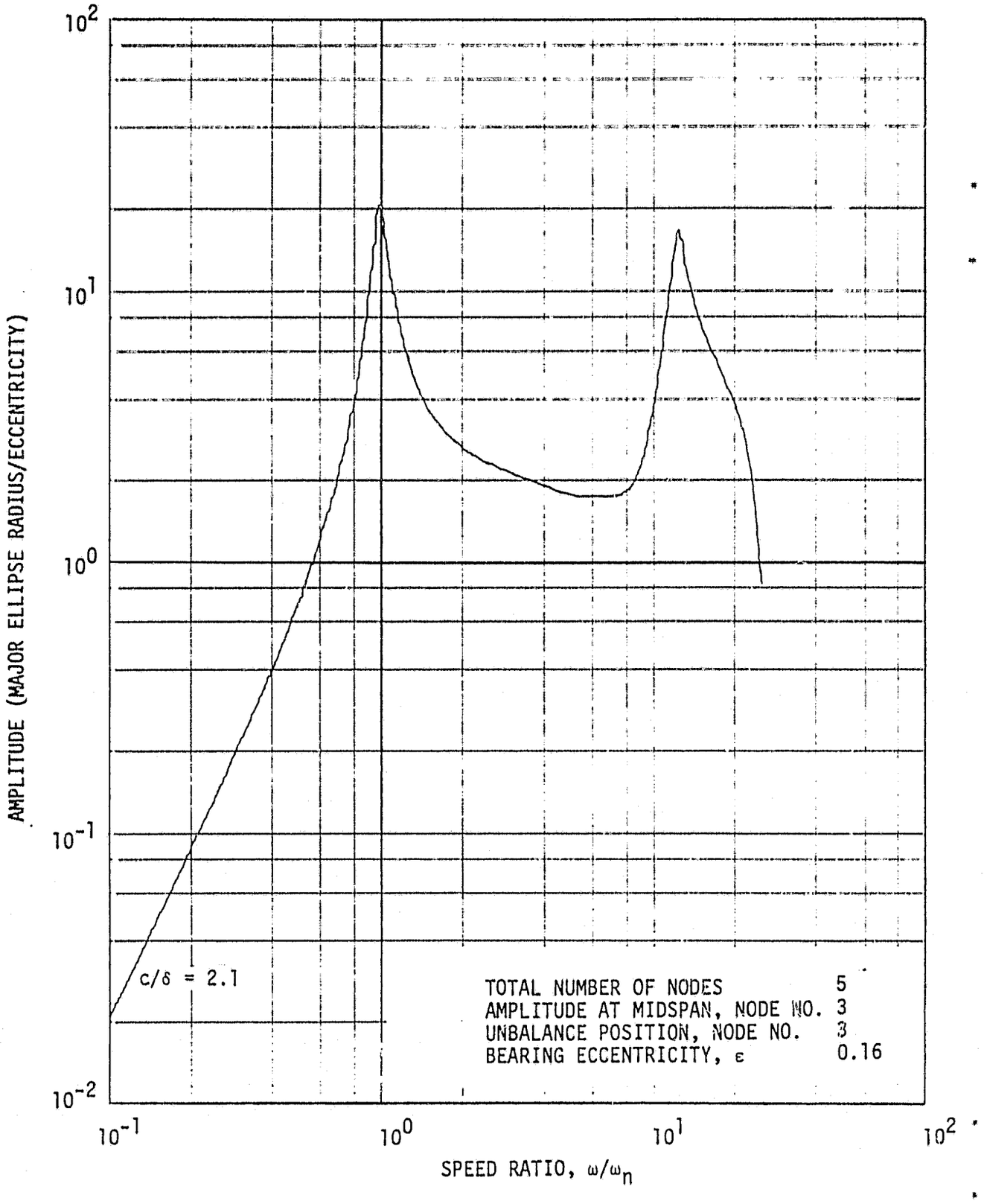

Figure 36. Equivalent Rotor Response. Case 2. Flexible Bearings.

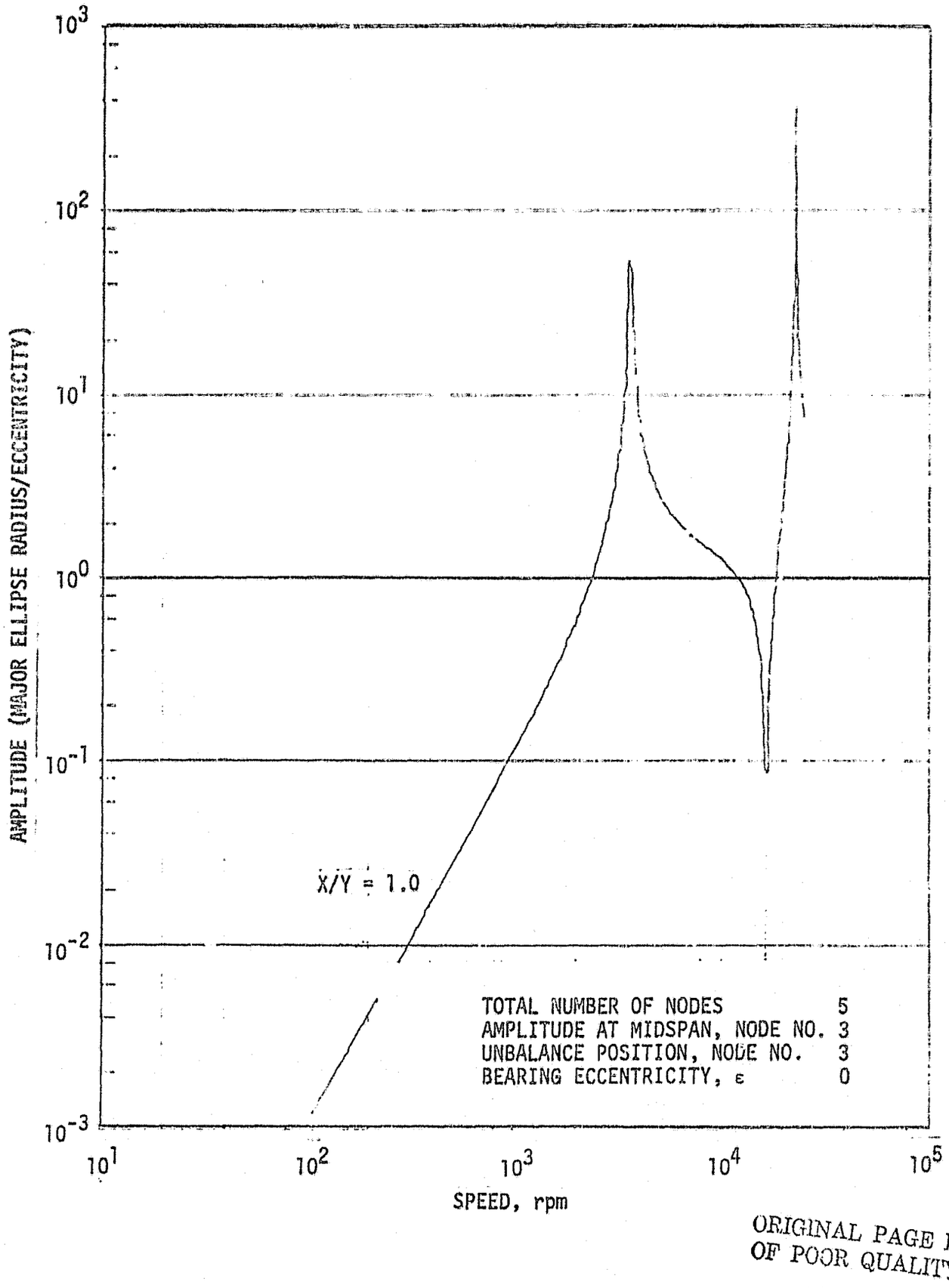

Figure 37. Response of Stepped Rotor. Case 3. Rigid Bearings.

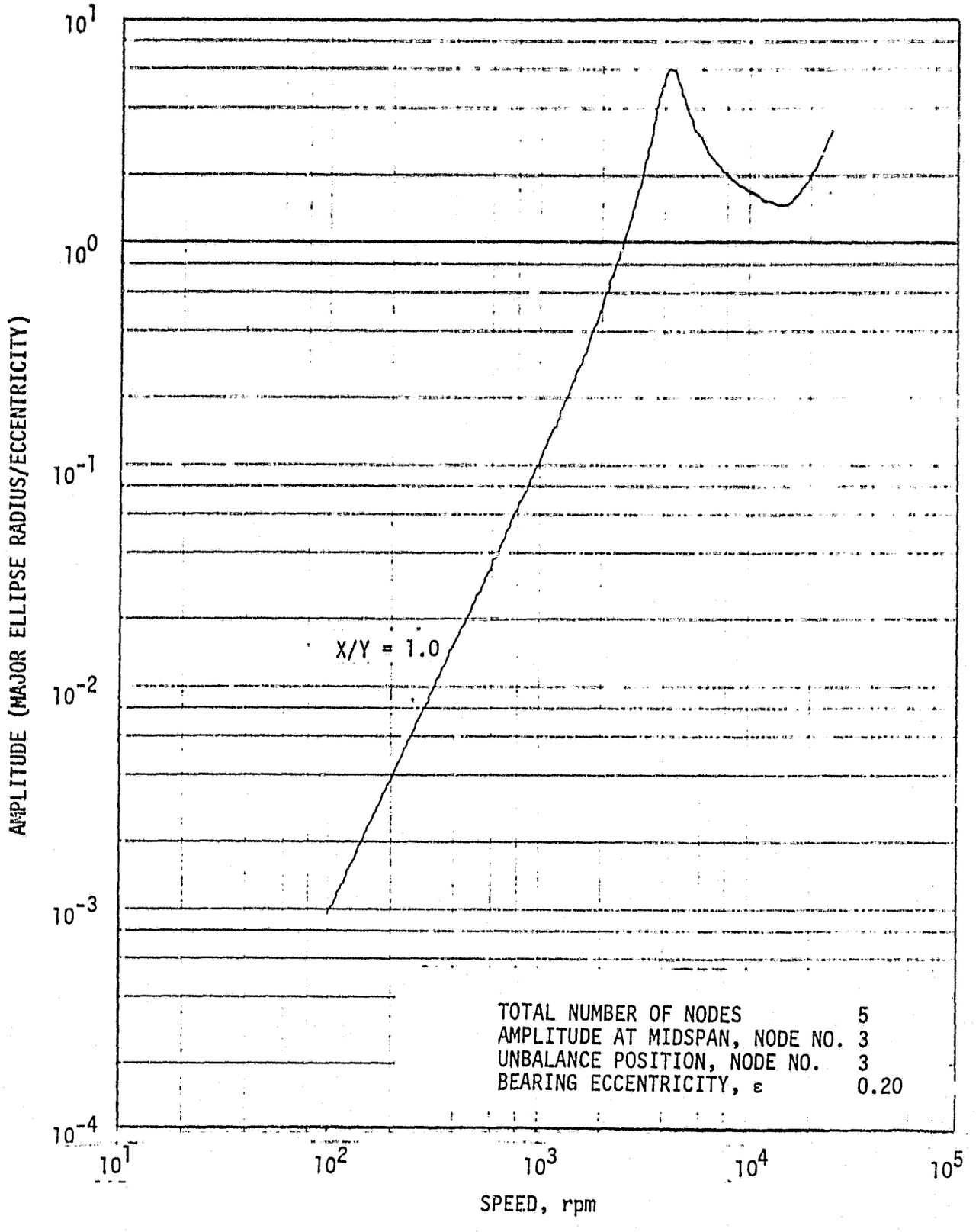

Figure 38. Response of Stepped Rotor. Case 3. Flexible Bearings.

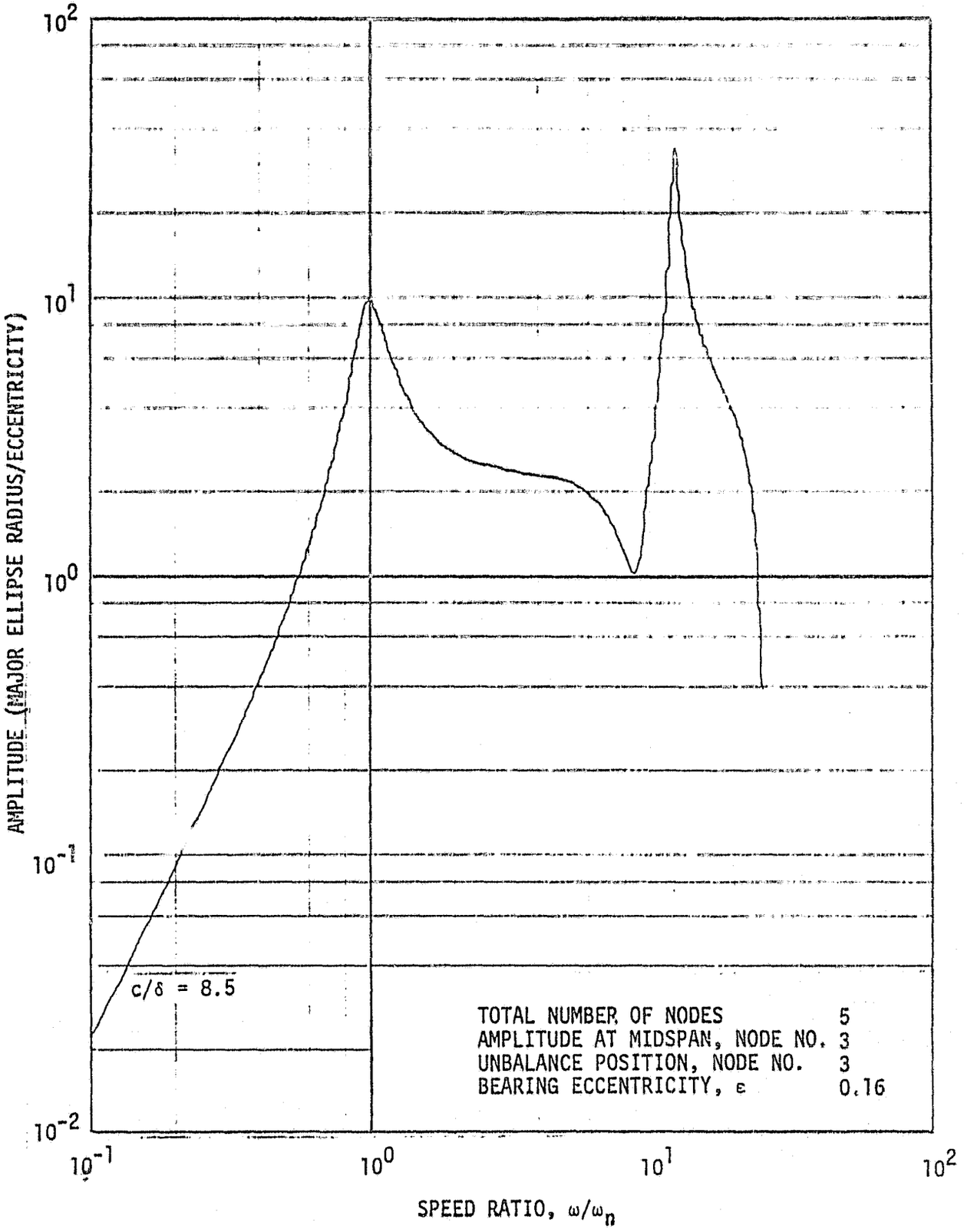

Figure 39. Response of Equivalent Rotor. Case 3. Flexible Bearings.

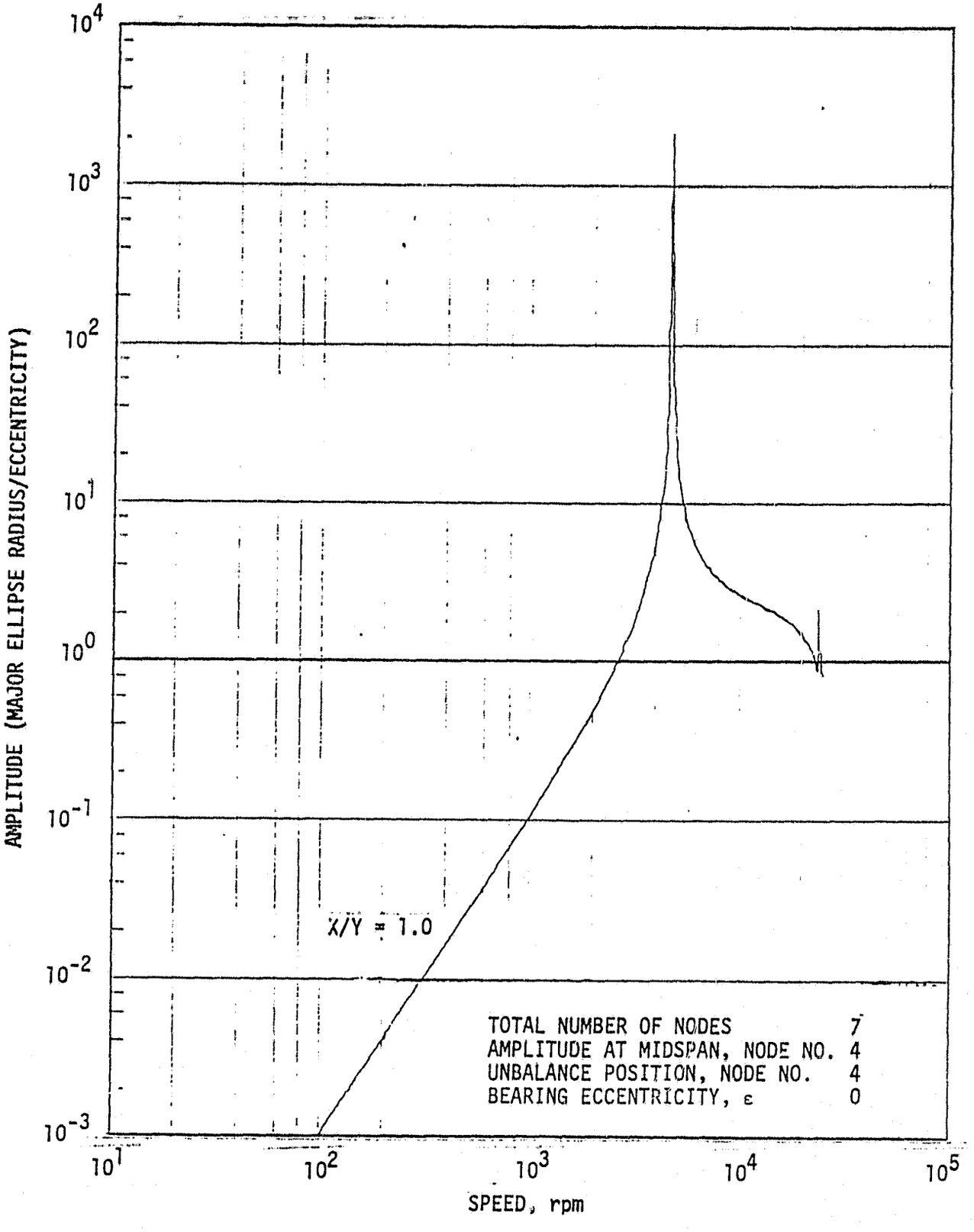

Figure 40. Response of Stepped Rotor. Case 4. Rigid Bearings.

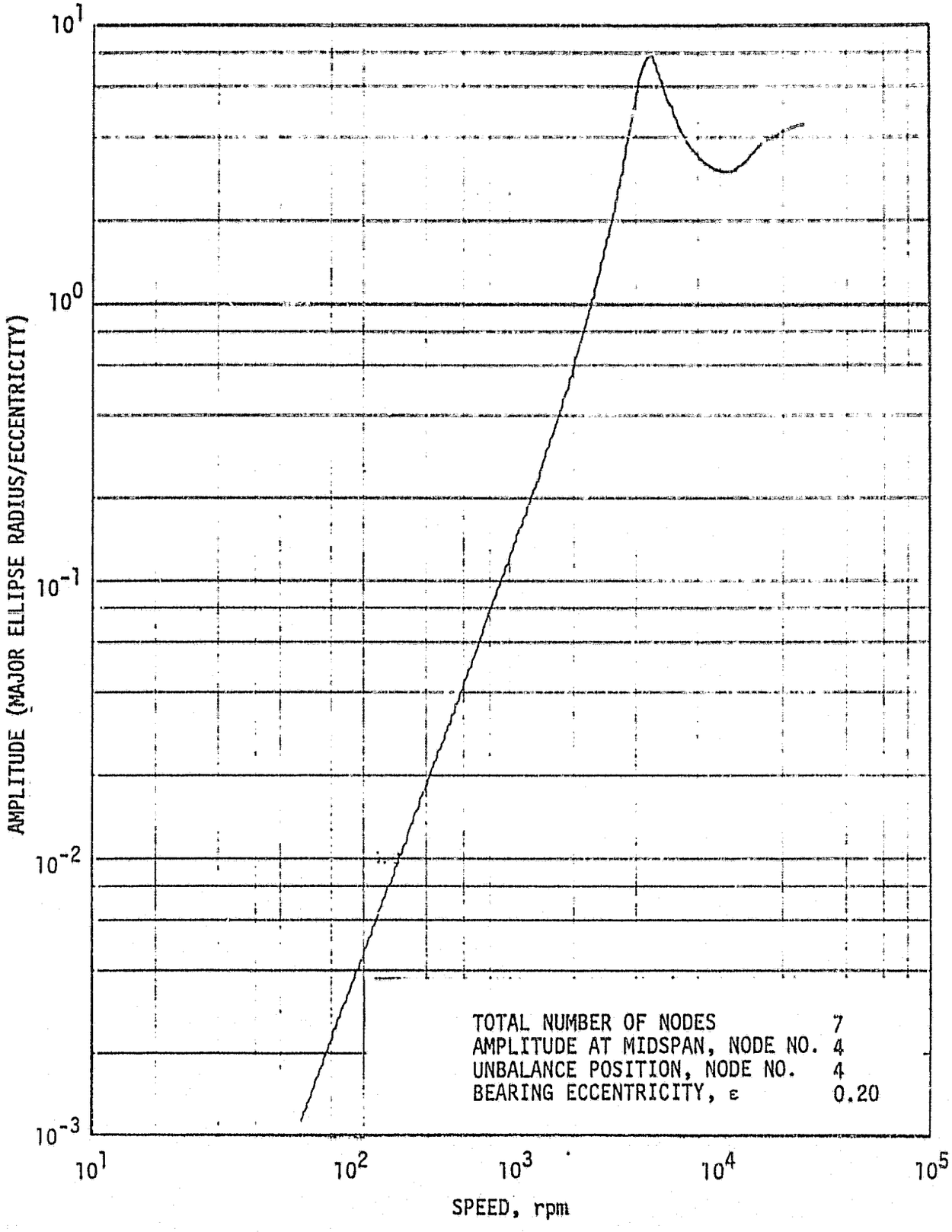

Figure 41. Response of Stepped Rotor. Case 4. Flexible Bearings.

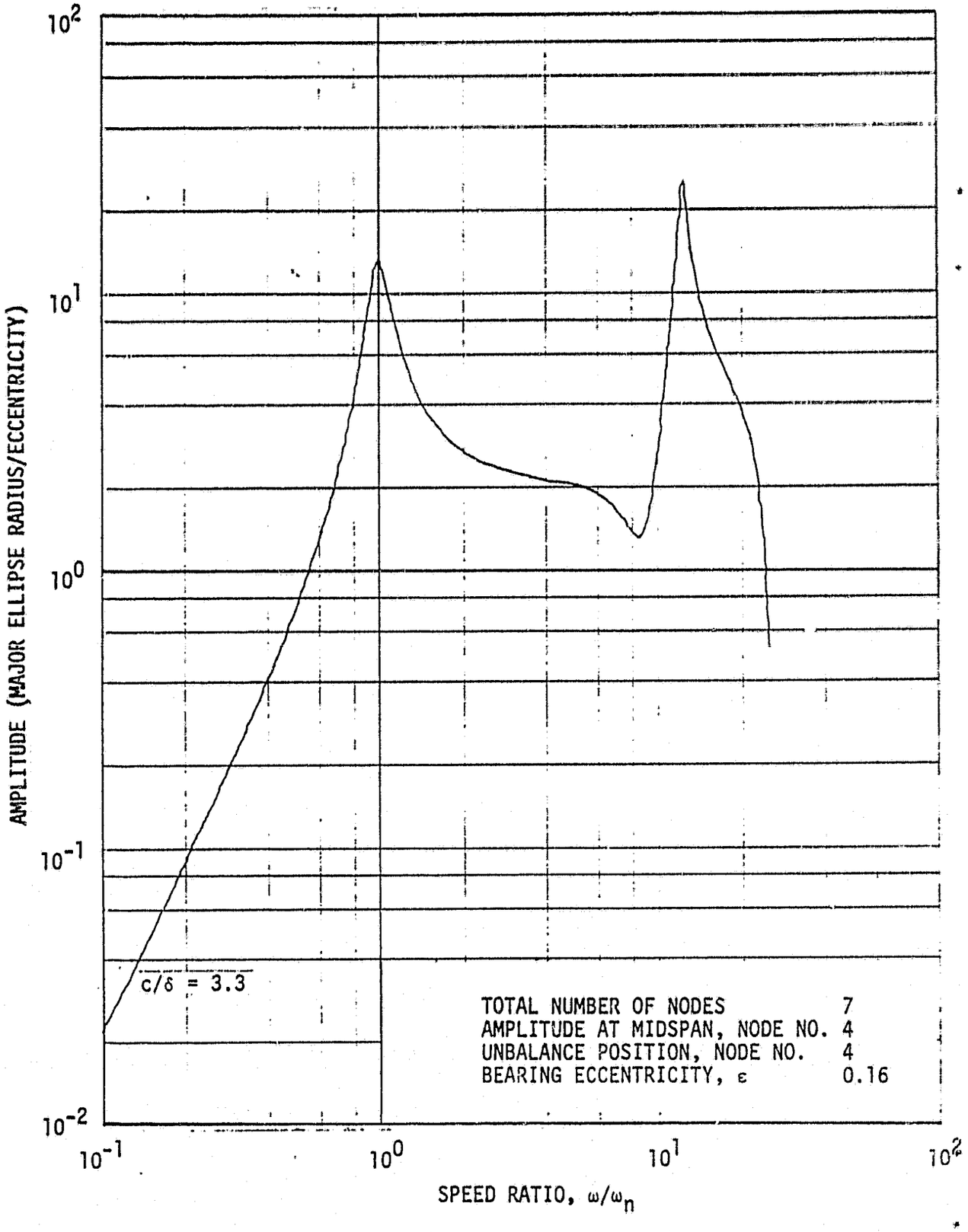

Figure 42. Response of Equivalent Rotor. Case 4. Flexible Bearings

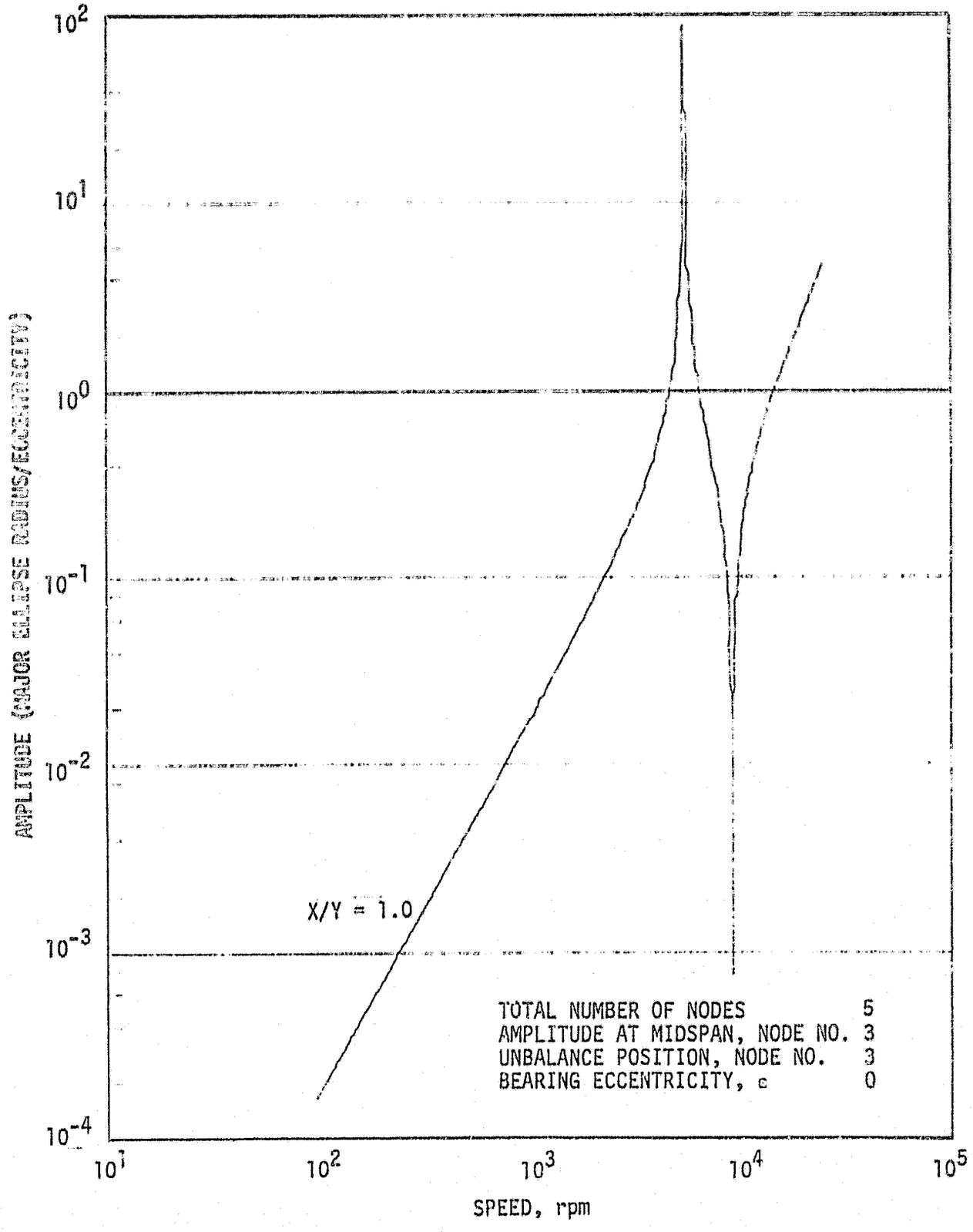

Figure 43. Response of Stepped Rotor. Case 5. Rigid Bearings.

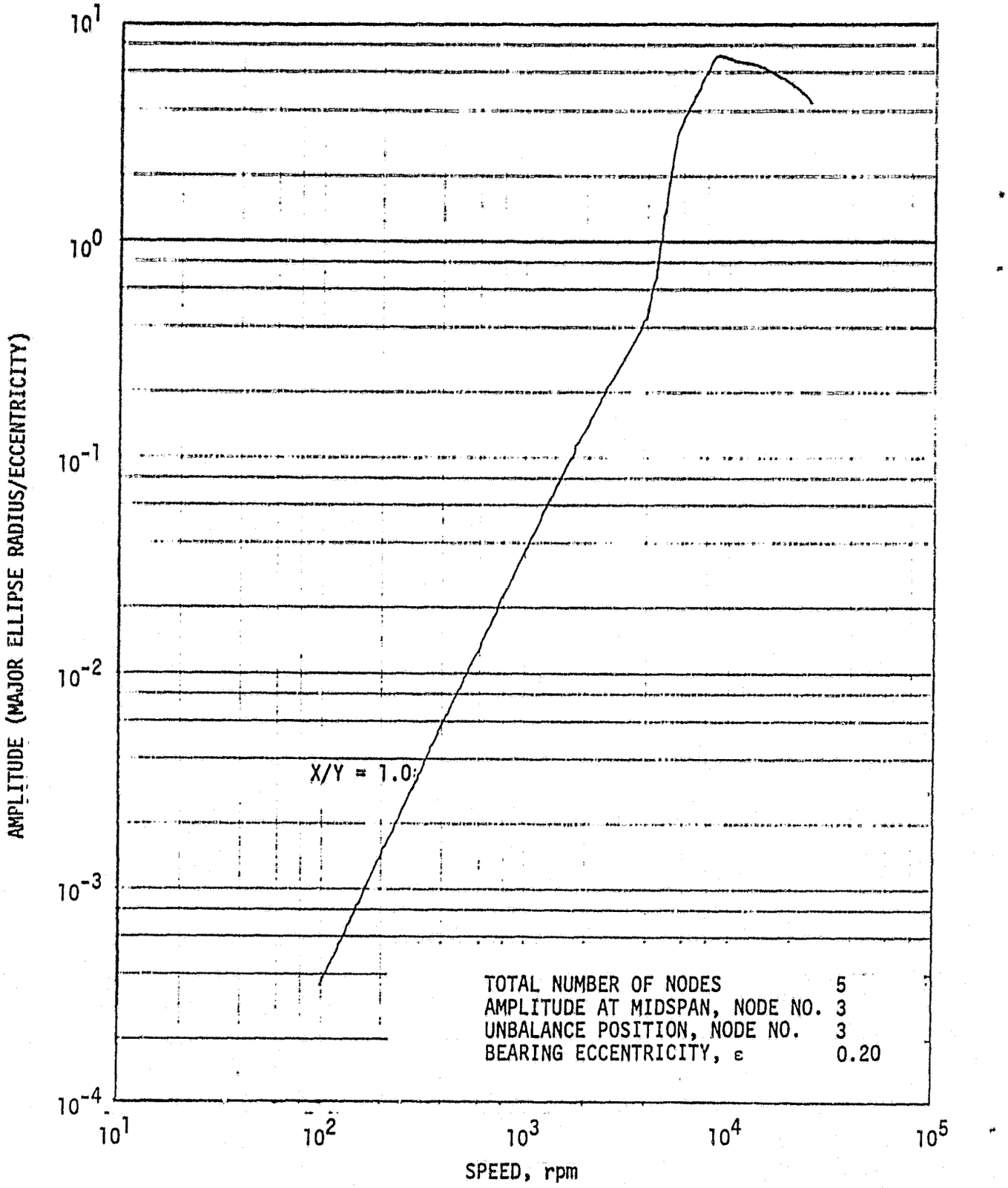

Figure 44. Response of Stepped Rotor. Case 5. Flexible Bearings.

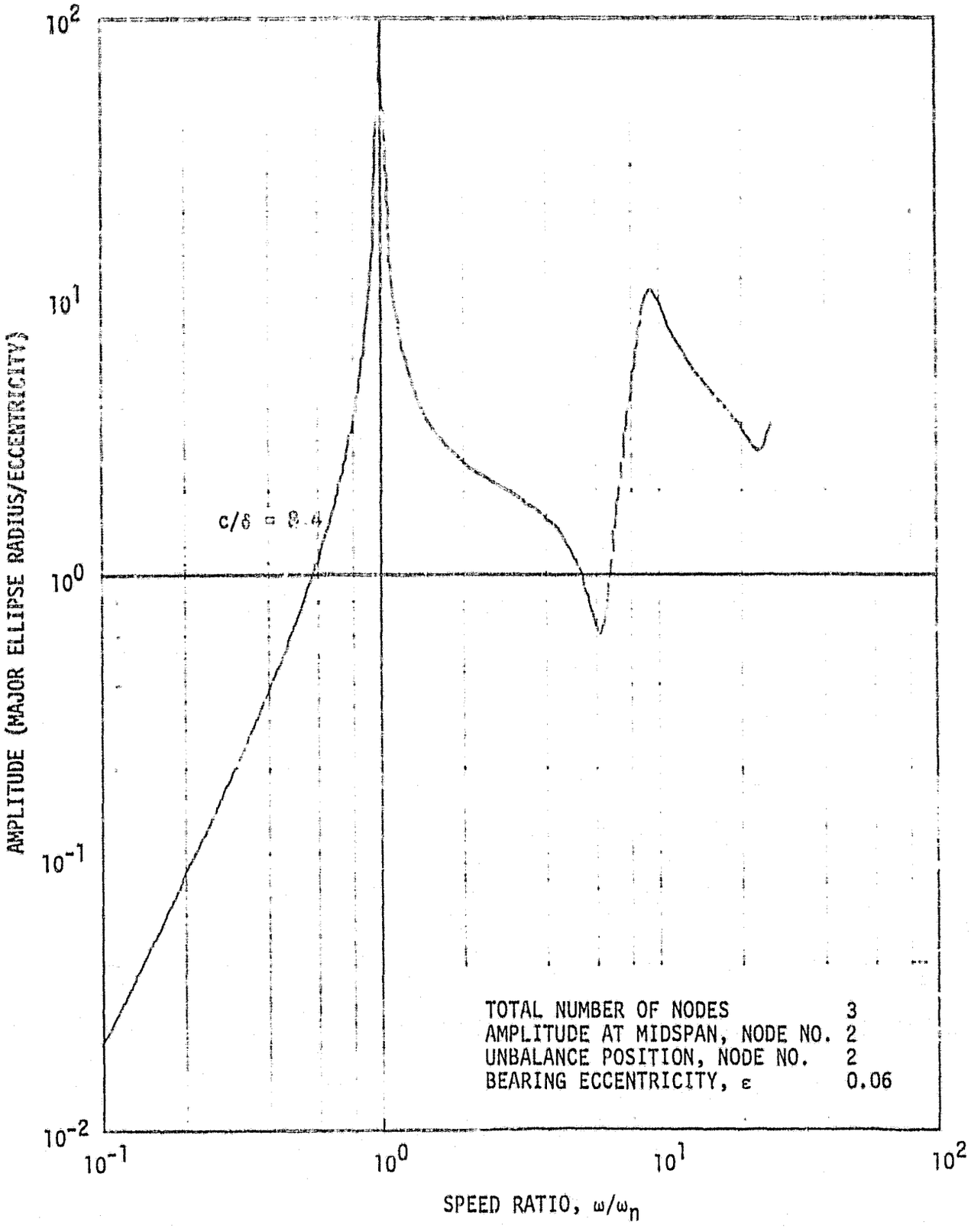

Figure 45. Response of Equivalent Rotor. Case 5. Flexible Bearings.

"Page missing from available version"

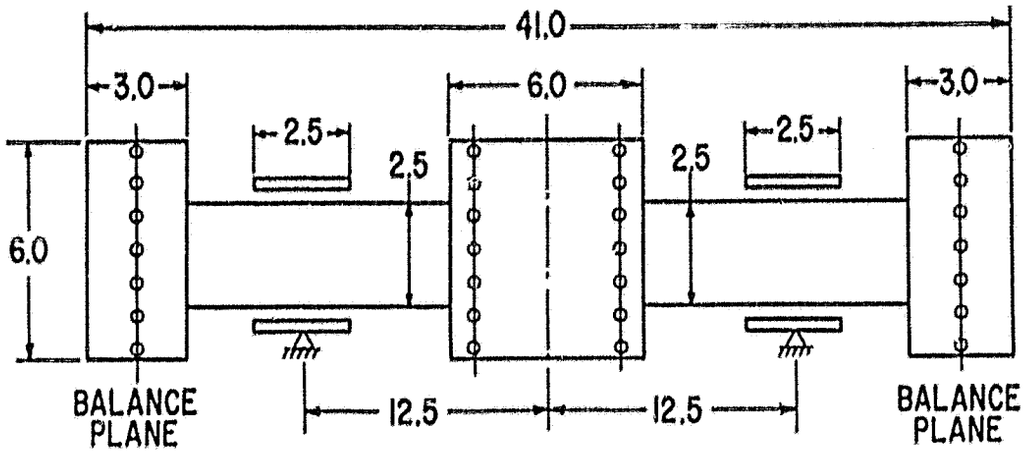

ROTOR WEIGHT: 88 LB.
END DISKS: 18 LB. EACH
CENTER DISK: 36 LB.
DRIVE: ELECTRIC MOTOR AT END
SPEED RANGE: 24,000 RPM
FLUID VISCOSITY: 0.65 CS (77°F)
0.51 CS (130°F)

BEARINGS: 4 SHOE TILTING PAD
L/D RATIO: 1.0
CLEARANCE RATIO: 3×10^{-3} IN./IN.
(MACHINED CLEARANCE)
PAD ARC LENGTH: 80 DEGREES
PIVOT POSITION: 44 DEGREES
FROM LEADING EDGE
GEOMETRIC PRELOAD: 0.5

Figure 46. Lund-Orcutt Rotor System Details.

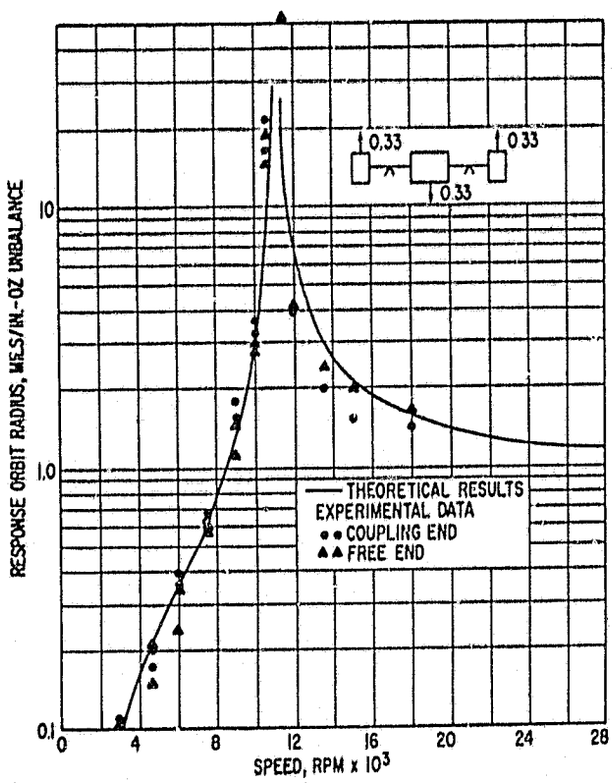

Figure 47. Unbalance Response Amplitudes of Lund-Orcutt Rotor in Free-Free Mode. From Ref. [5].

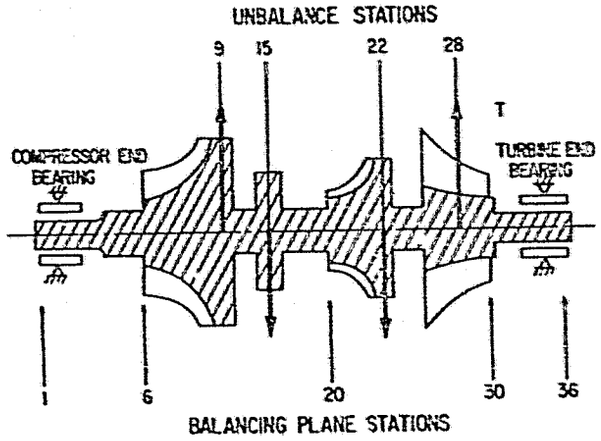

Figure 48. Rieger-Badgley Rotor System Details.

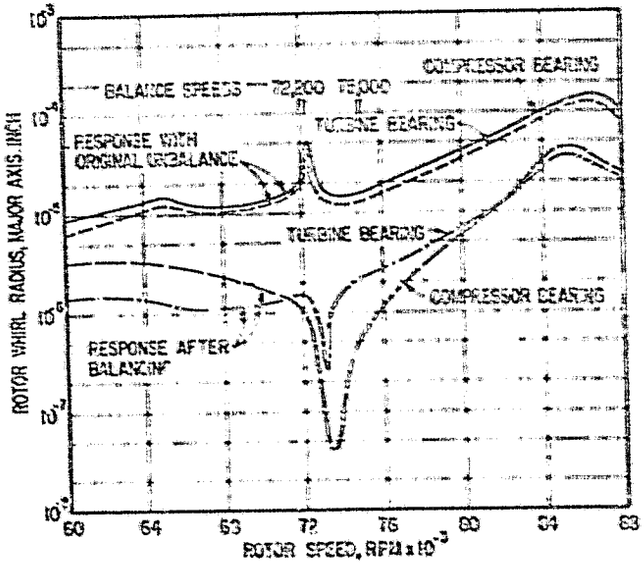

Figure 49. Unbalance Response Amplitudes of Reiger-Badgley Rotor. From Ref. [15].

"Page missing from available version"

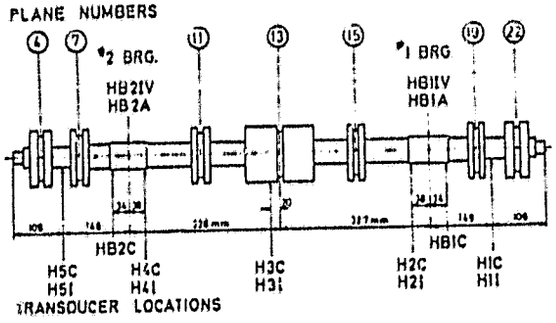

Figure 50. Lund-Tonneson Rotor System Details.

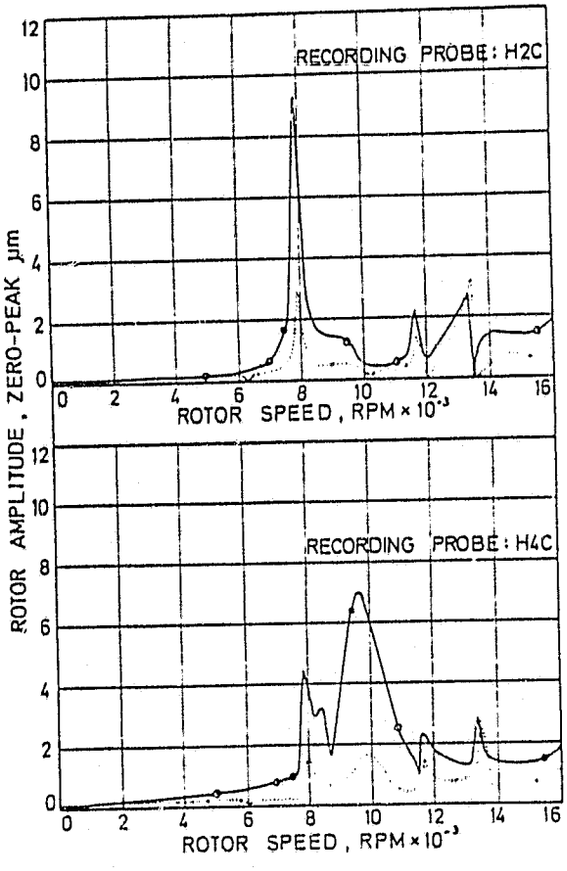

Figure 51. Unbalance Response Amplitudes of Lund-Tonneson Rotor. From Ref. [16].

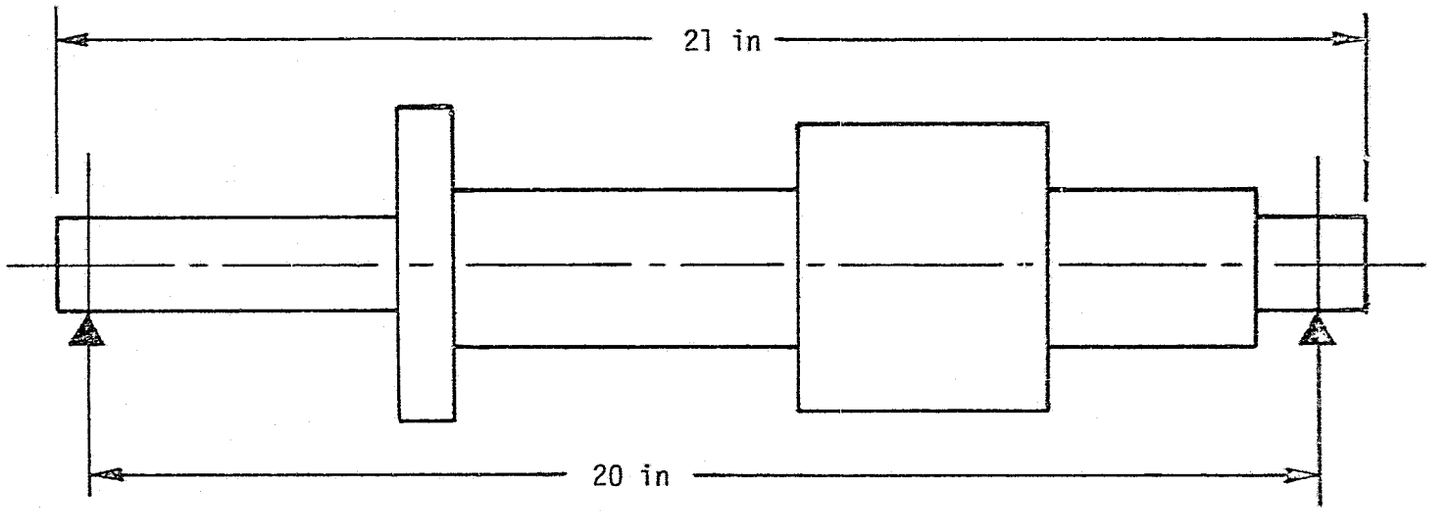

Figure 52. Gas Turbine Rotor Details.

"Page missing from available version"

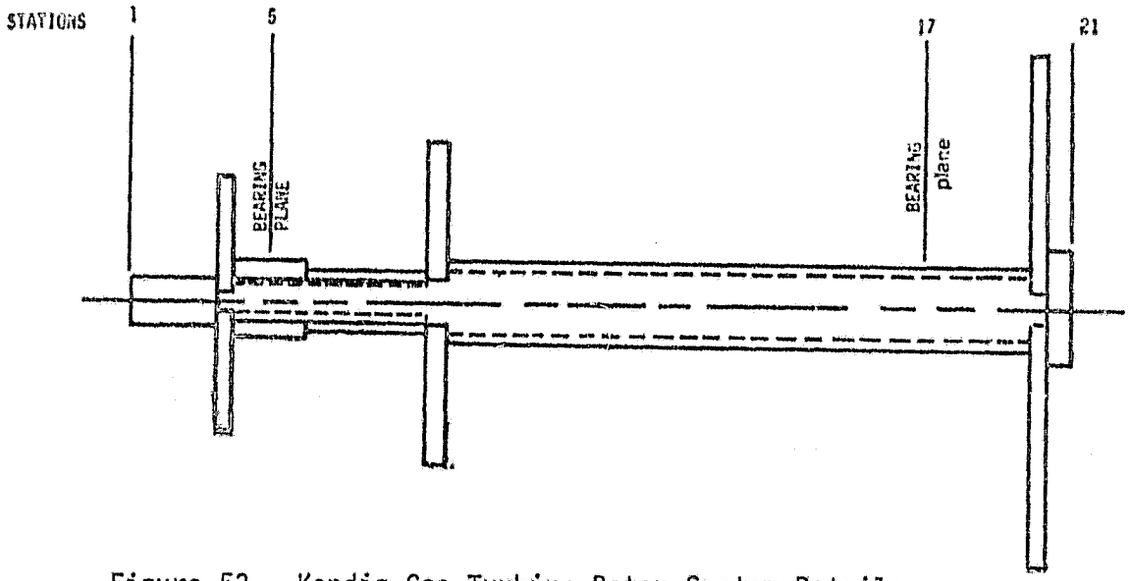

Figure 53. Kendig Gas Turbine Rotor System Details.

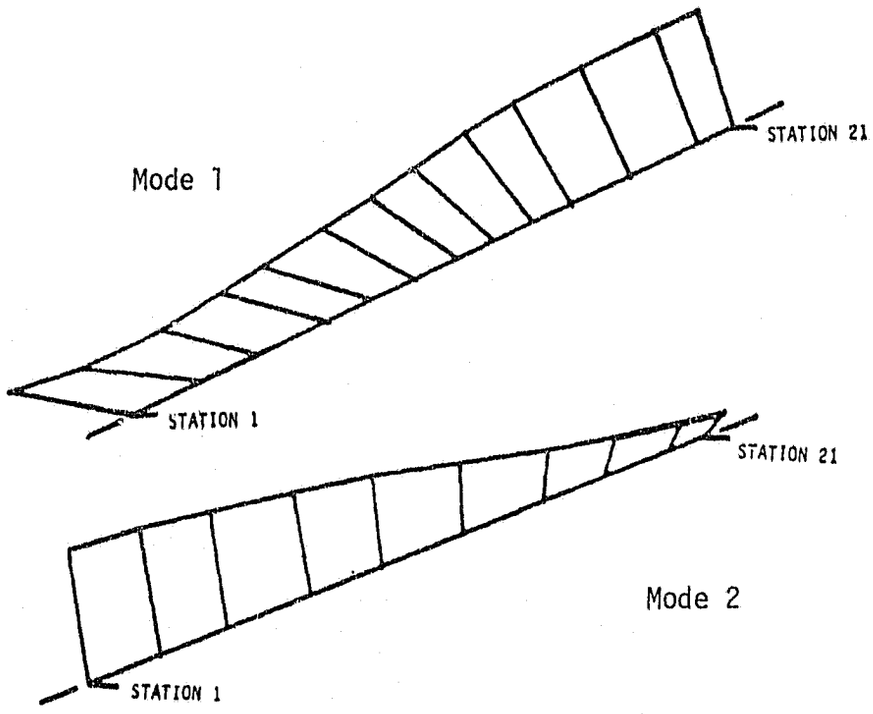

Figure 54. Gas Turbine Unbalance Response.

"Page missing from available version"

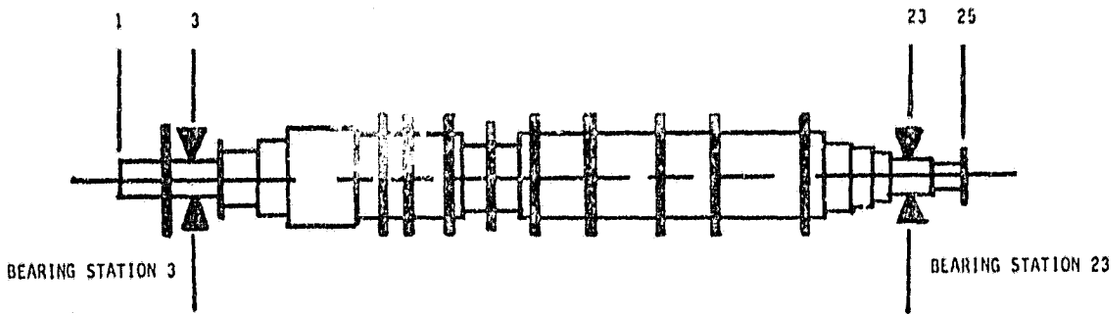

Figure 55. Kendig Steam Turbine Rotor System Details.

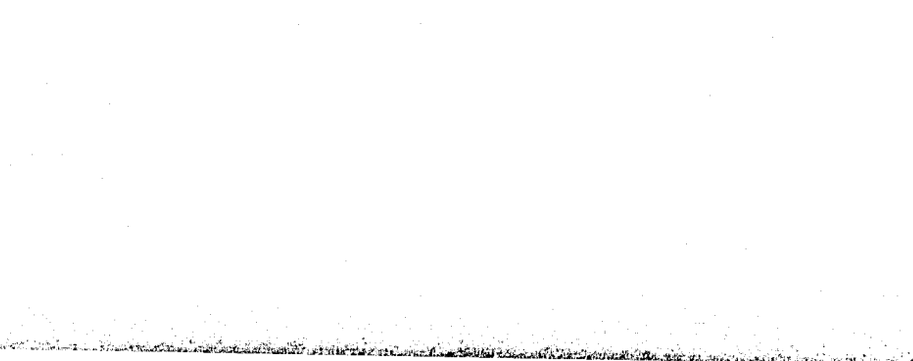

Figure 56. Steam Turbine Unbalance Response.